

**Westinghouse Electric Company LLC LTR-CDME-05-209-NP, "Steam Generator Tube
Alternate Repair Criteria for the Portion of the Tube Within the Tubesheet at the Wolf
Creek Generating Station."
(NON-PROPRIETARY)**

LTR-CDME-05-209-NP

**Steam Generator Tube Alternate Repair Criteria
for the Portion of the Tube Within the Tubesheet
at the Wolf Creek Generating Station**

January 2006

Author: */s/ Robert F. Keating*

Robert F. Keating

Major Component Replacements & Engineering

Verified: */s/ Hermann O. Lagally*

Hermann O. Lagally

Chemistry Diagnostics & Materials Engineering

Westinghouse Electric Company LLC

P.O. Box 355

Pittsburgh, PA 15230-0355

© 2006 Westinghouse Electric Company LLC

All Rights Reserved

Official Record Electronically Approved in EDMS

This page intentionally blank.

Abstract

Nondestructive examination indications of primary water stress corrosion cracking were found in the Westinghouse Model D5 Alloy 600 thermally treated steam generator tubes at the Catawba 2 nuclear power plant in the fall of 2004. Most of the indications were located in the tube-to-tubesheet welds with a few of the indications being reported as extending into the parent tube. In addition, a small number of tubes were reported with indications about 3/4 inch above the bottom of the tube within a region referred to as the tack-expansion, and multiple indications were reported in one tube at internal bulge locations in the upper third of the tubesheet. The tube end weld indications were dominantly axial in orientation and almost all of the indications were concentrated in one steam generator. Circumferential cracks were also reported at internal bulge locations in two of the Alloy 600 thermally treated steam generator tubes at the Vogtle 1 plant site in the spring of 2005. Internal tube bulges within the tubesheet are created in a number of locations as an artifact of the manufacturing process. Based on interpretations of requirements published by the NRC staff in GL 2004-01 and IN 2005-9, the Wolf Creek Nuclear Operating Corporation requested that a recommendation be developed for future examinations of the tubesheet regions of the steam generator tubes at the Wolf Creek Generating Station. An evaluation was performed that considered the requirements of the ASME Code, Regulatory Guides, NRC Generic Letters, NRC Information Notices, the Code of Federal Regulations, NEI 97-06, and additional industry requirements. The conclusion of the technical evaluation is that: 1) the structural integrity of the primary-to-secondary pressure boundary is unaffected by tube degradation of any magnitude below a tube location-specific depth ranging from 2.2 to 6.9 inches depending on the tube leg and bundle zone being considered, designated as H*, and, 2) that the accident condition leak rate integrity can be bounded by a specified factor of the normal operation leak rate from degradation at or below a calculated distance, designated as B*, from the top of the 21 inch thick tubesheet, including degradation of the tube end welds. These results follow from analyses demonstrating that the tube-to-tubesheet hydraulic joints make it extremely unlikely that any operating or faulted condition loads are transmitted below the H* elevation, and the contact pressure dependent leak rate resistance increases below the B* elevation within the tubesheet. The possibility of degradation at such locations in the Wolf Creek steam generator tubes exists based on the reported degradation at Catawba 2 and Vogtle 1. The determination of the required engagement depth was based on results from finite element model structural analyses and a steam line break to normal operation comparative leak rate evaluation. It was also concluded that the evaluation of the conditions on the hot leg would always bound those for the cold leg with regard to leak rate performance. The cold leg requirements are greater than the hot leg requirements with regard to pullout resistance (the above numbers bound both). The structural length is slightly less than that needed to restrict leak resistance to be the same during accident conditions at the center of the bundle. Application of the structural analysis and leak rate evaluation results to eliminate inspection and/or repair of tube indications in the region of the tube below the H* or B* elevation is interpreted to constitute a redefinition of the primary-to-secondary pressure boundary relative to the original design of the SG and requires the approval of the NRC staff through a license amendment.

This page intentionally blank.

Table of Contents

1.0	Introduction	11
2.0	Summary Discussion	17
3.0	Historical Background Regarding Tube Indications in the Tubesheet.....	20
4.0	Design Requirements for the Tube-to-Tubesheet Joint Region	22
5.0	Operating Conditions	24
5.1	Bounding Operating Conditions	24
5.2	Faulted Conditions	24
6.0	Steam Generator Tube Leakage and Pullout Test Programs Discussion	26
6.1	Model F Tube Pullout Test Program and Results	26
6.2	Leak Rate Testing Program.....	27
6.2.1	Model F Tube Joint Leakage Resistance Program	27
6.2.2	Model F Leakage Resistance Tests.....	30
6.3	Loss Coefficient on Contact Pressure Regression.....	30
7.0	Structural Analysis of Tube-to-Tubesheet Joint.....	41
7.1	Evaluation of Tubesheet Deflection Effects for Tube-to-Tubesheet Contact Pressure.....	42
7.1.1	Material Properties and Tubesheet Equivalent Properties.....	42
7.1.2	Finite Element Model	45
7.1.3	Tubesheet Rotation Effects.....	46
7.1.4	Wolf Creek Contact Pressures.....	49
7.2	Determination of Required Engagement Length of the Tube in the Tubesheet.....	51
8.0	Leak Rate Analysis of Cracked Tube-to-Tubesheet Joints	71
8.1	The Bellwether Principle for Normal Operation to Steam Line Break Leak Rates	71
8.2	Ligament Tearing Discussion.....	75
9.0	Determination of the B* Distance	81
9.1	Background Information	82
9.2	Flow Through a Crevice (Darcy's Equation)	83
9.3	Tube-to-Tubesheet Contact Pressure Variation	84
9.4	Determination of the B* Distance.....	85
9.5	Sensitivity of the B* Calculation	87
9.6	Conclusions Relative to B*	88
10.0	NRC Staff Discussion for One-Cycle B* Approval for Braidwood 2 & Wolf Creek.....	102
10.1	Joint Structural Integrity Discussion	102
10.1.1	Discussion of Interference Loads	103
10.1.2	Flexibility Discussion	105
10.1.3	Analysis	107
10.1.4	Conclusions	109
10.2	Joint Leakage Integrity Discussion	109

11.0 Conclusions	114
11.1 Analysis.....	114
11.2 Application for Wolf Creek	116
12.0 References	124

List of Tables

Table 6-1. Model F Leak Test Program Matrix	32
Table 6-2. Model F Leak Rate Testing Data	33
Table 6-4. Model F 0.25 Inch Displacement Data at 600°F	34
Table 7-1. Summary of Material Properties Alloy 600 Tube Material	55
Table 7-2. Summary of Material Properties for SA-508 Class 2a Tubesheet Material	55
Table 7-3. Summary of Material Properties SA-533 Grade A Class 2 Shell Material	55
Table 7-4. Summary of Material Properties SA-216 Grade WCC Channelhead Material	56
Table 7-5. Tube/Tubesheet Maximum & Minimum Contact Pressures and H* Depths for Wolf Creek Steam Generators	57
Table 7-7. Cumulative Forces Resisting Pull Out from the TTS Wolf Creek Hot Leg Normal Conditions – $T_{hot} = 620^{\circ}\text{F}$, $P_{sec} = 935$ psig	59
Table 7-8. Cumulative Forces Resisting Pull Out from the TTS Wolf Creek Faulted (SLB) Conditions, $P_{sec} = 0$ psig	60
Table 7-9. Cumulative Forces Resisting Pull Out from the TTS Wolf Creek FLB Conditions, Reduced T_{hot}	61
Table 7-10. Cumulative Forces Resisting Pull Out from the TTS Wolf Creek FLB Conditions, T_{hot} $= 620^{\circ}\text{F}$	62
Table 7-11. Summary of H* Calculations for Wolf Creek	63
Table 9-1. First Order Equation Coefficients for the Variation of Contact Pressures Through Tubesheet	90
Table 10-1. Typical Radial Flexibilities Times Elastic Modulus (in./psi)	111
Table 10-2. Example Contact Pressure Influence Factors for Model F & Model D5 SG Tubes at 600°F	111
Table 11-1. Calculated H* and B* Depths	119
Table 11-2. Inspection Program for H*/B*	120

This page intentionally blank.

List of Figures

Figure 1-1. Distribution of Indications in SG A at Catawba 2.....	15
Figure 1-2. Distribution of Indications in SG B at Catawba 2.....	15
Figure 1-3. Distribution of Indications in SG D at Catawba 2.....	16
Figure 2-1. As-Fabricated & As-Analyzed Tube-to-Tubesheet Welds.....	19
Figure 6-1. Example Leakage Test Schematic.....	35
Figure 6-2. Example Tube Hydraulic Expansion Process Schematic.....	36
Figure 6-3. Example Tube Joint Leakage Test Configuration.....	37
Figure 6-4. Schematic for the Test Autoclave Systems for Leak Rate Testing.....	38
Figure 6-5. Example Tube Joint Sample Pullout Test Configuration.....	39
Figure 6-6. Loss Coefficient Values for Model F Leak Rate Analysis.....	40
Figure 7-1. Definition of H* Zones.....	65
Figure 7-2. Finite Element Model of Model F Tubesheet Region.....	66
Figure 7-3. Contact Pressures for NOp at Wolf Creek, Reduced T_{hot} , $P_{sec} = 792$ psig.....	67
Figure 7-4. Contact Pressures for NOp at Wolf Creek, $T_{hot} = 620^{\circ}\text{F}$, $P_{sec} = 935$ psig.....	67
Figure 7-5. Contact Pressures for SLB Faulted Condition at Wolf Creek.....	68
Figure 7-6. Contact Pressures for FLB Condition at Wolf Creek, Reduced T_{hot}	68
Figure 7-7. Contact Pressures for FLB Condition at Wolf Creek, $T_{hot} = 620^{\circ}\text{F}$	69
Figure 8-1. Change in contact pressure at 20.0 inches below the TTS.....	78
Figure 8-2. Change in contact pressure at 16.9 inches below the TTS.....	78
Figure 8-3. Change in contact pressure at 12.6 inches below the TTS.....	79
Figure 8-4. Change in contact pressure at 10.5 inches below the TTS.....	79
Figure 8-5. Change in contact pressure at 8.25 inches below the TTS.....	80
Figure 8-6. Change in contact pressure at 6.0 inches below the TTS.....	80
Figure 9-1. Determination of H*.....	91
Figure 9-2. Determination of B*.....	92
Figure 9-3. Concepts for the Determination of B*.....	93
Figure 9-4. Schematic for the Determination of B* Parameters.....	93
Figure 9-5. First Order Linear Representation of Contact Pressure.....	94
Figure 9-6. Contact Pressure During Normal Operation (Model F).....	94
Figure 9-7. Contact Pressure During SLB (2560 psi at 297°F).....	95
Figure 9-8. NOp Contact Pressure vs. Depth Coefficients by Radius.....	95
Figure 9-9. SLB Contact Pressure vs. Depth Coefficients by Radius.....	96
Figure 9-10. Comparison of Contact Pressure Coefficients for NOp & SLB Conditions.....	96
Figure 9-11. Elevation Below the TTS for Invariant Contact Pressure.....	97
Figure 9-12. TTS Contact Pressure for NOp & SLB Conditions.....	97
Figure 9-13. Viscosity of Water as a Function of Pressure.....	98
Figure 9-14. Viscosity of Water at 2560 psi as a Function of Temperature.....	98
Figure 9-15. Upper Bound B* for Wolf Creek SGs for No Change in Resistance.....	99
Figure 9-16. Nominal B* for Wolf Creek SGs for No Change in Leak Rate.....	99
Figure 9-17. Graphical Determination of B* Depth from Flow Resistance.....	100
Figure 9-18. Approximate Determination of B* Depth from Contact Pressure.....	100

Figure 9-19. Elevation of Zero Contact Pressure for the Hot Leg	101
Figure 9-20. Elevation of Zero Contact Pressure for the Cold Leg	101
Figure 10-1. Geometry of the Tube-to-Tubesheet Interface	112
Figure 10-2. Model for Initial Contact Pressure	112
Figure 10-3. Determination of Contact Pressure, Normal or Accident Operation.....	113
Figure 11-1. Comparison of H* and B* Hot Leg Results.....	121
Figure 11-2. Comparison of H* and B* Cold Leg Results	121
Figure 11-3. Wolf Creek Hot Leg Inspection Depth Profile.....	122
Figure 11-4. Wolf Creek Cold Leg Inspection Depth Profile.....	122
Figure 11-5. Wolf Creek Hot Leg Inspection Depth Zones	123
Figure 11-6. Wolf Creek Cold Leg Inspection Depth Zones	123

**Steam Generator Tube Alternate Repair Criteria
for the Portion of the Tube Within the Tubesheet
at the Wolf Creek Generating Station**

1.0 Introduction

Indications of cracking were reported from the nondestructive, eddy current examination of the steam generator (SG) tubes during the fall 2004 outage at the Catawba 2 nuclear power plant operated by the Duke Power Company, References 1, 2, and 3. The tube indications at Catawba 2 were reported about 7.6 inches from the top of the tubesheet in one tube, and just above the tube-to-tubesheet welds in a region of the tube known as the tack expansion (TE) in several other tubes. Moreover, indications were also reported in the tube-end welds (TEWs), also known as tube-to-tubesheet welds, joining the tube to the tubesheet, with a small number of those indications extending into the tube material. The spatial distribution of indications by row and column number is shown on Figure 1-1 for SG A, Figure 1-2 for SG B, and Figure 1-3 for SG D at Catawba 2; there were no indications in SG C. The Catawba 2 plant has Westinghouse designed, Model D5 SGs fabricated with Alloy 600TT (thermally treated) tubes. Subsequently, one indication was reported in each of two SG tubes at the Vogtle Unit 1 plant operated by the Southern Nuclear Operating Company (Reference 4). The Vogtle SGs are of the Westinghouse Model F design, like those at Wolf Creek, with slightly smaller diameter and thickness A600TT tubes than at Catawba. It was concluded from those observations that there is the potential for similar tube indications to be reported during future inspections of the Wolf Creek SGs.

Note: No indications were found during the planned inspections of the Braidwood 2 SG tubes in April 2005, a somewhat similar inspection of the tubes in two Model F SGs at Wolf Creek in April 2005, or an inspection of the Model D5 tubes at Comanche Peak 2 in the spring of 2005. Nor during similar inspections of the Model D5 tubes at Byron 2 and Model F tubes at Vogtle 1 in the fall of 2005.

The SGs at the Model D5 plant sites were fabricated in the 1978 to 1980 timeframe using similar manufacturing processes with a few exceptions. For example, the fabrication technique used for the installation of the SG tubes at Braidwood 2 would be expected to lead to a much lower likelihood for crack-like indications to be present in the region known as the tack expansion relative to Catawba 2 because a different process for effecting the tack expansions was adopted prior to the time of the fabrication of the Braidwood 2 SGs.

The Model F SGs were fabricated in the 1979 through 1988 timeframe using similar manufacturing processes also with a few exceptions. For example, the fabrication technique used for the installation of the SG tubes at Vogtle 1 would be expected to lead to a much lower likelihood for crack-like indications to be present in the region known as the tack expansion relative to Catawba 2 because a different process for effecting the tack expansions was adopted prior to the time of the fabrication of the Vogtle 1 SGs. The same statement cannot be made with regard to the tack expansion region in the Wolf Creek SGs since they were fabricated at about the same time as the Catawba 2 SGs using the same tack expansion process.

The findings in the Catawba 2 and Vogtle 1 SG tubes present three distinct issues with regard to future inspections of A600TT SG tubes which have been hydraulically expanded into the tubesheet:

- 1) indications in internal bulges within the tubesheet (created in a number of tubes as an artifact of the manufacturing process),
- 2) indications at the elevation of the tack expansion transition, and,
- 3) indications in the tube-to-tubesheet welds, including some extending into the tube.

The scope of this document is to:

- a) address the applicable requirements, including the original design basis, Reference 11, and regulatory issues, Reference 13, and,
- b) provide analysis support for technical arguments to limit tube inspection in the tubesheet region to an area above which degradation could result in potentially not meeting the SG performance criteria, i.e., the depths specified in Section 7.0 of this report.

An evaluation was performed that considered the requirements of the ASME Code, Regulatory Guides, NRC Generic Letters, NRC Information Notices, the Code of Federal Regulations, NEI 97-06, and additional industry requirements. The conclusion of the technical evaluation is that:

- 1) the structural integrity of the primary-to-secondary pressure boundary is unaffected by tube degradation of any magnitude below a tube location-specific depth designated as H^* , and,
- 2) the accident condition leak rate integrity can be bounded by twice the normal operation leak rate from degradation at or below a depth designated herein as B^* from the top of the 21 inch thick tubesheet.

These results follow from analyses demonstrating that the tube-to-tubesheet hydraulic joints make it extremely unlikely that any operating or faulted condition loads are transmitted below the H^* elevation, and that the tube-to-tubesheet contact leak rate resistance increases below the B^* elevation within the tubesheet. The determination of the required engagement depth was based on the use of finite element model structural analyses and of a bounding leak rate evaluation based on the change in contact pressure between the tube and the tubesheet between normal operation and postulated accident conditions. The results provide the technical rationale to eliminate inspection of the region of the tube below the H^* or B^* elevation. Such an approach is interpreted to constitute a redefinition of the primary-to-secondary pressure boundary relative to the original design of the SG and requires the approval of the NRC staff through a license amendment.

A similar type of Technical Specification change was approved, on a one-time basis, to limit inspections of the Wolf Creek Model F and Braidwood 2 Model D5 SGs during the spring 2005 inspection campaigns, for example see References 7 and 8 respectively. Subsequent approvals were also obtained for use at Byron 2 and Vogtle 2 for their fall 2005 inspection campaigns,

Reference 9 for example for the latter. This report was prepared to justify the specialized probe, e.g., RPC (rotating probe coil), exclusion zone to the portion of the tube below about 8 to 11 inches from the top of the tubesheet, depending on the tube leg, and to provide the necessary information for a detailed NRC staff review of the technical basis for that request. The major difference between the current evaluation of the Wolf Creek SGs and prior applications is the identification of tube location-specific depths for the inspection instead of simply using an arbitrary, bounding value of 17 inches from the top of the tubesheet.

The H^* values were determined to assure meeting the structural performance criteria for the operating SG tubes as delineated in NEI 97-06, Revision 2, Reference 14. The B^* values were determined based on meeting the accident condition leak rate performance criteria. Compliance is based on demonstrating both structural and leakage integrity during normal operation and postulated accident conditions. The structural model was based on standard analysis techniques and finite element models as used for the original design of the SGs and documented in numerous submittals for the application of criteria to deal with tube indications within the tubesheet of other models of Westinghouse designed SGs with tube-to-tubesheet joints fabricated by other techniques, e.g., explosive expansion.

All full depth expanded tube-to-tubesheet joints in Westinghouse-designed SGs have a residual radial preload between the tube and the tubesheet. Early vintage SGs involved hard rolling which resulted in the largest magnitude of the residual interface pressure. Hard rolling was replaced by explosive expansion which resulted in a reduced magnitude of the residual interface pressure. Finally, hydraulic expansion replaced explosive expansion for the installation of SG tubes, resulting in a further reduction in the residual interface pressure. In general, it was found that the leak rate through the joints in hard rolled tubes is insignificant. Subsequent testing demonstrated that the leak rate resistance of explosively expanded tubes was not as great as that of hard rolled tubes and prediction methods based on empirical data to support theoretical models were developed to deal with the potential for leakage. The same approach was followed to develop a prediction methodology for hydraulically expanded tubes. However, the model has been under review since its inception, with the intent of verifying its accuracy because it involved analytically combining the results from independent tests of leak rate through cracks with the leak rate through the tube-to-tubesheet crevice. The leak rate model associated with the initial development of H^* to meet structural performance criteria is such a model; technical acceptance could be time consuming since it has not been previously reviewed by the NRC staff. An alternative approach, provided in this report, was developed for application at Wolf Creek from engineering expectations of the relative leak rate between normal operation and postulated accident conditions based on a first principles engineering evaluation.

A summary of the evaluation is provided in Section 2.0 of this report. The historical background and design requirements for the tube-to-tubesheet joint are discussed in Sections 3.0 and 4.0 respectively. Section 5.0 addresses plant operating conditions at Wolf Creek. Section 6.0 discusses the tube pullout and leakage test programs that are applicable to the Model F SGs at Wolf Creek. A summary of the conclusions from the structural analysis of the joint is provided in Section 7.0, the leak rate analysis in Section 8.0, determination of the requisite inspection depth based on leak

rate considerations is in Section 9.0, a review of the qualitative arguments used by the NRC Staff for the tube joint inspection length approved for other plants is discussed in Section 10.0, conclusions from the structural and leak rate evaluations and recommended tube inspection plans are contained in Section 11.0 of this report.

SG - 2A +Point Indications Within the Tubesheet

Catawba EOC13 DDP D5

E 1 INDICATION WITHIN 0.25" OF HOT LEG TUBE END
■ 66 PLUGGED TUBE

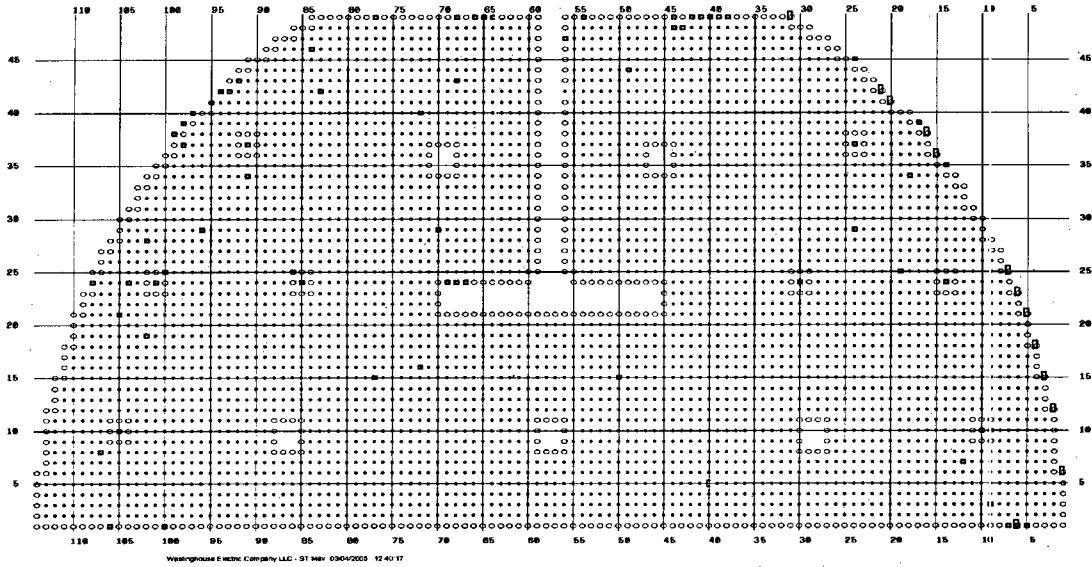


Figure 1-1. Distribution of Indications in SG A at Catawba 2

SG - 2B +Point Indications Within the Tubesheet

Catawba EOC13 DDP D5

Z 1 MULTIPLE INDICATIONS AT APPROXIMATELY 7" BELOW HOT LEG TOP OF TUBESHEET
E 192 INDICATION WITH 0.25" OF HOT LEG TUBE END
W 1 INDICATIONS WITHIN 0.25" AND BETWEEN 0.25" AND 0.80" OF HOT LEG TUBE END
B 0 INDICATION BETWEEN 0.26" AND 0.80" OF HOT LEG TUBE END
■ 58 PLUGGED TUBE

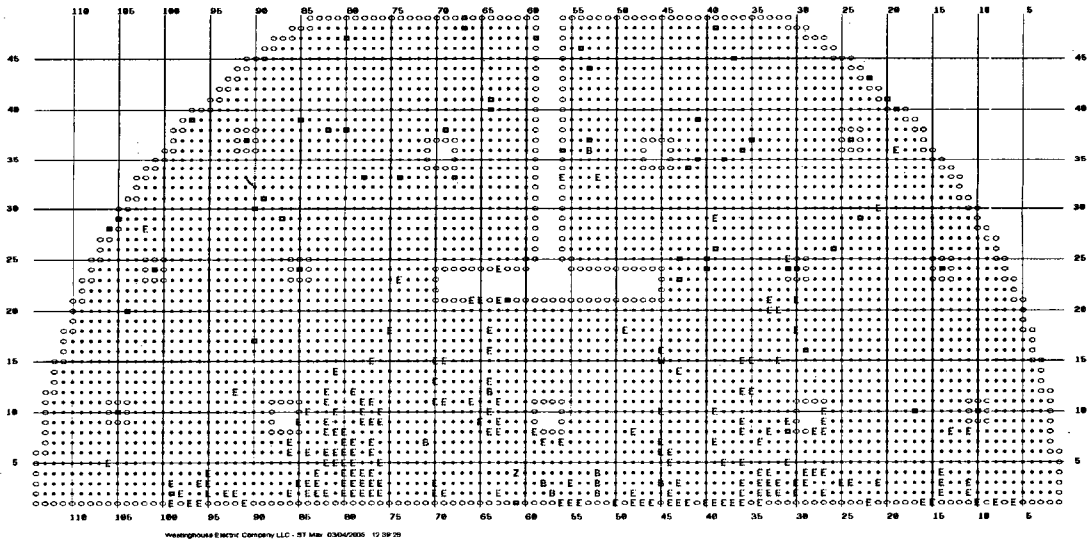


Figure 1-2. Distribution of Indications in SG B at Catawba 2

SG - 2D +Point Indications Within the Tubesheet

Catawba EOC13 DDP D5

E 7 INDICATION WITHIN 0.25" OF
HOT LEG TUBE END
■ 85 PLUGGED TUBE

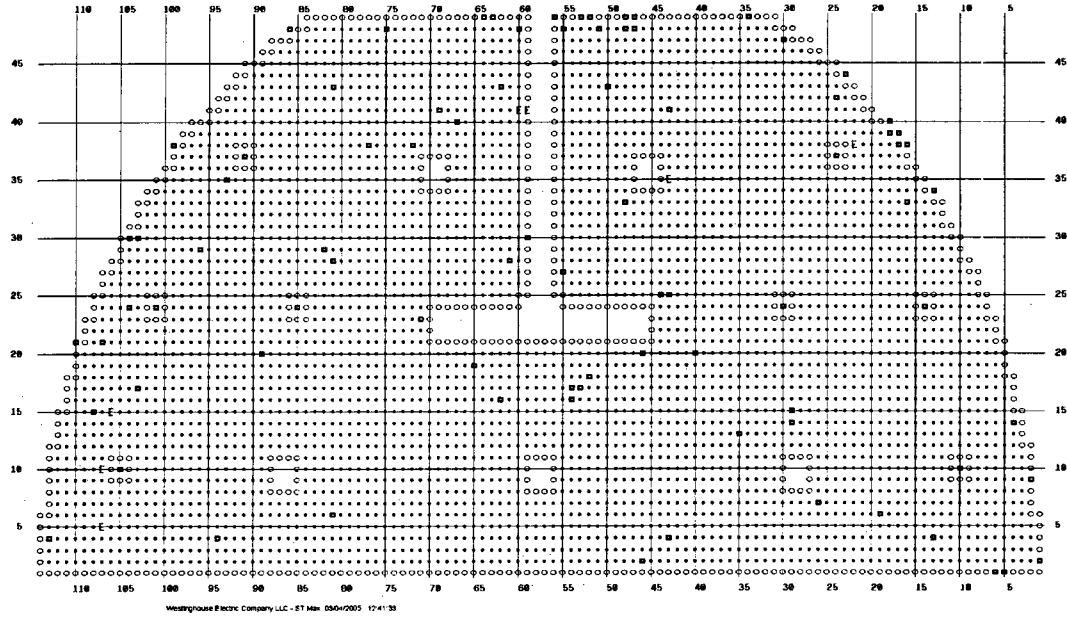


Figure 1-3. Distribution of Indications in SG D at Catawba 2

2.0 Summary Discussion

Evaluations were performed to assess the need for addressing degradation in the region of the SG tubes within the tubesheet at the Wolf Creek Generating Station. The conclusions from the evaluation are that a redefinition of the pressure boundary can be effected while still assuring that the structural and leak rate performance criteria would be met during both normal operation and limiting postulated accident conditions.

Implementation of the redefinition of the pressure boundary results in the elimination of examination of the tubes below a depth on the order of 7¹ inches from the top of the tubesheet, which includes the region of the tube referred to as the tack expansion or the tack expansion transition near the bottom of the tubesheet. In addition, consideration was given to the need to perform inspections of the tube-to-tubesheet weld in spite of the fact that the weld is specifically not part of the tube in the sense of the plant technical specification, see Reference 2. It is concluded that there is no need to inspect the tube-to tubesheet welds for degradation because the tube in these regions has been shown to meet structural and leak rate criteria regardless of the level of degradation. Furthermore, it could also be concluded that for some of the tubes, depending on radial location in the tubesheet, there is no need to inspect the region of the tube below the shifted neutral plane of the tubesheet with regard to contact pressure,² roughly 8.3 inches below the top. The results from the evaluations performed as described herein demonstrate that the inspection of the tube within about 10 inches of the tube-to-tubesheet weld and of the weld is not necessary for structural adequacy of the SG during normal operation or during postulated faulted conditions, nor for the complying with leak rate limits during postulated faulted events.

In summary:

- The structural integrity requirements of NEI 97-06, Reference 14, are met by sound tube engagement lengths ranging from 2.2 to 6.9 inches from the top of the tubesheet, see Table 7-12, thus the region of the tube below those elevations, including the tube-to-tubesheet weld is not needed for structural integrity during normal operation or accident conditions.
- NEI 97-06, Reference 14, defines the tube as extending from the tube-to-tubesheet weld at the tube inlet to the tube-to-tubesheet weld at the tube outlet, but specifically excludes the tube-to-tubesheet weld from the definition of the tube. The acceptance of the definition by the NRC staff was recorded in the Federal Register on March 2, 2005, Reference 16.
- The welds were originally designed and analyzed as primary pressure boundary in accordance with the requirements of Section III of the 1971 edition of the ASME Code,

¹ The value of 7 inches corresponds to the worst location in the tubesheet. The value can be considerably less towards the periphery.

² The neutral plane of the tubesheet is shifted away from the center because of the tensile stress in the tubesheet and the internal pressure in the tube.

Summer 1973 Addenda, References 11, 12 and 17. The analyses are documented in Reference 12 for the Wolf Creek SGs. The typical as-fabricated and the as-analyzed weld configurations are illustrated on Figure 2-1.

- Section XI of the ASME Code, Reference 18 (1971) through 19 (2004), deals with the inservice inspection of nuclear power plant components. The ASME Code specifically recognizes that the SG tubes are under the purview of the NRC through the implementation of the requirements of the Technical Specifications as part of the plant operating license.

The hydraulically expanded tube-to-tubesheet joints in Model F SGs are not leak-tight without the tube end weld and considerations were also made with regard to the potential for primary-to-secondary leakage during postulated faulted conditions. However, the leak rate during postulated accident conditions would be expected to be less than that during normal operation for indications near the bottom of the tubesheet (including indications in the tube end welds) based on the observation that while the driving pressure increases by about a factor of almost two, the flow resistance increases because the tube-to-tubesheet contact pressure also increases. Depending on the depth within the tubesheet, the relative increase in resistance could easily be larger than that of the pressure potential. Therefore, the leak rate under normal operating conditions could exceed its allowed value before the accident condition leak rate would be expected to exceed its allowed value. This approach is termed an application of the "bellwether principle." The evaluations were performed to specifically determine relative changes in the leak rate resistance as a function of tube location from the center of the tubesheet and degradation distance from the top of the tubesheet. The assessment envelopes postulated circumferential cracking of the tube or the tube-to-tubesheet weld that is 100% deep by 360° in extent because it is based on the premise that the tube and weld are not present below the analyzed elevations.

Based on the information summarized above, no inspection of the tube-to-tubesheet welds, tack roll region or bulges below the distance determined to have the potential for safety significance as specified in Reference 5, i.e., the H* depths, would be considered to be the minimum distance to be necessary to assure compliance with the structural requirements for the SGs. In addition, based on the results from consideration of application of the bellwether principle regarding potential leakage during postulated accident conditions, inspection depths as a function of tube location established using the results from these analyses are conservative and justified.

The length determined for structural compliance purposes may or may not bound the required length for leak rate compliance as discussed in Sections 7.0 and 8.0 of this report depending on the allowable relative leak rates. For example, compare the results in Table 7-12 to those in Table 9-2. The application of the bellwether approach to the leak rate analysis as described in Section 8.1 of this report negates the need to consider specific leak rates because it relies only on the relative magnitude of the joint contact pressures between the tube and the tubesheet.

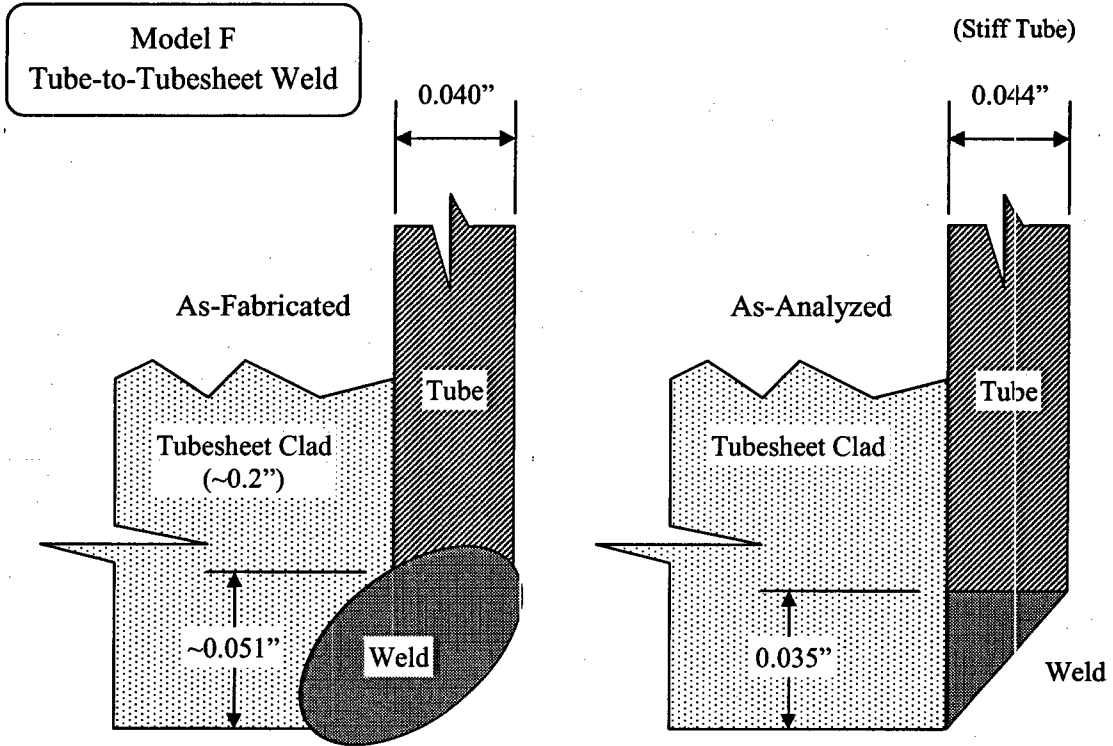


Figure 2-1. As-Fabricated & As-Analyzed Tube-to-Tubesheet Welds

3.0 Historical Background Regarding Tube Indications in the Tubesheet

There has been extensive experience associated with the operation of SGs wherein it was believed, based on NDE, that throughwall tube indications were present within the tubesheet. The installation of the SG tubes usually involves the development of a short interference fit, referred to as the tack expansion, at the bottom of the tubesheet. The tack expansion was usually effected by a hard rolling process through October of 1979 and thereafter, in most instances, by the Poisson expansion of a urethane plug inserted into the tube end and compressed in the axial direction. The rolling process by its very nature is considered to be more intensive with regard to metalworking at the inside surface of the tube and would be expected to lead to higher residual surface stresses. The manufacturing procedures and drawing requirements indicate that the rolling process was used during fabrication of the Wolf Creek SGs. The tube-to-tubesheet weld was then performed to create the ASME Code pressure boundary between the tube and the tubesheet.³

The development of the F* alternate repair criterion (ARC) in 1985-1986 for tubes hard rolled into the tubesheet was prompted by the desire to account for the inherent strength of the as-fabricated tube-to-tubesheet joint away from the weld and to allow tubes with degradation within the tubesheet to remain in service, Reference 20. The result of the development activity was the demonstration that the tube-to-tubesheet weld was superfluous with regard to the structural and leakage integrity of the rolled joint between the tube and the tubesheet. Once the plants were in operation, the structural and leakage resistance requirements for the joints were based on the plant Technical Specifications, and a means of demonstrating joint integrity that was acceptable to the NRC staff was delineated in Reference 15. License amendments were sought and granted for several plants with hard rolled tube-to-tubesheet joints to omit the inspection of the tube below a depth of about 1.5 inches from the top of the tubesheet. Similar criteria, designated as W*, were developed for explosively expanded tube-to-tubesheet joints in Westinghouse designed SGs in the 1991-1992 timeframe, Reference 22. The W* criteria were first applied to operating SGs in 1999 based on a generic evaluation for Model 51 SGs, Reference 23, and the subsequent safety evaluation by the NRC staff, Reference 24. However, the required engagement length to meet structural and leakage requirements was on the order of 4 to 6 inches because an explosively expanded joint does not have the same level of residual interference fit as that of a rolled joint. It is noted that the length of joint necessary to meet the structural performance criteria is not the same as, and is usually shorter than, that needed to meet the leakage integrity requirements.

The post-weld expansion of the tube into the tubesheet in the Wolf Creek SGs was effected by a hydraulic expansion of the tube instead of rolling or explosive expansion. The hydraulically formed joints do not exhibit the level of interference fit that is present in rolled or explosively expanded joints; however, when the thermal and internal pressure expansion of the tube is considered during normal operation and postulated accident conditions, appropriate conclusions regarding the need for the weld similar to those for the other two types of joint can be made.

³ The actual weld is between the Alloy 600 tube and weld buttering, a.k.a. cladding, on the bottom of the carbon steel tubesheet.

Evaluations were performed in 1996 and 1997 of the effect of tube-to-tubesheet weld damage that occurred from an object in the bowl of a Model F SG with tube-to-tubesheet joints similar to those in the Wolf Creek SGs on the structural and leakage integrity of the joint, References 25 and 26 respectively. It was concluded in that evaluation that the strength of the tube-to-tubesheet joint is sufficient to prevent pullout in accordance with the requirements of the performance criteria of Reference 14 and that a significant number of tubes could be damaged without violating the performance criterion related to the primary-to-secondary leak rate during postulated accident conditions. Both documents noted that the leak rate during normal operation would likely bound that to be expected during postulated accident conditions. A similar evaluation was performed for SG D at Wolf Creek with similar conclusions, Reference 27.

4.0 Design Requirements for the Tube-to-Tubesheet Joint Region

This section provides a review of the applicable design and analysis requirements, including the ASME Code pre-service design requirements of Section III and the operational/maintenance requirements of Section XI. The following is the Westinghouse interpretation of the applicable analysis requirements and criteria for the condition of TEW cracking. Recommendations that include code requirements and the USNRC and NEI positions are expressed in References 13 and 14 respectively. Reference 13 notes that:

“In accordance with Section III of the Code, the original design basis pressure boundary for the tube-to-tubesheet joint included the tube and tubesheet extending down to and including the tube-to-tubesheet weld. The criteria of Section III of the ASME Code constitute the “method of evaluation” for the design basis. These criteria provide a sufficient basis for evaluating the structural and leakage integrity of the original design basis joint. However, the criteria of Section III do not provide a sufficient basis by themselves for evaluating the structural and leakage integrity of a mechanical expansion joint consisting of a tube expanded against the tubesheet over some minimum embedment distance. If a licensee is redefining the design basis pressure boundary and is using a different method of evaluation to demonstrate the structural and leakage integrity of the revised pressure boundary, an analysis under 10 CFR 50.59 would determine whether a license amendment is required.”

The industry definition of Steam Generator tubing excludes the tube-end weld from the pressure boundary as noted in NEI 97-06 (Reference 14):

“Steam generator tubing refers to the entire length of the tube, including the tube wall and any repairs to it, between the tube-to-tube sheet weld at the tube inlet and the tube-to-tube sheet weld at the tube outlet. The tube-to-tube sheet weld is not considered part of the tube.”

The NRC has indicated its concurrence with this definition, see Reference 16 for example. In summary, from a non-technical viewpoint, no specific inspection of the tube-end welds would be required because:

1. The industry definition of the tube excludes the tube-end weld,
2. The ASME Code defers the judgment regarding the redefined pressure boundary to the licensing authority under 10CFR50.59,
3. The NRC has accepted this definition; therefore, by inference, may not consider cracked welds to be a safety issue on a level with that of cracked tubes, and
4. There is no qualified technique that can realistically be applied to determine if the tube-end welds are cracked.

However, based on the discussion of Information Notice 2005-09, Reference 2, it is clear that the NRC staff has concluded that “the findings at Catawba illustrate the importance of inspecting the parent tube adjacent to the weld and the weld itself for degradation.” The technical considerations documented herein obviate the need for consideration of any and all non-technical arguments.

5.0 Operating Conditions

The Wolf Creek Generating Station is a four-loop nuclear power plant with Westinghouse designed and fabricated Model F SGs; there are 5626 tubes in each SG. The design of these SGs includes Alloy 600 thermally treated (A600TT) tubing, full-depth hydraulically expanded tubesheet joints, and broached hole quatrefoil tube support plates constructed of stainless steel.

5.1 Bounding Operating Conditions

Values that bound the current Wolf Creek SG thermal and hydraulic parameters during normal operation are tabulated below (Note: these values assume a 10% SG tube plugging level.):

Parameter and Units		Bounding NOp Conditions ⁽¹⁾	
		Case 1	Case 2
Power – NSSS	MWt	3579	3579
Reactor Vessel Outlet Temperature	°F	603.4	620.0
Reactor Coolant System Pressure	psig	2235	2235
SG Steam Temperature	°F	519.3	538.4
SG Steam Pressure	psig	807	950
Primary-to-Secondary Pressure Difference	psi	1428	1285
Steam Line Break Pressure Difference	psig	2560	2560
Ratio of Accident to Normal Pressure	SLB / NOp	1.79	1.99
(1) Reference 28.			

5.2 Faulted Conditions

In addition to the RG 1.121 criteria, it is necessary to satisfy the updated safety analysis report (USAR) accident condition assumptions for primary-to-secondary leak rates. Calculated primary-to-secondary side leak rate during postulated events should:

- 1) not exceed the total charging pump capacity of the primary coolant system, and
- 2) be such that the off-site radiological dose consequences do not exceed Title 10 of the Code of Federal Regulations (10 CFR) Part 100 guidelines.

The accident condition primary-to-secondary leakage must be limited to acceptable values established by plant specific USAR evaluations. Pressure differentials associated with a postulated accident condition event can result in leakage from a throughwall crack through the interface

between a hydraulically expanded tube in the tubesheet and the tube hole surface. Therefore, a steam generator leakage evaluation for faulted conditions is provided in this report. The accidents that are affected by primary-to-secondary leakage are those that include, in the activity release and off-site dose calculation, modeling of leakage and secondary steam release to the environment. Steamline break (SLB) is the limiting condition because:

- 1) the SLB primary-to-secondary leak rate in the faulted loop is assumed to be greater than the operating leak rate because of the sustained increase in differential pressure, and
- 2) leakage in the faulted steam generator is assumed to be released directly to the environment.

For evaluating the radiological consequences due to a postulated SLB, the activity released from the affected SG (which is connected to the broken steam line) is released directly to the environment. The unaffected steam generators are assumed to continually discharge steam and entrained activity via the safety and relief valves up to the time when initiation of the RHR (reactor heat removal) system can be accomplished. The radiological consequences evaluated, based on meteorological conditions, usually assume that all of this flow goes to the affected SG. With the analytically determined level of leakage, the resultant doses are expected to be well within the guideline values of 10 CFR 100.

6.0 Steam Generator Tube Leakage and Pullout Test Programs Discussion

Data were available with regard to pullout and leak rate testing for the Model F SG geometry, for example, the original testing of Reference 26 was performed to investigate postulated extreme effects on the tube-to-tubesheet weld from a loose part on the primary side of one Model F SG. These data were subsequently used to support the model specific development of the required H* engagement length to resist pullout and to characterize the leak rate from throughwall tube indications within the tubesheet as a function of the contact pressure between the tube and the tubesheet, e.g., Reference 10 was originally written for the Wolf Creek SGs. The testing also provides valuable information regarding the calculation of B* once a relative SLB to NOP leak rate has been identified.⁴ The data from the Model F testing programs were used to support the development of the inspection criteria delineated in this report.

- The results from strength tests were used to establish the joint lengths needed to meet the structural performance criteria during normal operation and postulated accident conditions, the required engagement length being designated as H*. The inherent strength of the joint coupled with the results from a finite element model of the loading conditions is used to calculate the required H* values subsequently described in Section 7.0.
- The results from leak rate tests were used to support the methodology to quantify the leak rate during postulated accident conditions as a function of the leak rate during normal operation. The required engagement length to meet a specific leak rate objective is designated as B*. For example, it may be desired to determine the engagement length needed so that the leak rate expected during a postulated accident event is no more than twice that during normal operation. The calculation of the relative leak rates as a function of engagement length is described in Section 9.0 of this report.

The test programs, their results, and the analysis of the results are described in the following sections.

6.1 Model F Tube Pullout Test Program and Results

Two testing programs were performed to determine the pullout resistance of Model F tube-to-tubesheet joints at [

]^{a,c,e}. All of the test results are listed in Table 6-3. The mechanical loading, [

]^{a,c,e} The objective was to develop input information for analytically determining tube-to-tubesheet contact pressure and pullout resistance (lb/inch – axial). In this configuration, there is no contribution to tube-to-

⁴ It is noted that the discussion in Section 9.0 shows that the B* depths are not very sensitive to changes in the correlating parameters between the leak rate and contact pressure.

tubesheet contact pressure from tube internal pressurization. Internal pressurization also resists Poisson contraction associated with the axial load.

The data from the series of pullout tests are listed in Table 6-3 and in Table 6-4 for the 0.25 inch displacement data at 600°F. [

] ^{a,c,e} The use of a larger coefficient of friction results in calculating a lower value of the contact pressure. Subsequent use of the lower coefficient of friction results in calculating a larger required engagement length. A conservative value used for the pullout force in the H* calculations was the lower 95th percentile, i.e., [] ^{a,c,e} lb./inch. The 95th percentile was used because the standard deviation value was so small. It is possible that the [] ^{a,c,e}.

6.2 Leak Rate Testing Program

The purpose of the testing program was to provide quantified data with which to determine the [

] ^{a,c,e} As discussed in detail in Section 9.2, the analytical model for the leak rate is referred to as the Darcy or Hagen-Poiseuille formulation. The volumetric flow is a function of the pressure potential, the inverse of the crevice length, the inverse of the fluid viscosity, and the inverse of a resistance term characteristic of the geometry of the tube-to-tubesheet joint and referred to as the loss coefficient. Thus, the purpose of the testing programs is to obtain data with which to determine the loss coefficient.

6.2.1 Model F Tube Joint Leakage Resistance Program

A total of [

] ^{a,c,e}

[

] ^{a,c,e} The leakage resistance data were calculated for the test conditions listed in Table 6-1.

6.2.1.1 Model F Test Specimen Configuration

The intent of the test samples was to model key features of the Model F tube-to-tubesheet joint for [] ^{a,c,e}. Model F tubesheet simulating collars which duplicated the radial stiffness of a Model F tubesheet unit cell with an outside diameter of [] ^{a,c,e} were fabricated with a length of [] ^{a,c,e} thickness of the steam generator tubesheet. This allowed for the introduction and collection of leakage in unexpanded sections of the tube, while retaining conservative or typical hydraulic expansion lengths. The collars were drilled to the nominal design value inside diameters with the surface finish corresponding to SG drawing tolerances. In addition, the run-out tolerance for the collar drilling operation was held to within ± 0.002 inch of the tubesheet nominal hole diameter.

The collars were fabricated from [

] ^{a,c,e}.

Model F A600TT tubing with a yield strength approximately the same as that of the tubes in the operating plants, which ranges from [] ^{a,c,e}. The material used was from a certified heat and lot conforming to ASME SB163, Section III Class 1 and was maintained in a Quality Systems-controlled storeroom prior to use.

The intent of the leakage portion of the test program was to determine the leakage resistance of simulated Model F tube-to-tubesheet joints, disregarding the effect of the tube-to-tubesheet weld and the [

] ^{a,c,e}

[

] ^{a,c,e}, see Figure 6-1. The welds were a feature of the test specimen design and made no contribution to the hydraulic resistance.

6.2.1.2 Model F Test Sample Assembly

The SG factory tube installation drawing specifies a [

] ^{a,c,e}, to facilitate the tube weld to the cladding on the tubesheet face and it was omitted from the test. Following welding of the tube to the tubesheet, a full-length hydraulic expansion of the tube into the tubesheet is performed. The hydraulic expansion pressure range for the Model F SGs was approximately [] ^{a,c,e}. The majority of the test samples were expanded using a specified pressure of [] ^{a,c,e} to conservatively bound the lower expansion pressure limit used for SG fabrication.

The tube expansion tool used in the factory consisted of a pair of seals, spaced by a tie rod between them. The hydraulically expanded zone was positioned relative to the lower surface of the tubesheet, overlapping the upper end of the tack expanded region. It extended to within a short distance of the upper surface of the tubesheet. This produced a hydraulically expanded length of approximately [] ^{a,c,e} inch nominal tubesheet thickness. The majority of the test specimens were fabricated using [

] ^{a,c,e}. Previous test programs which employed a segmented approach to expansion confirmed the expectation that uniform results from one segment to the next would result. This approach produced the desired expansion pressures for a conservative length of [] ^{a,c,e} inch-expanded length being simulated. The remaining length of tube was expanded to the pressure at which the expansion bladder failed, usually between [] ^{a,c,e}. These samples are described as “Segmented Expansion” types. A tube expansion schematic is shown on Figure 6-2.

Data were also available from a small group of the test samples that had been previously fabricated using a [] ^{a,c,e} tool which had been fabricated expressly for such tests. These samples were described as “Full Depth Expansion” types. The expansion method with regard to the segmented or full length aspect does not have a bearing on the test results.

6.2.2 Model F Leakage Resistance Tests

The testing reported herein was performed according to a test procedure which outlined two types of leak tests as follows:

1. Model F elevated temperature primary-to-secondary leak tests were performed using an

[

] ^{a,c,e} These tests were performed following the room temperature primary-to-secondary side leak tests on the chosen samples. The test results showed a [

] ^{a,c,e}.

2. Model F room temperature primary-to-secondary side leak tests were performed on all test samples,

] ^{a,c,e}. These tests were performed following the elevated temperature primary-to-secondary side leak tests on the chosen samples.

6.2.2.1 Model F Leak Test Results

The elevated temperature leak tests on segmented expansion collars averaged approximately [

] ^{a,c,e}. (As a point of reference, there are approximately 75,000 drops in one gallon.) Leakage data were also recorded at room temperature conditions to provide input for the low contact pressure portion of the flow loss coefficient-versus-contact pressure correlation.

6.3 Loss Coefficient on Contact Pressure Regression

Loss coefficient values were calculated using the Darcy flow model discussed later in Section 9.2. The results are reported in Table 6-2 for the Model F. A logarithmic-linear (log-linear) regression and an uncertainty analysis were performed for the Model F SG data. Figure 6-6 provides a plot of the loss coefficient versus contact pressure with the linear regression trendline for the combined data represented as a thick, solid black line (this same plot was presented in Reference 5). The

regression trendline is represented by the log-linear relation,

$$\ln(K) = b_0 + b_1 P_c \quad (6-1)$$

where b_0 = the $\ln(K)$ intercept of the log-linear regression trendline, and,
 b_1 = the slope of the log-linear regression trendline.

The values obtained for the intercept and slope coefficients were []^{a,c,e} for Model F computations respectively. The []

^{a,c,e} In conclusion, the log-linear fit to the combined Model F loss coefficient data follow a relation of the form,

$$K = e^{b_0 + b_1 P_c} \quad (6-2)$$

The absolute leak rates *per se* are not used in the determination of B* and the confidence curve on the charts is provided for information only. Results of sensitivity studies using confidence limit values for the coefficients are discussed in Section 9.5. Since the B* value is based on the ratio of the SLB leak rate to the NOP leak rate it is not significantly sensitive to changes in the correlation slope or intercept.

Table 6-1. Model F Leak Test Program Matrix

a,c,e

Table 6-3. Model F Pullout Test Data

a,c,e

Table 6-4. Model F 0.25 Inch Displacement Data at 600°F

a,c,e

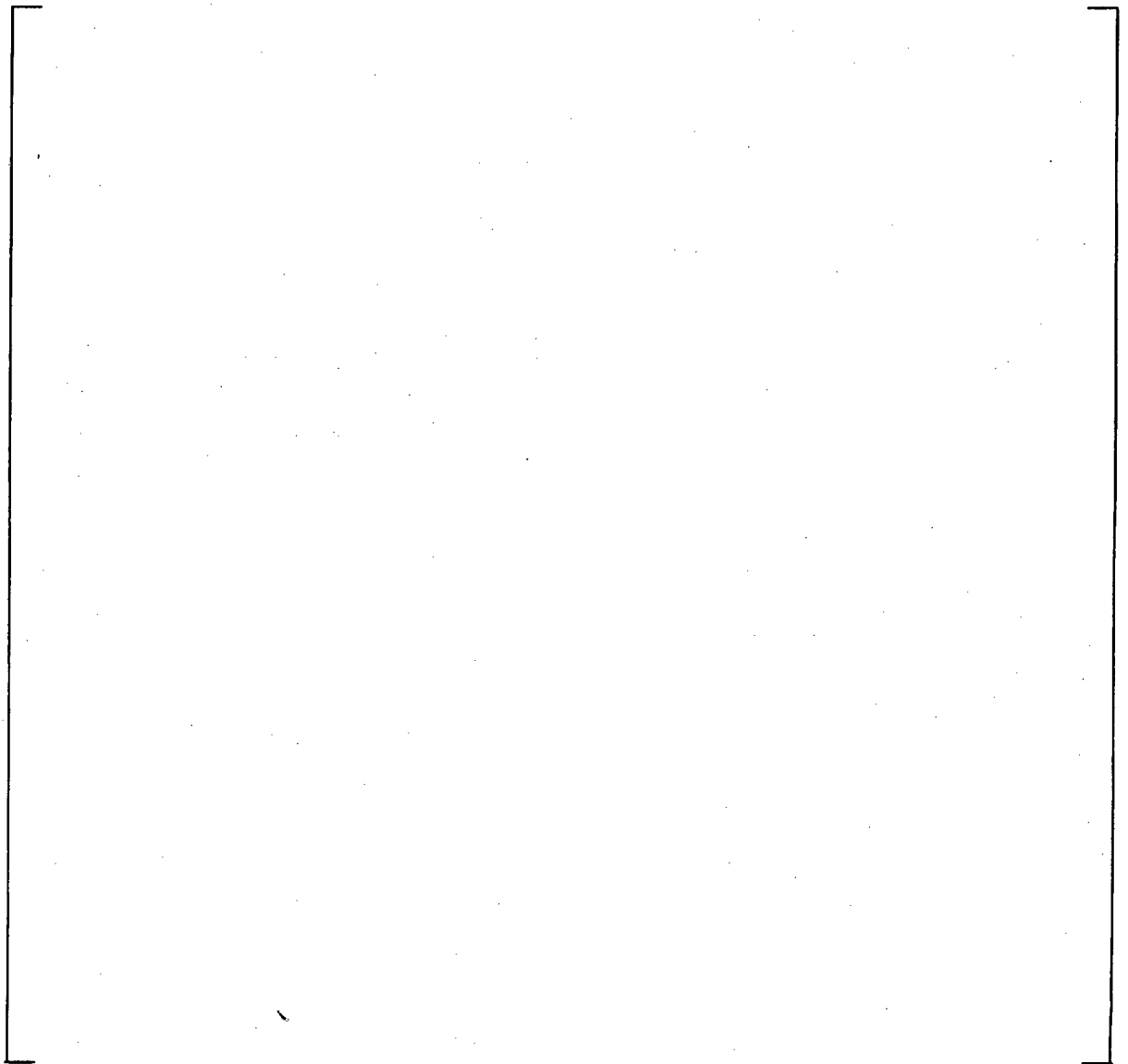


Figure 6-1. Example Leakage Test Schematic

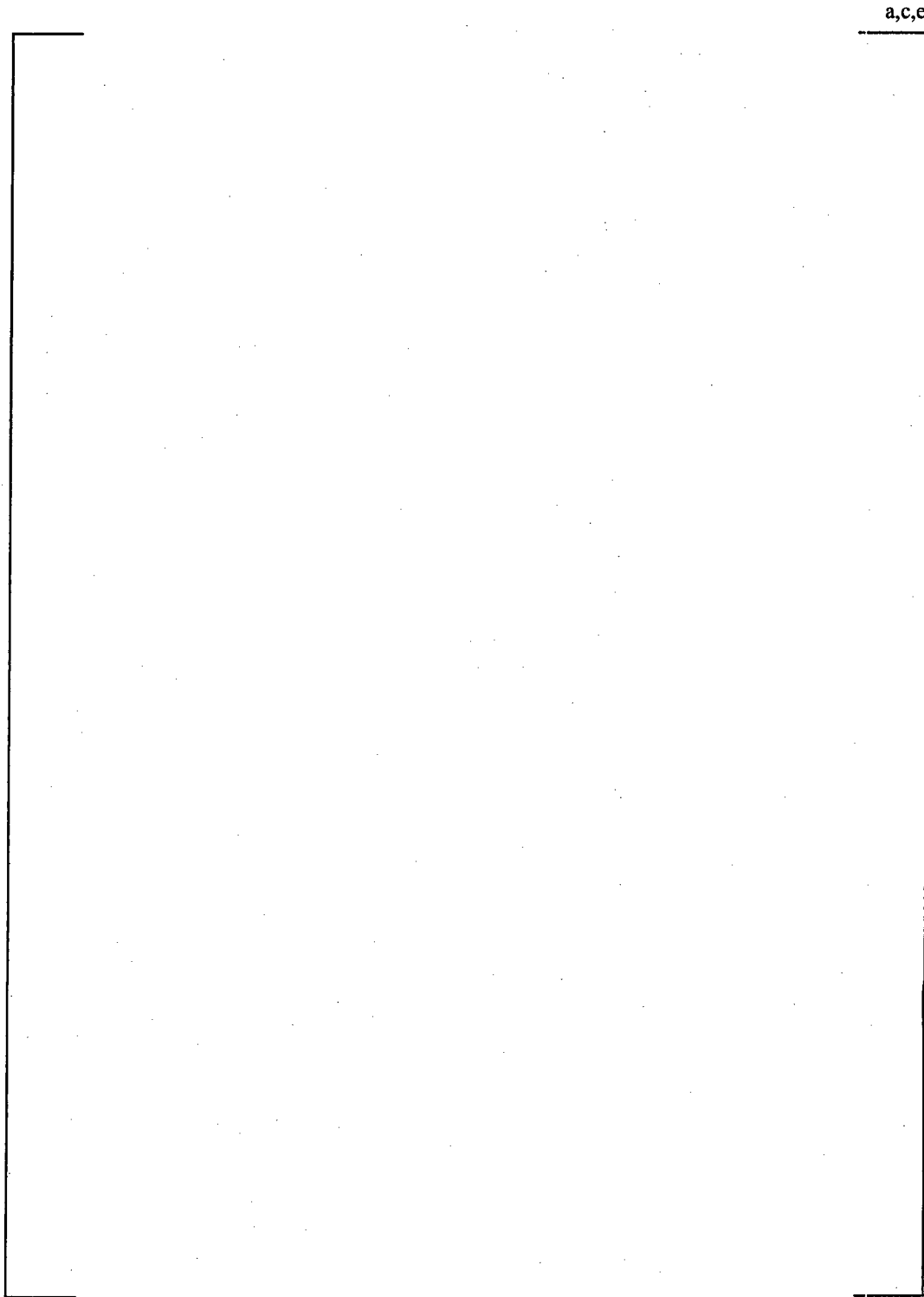


Figure 6-2. Example Tube Hydraulic Expansion Process Schematic

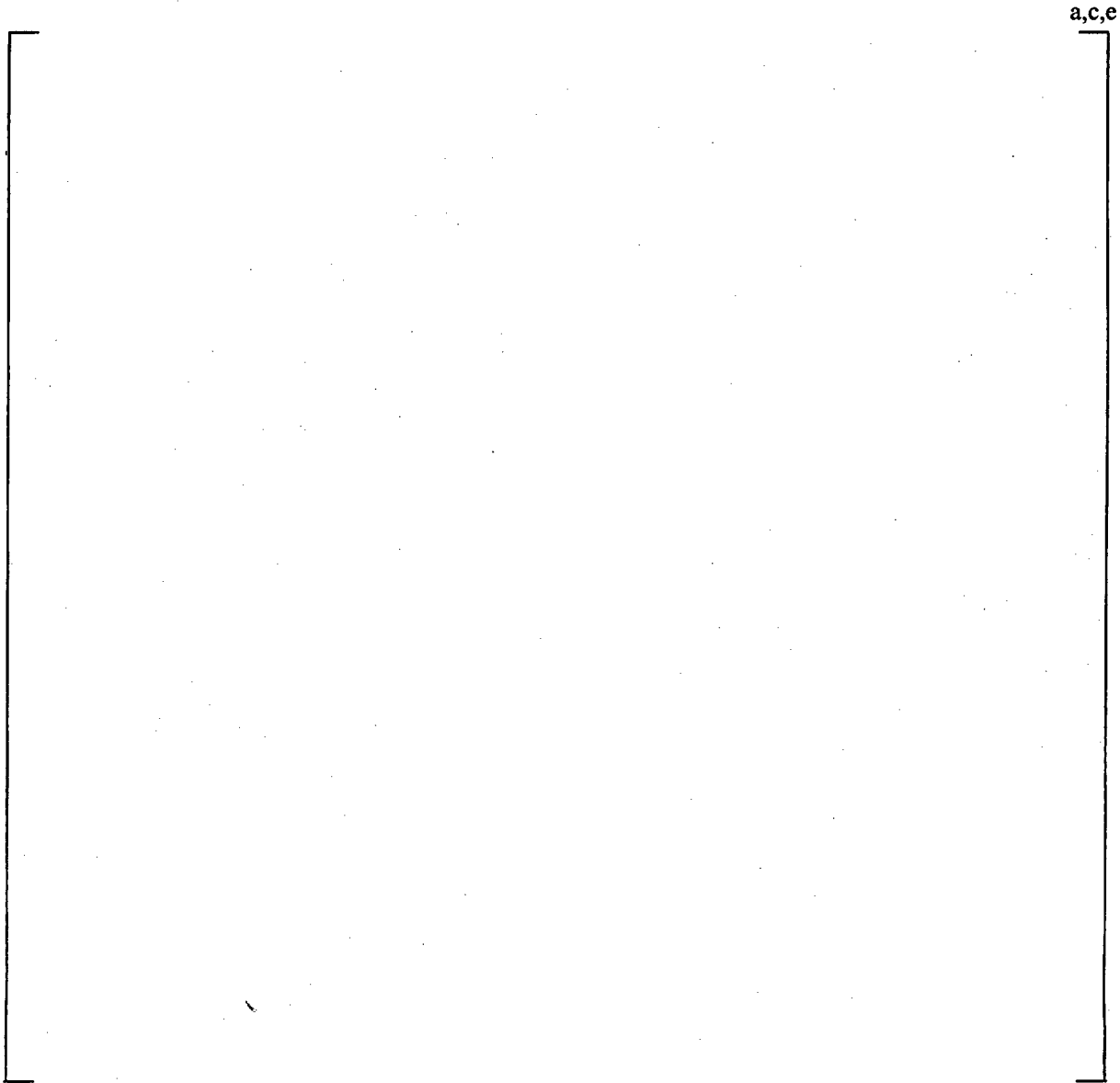


Figure 6-3. Example Tube Joint Leakage Test Configuration

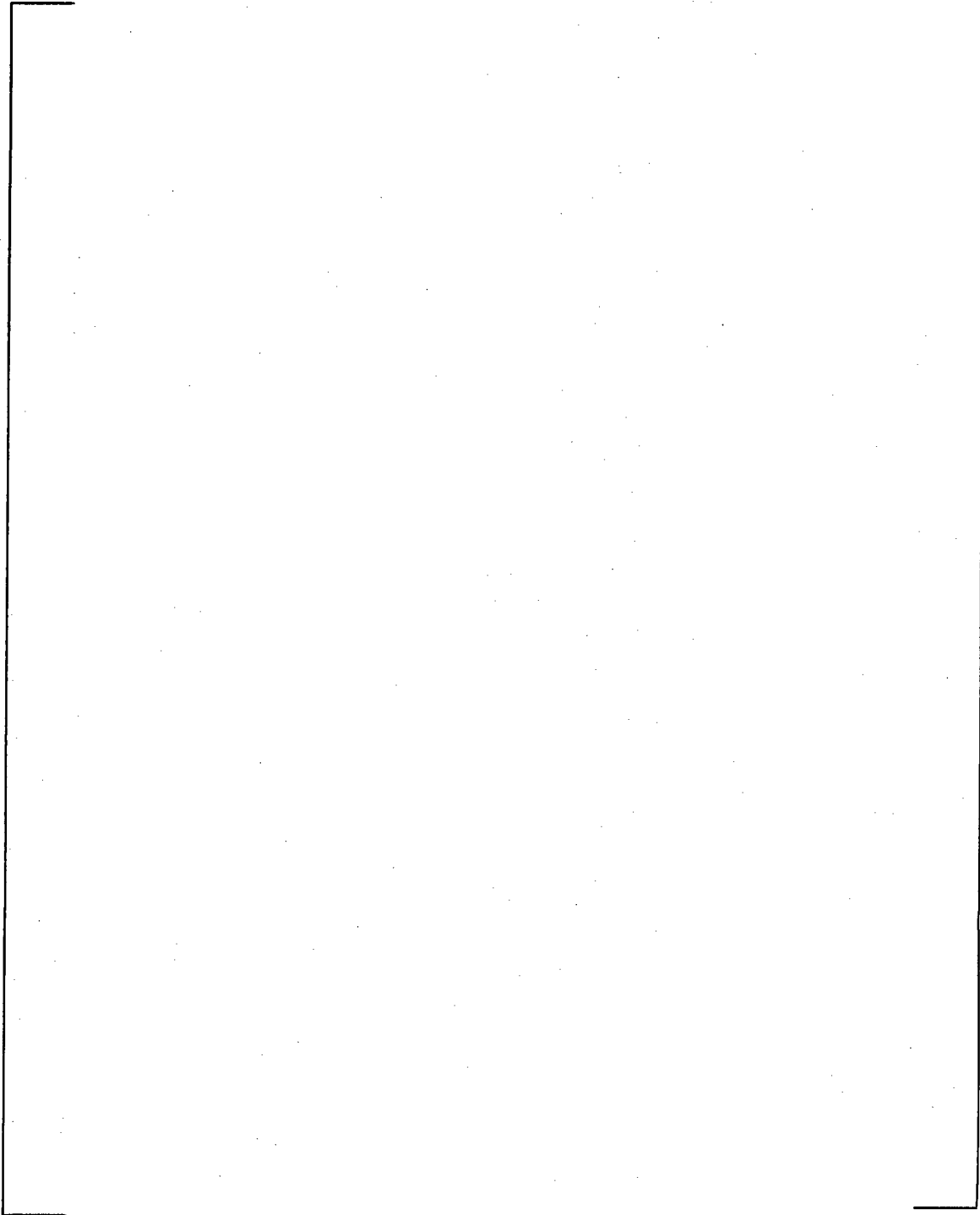
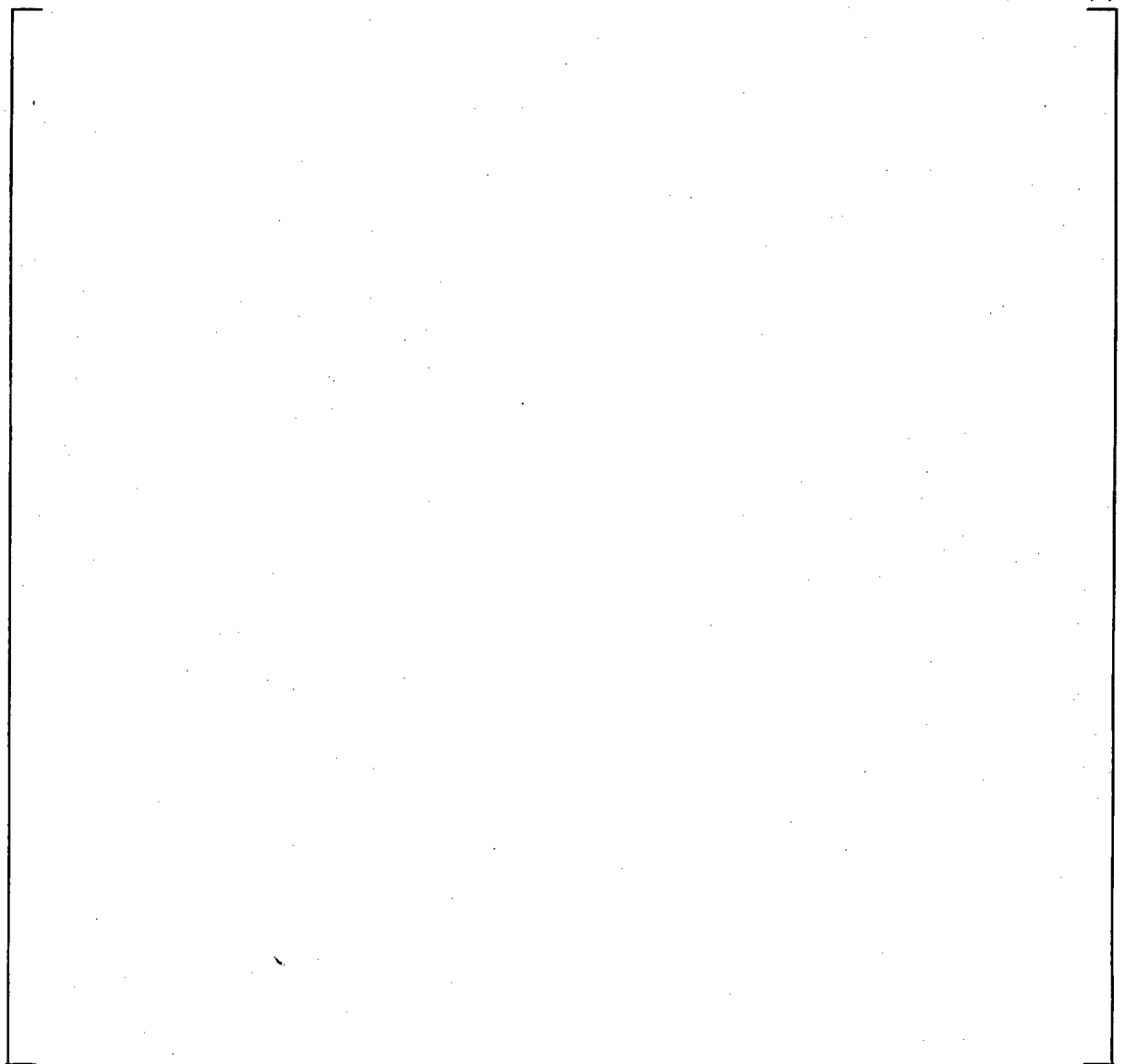


Figure 6-4. Schematic for the Test Autoclave Systems for Leak Rate Testing



a,c,e

Figure 6-5. Example Tube Joint Sample Pullout Test Configuration



Figure 6-6. Loss Coefficient Values for Model F Leak Rate Analysis

7.0 Structural Analysis of Tube-to-Tubesheet Joint

This section summarizes the structural aspects and analysis of the entire tube-to-tubesheet joint region. The tube end weld was originally designed as a pressure boundary structural element in accordance with the requirements of Section III of the ASME (American Society of Mechanical Engineers) Boiler and Pressure Vessel Code, Reference 11. The design and construction code for the Wolf Creek SGs was the 1971 edition with the Summer 1973 addenda. This means that there were no strength considerations made with regard to the expansion joint between the tube and the tubesheet, including the tack expansion regardless of whether it was achieved by rolling or Poisson expansion of a urethane plug.

An extensive empirical and analytical evaluation of the structural capability of the as-installed tube-to-tubesheet joints based on considering the weld to be absent was performed specifically for the Wolf Creek Model F SGs and the results are reported below. Typical Model F hydraulic expansion joints with lengths comparable to those being proposed in what follows for limiting specialized probe examination were tested for pullout resistance strength at temperatures ranging from 70 to 600°F. The results of the tests coupled with those from finite element evaluations of the effects of temperature and primary-to-secondary pressure on the tube-to-tubesheet interface loads have been used to determine the engagement lengths that would be sufficient to equilibrate the axial loads resulting from consideration of 3 times the normal operating and 1.4 times the limiting accident condition pressure differences (delineated in Section 2.0). Variation in required engagement length is a function of tube location, i.e., row and column, and decreases away from the center of the SG where the maximum value applies. The tubesheet bows, i.e., deforms, upward from the primary-to-secondary pressure difference and results in the tube holes becoming dilated above the neutral plane of the tubesheet, which is a little below the mid-plane because of the effect of the tensile membrane stress from the pressure loading. The amount of dilation is a maximum very near the radial center of the tubesheet (restricted by the divider plate) and diminishes with increasing radius outward. Moreover, the tube-to-tubesheet joint becomes tighter below the neutral axis and is a maximum at the bottom of the tubesheet⁵. In conclusion, the need for the weld is obviated by the interference fit between the tube and the tubesheet. Axial loads are not transmitted to the portion of the tube below the H* distance during operation or faulted conditions, by factors of safety of at least 3 and 1.4 respectively, including postulated loss of coolant accidents (LOCA), and inspection of the tube below the H* distance including the tube-to-tubesheet weld is not technically necessary. Also, even if the expansion joint were not present, there would be no effect on the strength of the weld from axial cracks, and tubes with circumferential cracks up to about 180° by 100% deep would have sufficient strength to meet the nominal ASME Code structural requirements, based on the margins of safety reported in Reference 12.

An examination of Table 7-6 through Table 7-10 illustrates that the holding strength of the tube-to-tubesheet joint in the vicinity of a depth of 11 inches is much greater than at the top of the

⁵ There is a small reversal of the bending stress beyond a radius of about 55 inches because the support ring prevents rotation and the hole dilation is at the bottom of the tubesheet.

tubesheet in the range of H^* as listed in Table 7-11. The radii reported in these tables were picked to conservatively represent the entire radial zones of consideration as defined on Figure 7-1. For example, Zone C has a maximum radius of 30.2 inches. However, in order to establish H^* values that were conservative throughout the zone, the tube location for which the analysis results were most severe above the neutral axis were reported, i.e., those values calculated for a tube at a radius of 4.02 inches. The values are everywhere conservative above the neutral surface of the tubesheet for tubes in Zone C. Likewise for tubes in Zone B under the heading 48.61 inches where the basis for the calculation was a tube at a radius of 34.4 inches. To illustrate the extreme conservatism associated with the holding strength of the joint at and below the neutral surface of the tubesheet, and to identify the proper tube radii for consideration the following is noted:

- In the center of the tubesheet the incremental holding strength in the 2.5 inch range from 8 to 10.5 inches below the top of the tubesheet during NOp is about 1260 lbf per inch. The performance criterion for $3 \cdot \Delta P$ is roughly met by the first 1.1 inch of engagement above the lower elevation. At a radius of 58 inches the corresponding length of engagement needed is about 1.1 inches.
- The corresponding values for steam line break conditions are 1.25 and 1.15 inches at radii of 4.02 and 58.3 inches respectively. In other words, while a value of 6.3 inches was determined for H^* from the top of the tubesheet⁶, a length of 1.15 to 1.25 inches would be sufficient at middle of the tubesheet.

7.1 Evaluation of Tubesheet Deflection Effects for Tube-to-Tubesheet Contact Pressure

A finite element model was developed for the Model F tubesheet, channel head, and shell region to determine the tubesheet hole dilations in the Wolf Creek SGs. [

tube.]^{a,c,e} loads in the

7.1.1 Material Properties and Tubesheet Equivalent Properties

The tubes in the Wolf Creek SGs were fabricated of A600TT material. Summaries of the applicable mechanical and thermal properties for the tube material are provided in Table 7-1. The tubesheets were fabricated from SA-508, Class 2a, material for which the properties are listed in Table 7-2. The shell material is SA-533 Grade A Class 2, and its properties are in Table 7-3. Finally, the channel head material is SA-216 Grade WCC, and its properties are in Table 7-4. The material properties were obtained from the ASME B&PV (Boiler and Pressure Vessel) Code, Reference 37.

⁶ A B^* value of about 6.8 inches will be specified in Table 9-2 for equal resistance during SLB and NOp.

The perforated tubesheet in the Model F channel head assembly is treated as an equivalent solid plate in the global finite element analysis. An accurate model of the overall plate behavior was achieved by using the concept of an equivalent elastic material with anisotropic properties. For square tubesheet hole patterns, the equivalent material properties depend on the orientation of loading with respect to the symmetry axes of the pattern. An accurate approximation was developed in Reference 31, where energy principles were used to derive effective average isotropic elasticity matrix coefficients for the in-plane loading. The average isotropic stiffness formulation gives results that are consistent with those using the Minimum Potential Energy Theorem, and the elasticity problem thus becomes axisymmetric. The solution for strains is sufficiently accurate for design purposes, except in the case of very small ligament efficiencies, which are not of issue for the evaluation of the SG tubesheet.

The stress-strain relations for the axisymmetric perforated part of the tubesheet are given by:

$$\begin{bmatrix} \sigma_R^* \\ \sigma_\theta^* \\ \sigma_z^* \\ \tau_{RZ}^* \end{bmatrix} = \begin{bmatrix} D_{11} & D_{12} & D_{13} & 0 \\ D_{21} & D_{22} & D_{23} & 0 \\ D_{31} & D_{32} & D_{33} & 0 \\ 0 & 0 & 0 & D_{44} \end{bmatrix} \begin{bmatrix} \epsilon_R^* \\ \epsilon_\theta^* \\ \epsilon_z^* \\ \gamma_{RZ}^* \end{bmatrix}$$

with the elasticity coefficients are calculated as:

$$\begin{aligned} D_{11} = D_{22} &= \frac{\bar{E}_p^*}{f(1+\bar{\nu}_p^*)} \left[1 - \frac{\bar{E}_p^*}{E_z^*} \nu^2 \right] + \frac{1}{2} \left[\bar{G}_p^* - \frac{\bar{E}_p^*}{2(1+\bar{\nu}_p^*)} \right] \\ D_{21} = D_{12} &= \frac{\bar{E}_p^*}{f(1+\bar{\nu}_p^*)} \left[\bar{\nu}_p^* + \frac{\bar{E}_p^*}{E_z^*} \nu^2 \right] - \frac{1}{2} \left[\bar{G}_p^* - \frac{\bar{E}_p^*}{2(1+\bar{\nu}_p^*)} \right] \\ D_{13} = D_{23} = D_{31} = D_{32} &= \frac{\bar{E}_p^* \nu}{f} \\ D_{33} &= \frac{E_z^*(1-\bar{\nu}_p^*)}{f} \text{ and } D_{44} = \bar{G}_z^* \\ \text{where } f &= 1 - \bar{\nu}_p^* - 2 \frac{\bar{E}_p^*}{E_z^*} \nu^2 \text{ and } \bar{G}_p^* = \frac{\bar{E}_d^*}{2(1+\bar{\nu}_d^*)}. \end{aligned}$$

Here,

- \bar{E}_p^* = Effective elastic modulus for in-plane loading in the pitch direction,
- E_z^* = Effective elastic modulus for loading in the thickness direction,
- $\bar{\nu}_p^*$ = Effective Poisson's ratio for in-plane loading in the pitch direction,
- \bar{G}_p^* = Effective shear modulus for in-plane loading in the pitch direction,
- \bar{G}_z^* = Effective modulus for transverse shear loading,
- \bar{E}_d^* = Effective elastic modulus for in-plane loading in the diagonal direction,
- $\bar{\nu}_d^*$ = Effective Poisson's ratio for in-plane loading in the diagonal direction, and,
- ν = Poisson's ratio for the solid material.

The tubesheet is a thick plate and the application of the pressure load results in a generalized plane strain condition. The pitch of the square, perforated hole pattern is 0.98 inches and nominal hole diameters are 0.703 inch. The ID of the tube after expansion into the tubesheet is taken to be about 0.625 inch based on an approximation of 1% thinning during installation associated with constant material volume. Equivalent properties of the tubesheet are calculated without taking credit for the stiffening effect of the tubes.

$$\text{Ligament Efficiency, } \eta = \frac{h_{\text{nominal}}}{P_{\text{nominal}}}$$

where: $h_{\text{nominal}} = P_{\text{nominal}} - d_{\text{maximum}}$
 $P_{\text{nominal}} = 0.980$ inches, the pitch of the square hole pattern
 $d_{\text{maximum}} = .706$ inches, the tube hole diameter

Therefore, $h_{\text{nominal}} = 0.2745$ inches (0.980-0.706), and $\eta = 0.2796$ when the tubes are not included. From Slot, Reference 32, the in-plane mechanical properties for Poisson's ratio of 0.3 are:

Property	Value
E_p^* / E	= 0.3977
ν_p^*	= 0.1630
E_d^* / E	= 0.2137
ν_d^*	= 0.5531
E^* / E	= 0.3057
ν^*	= 0.3580

where the subscripts p and d refer to the pitch and diagonal directions, respectively. These values are substituted into the expressions for the anisotropic elasticity coefficients given previously. In the global model, the X-axis corresponds to the radial direction, the Y-axis to the vertical or tubesheet thickness direction, and the Z-axis to the hoop direction. The directions assumed in the derivation of the elasticity coefficients were X- and Y-axes in the plane of the tubesheet and the Z-axis through the thickness. In addition, the order of the stress components in the WECAN/Plus (Reference 33) elements used for the global model is σ_{xx} , σ_{yy} , τ_{xy} , and σ_{zz} . The mapping between the Reference 31 equations and WECAN/+ is therefore:

Coordinate Mapping	
Reference 31	WECAN/+
1	1
2	4
3	2
4	3

Table 7-2 gives the modulus of elasticity, E, of the tubesheet material at various temperatures. Using the equivalent property ratios calculated above in the equations presented at the beginning of this section yields the elasticity coefficients for the equivalent solid plate in the perforated region of the tubesheet for the finite element model.

7.1.2 Finite Element Model

The analysis of the contact pressures utilizes conventional (thick shell equations) and finite element analysis techniques. A finite element analysis (FEA) model was developed for the Model F SG channel head/ tubesheet/ shell region in order to determine the tubesheet rotations. The elements used for the models of the channel head/ tubesheet/ shell region were the quadratic version of the 2-D axisymmetric isoparametric elements STIF53 and STIF56 of WECAN-Plus (Reference 33). The model for the Model F SG is shown on Figure 7-2.

The unit loads applied to this model are listed below:

Unit Load	Magnitude
Primary Side Pressure	1000 psi
Secondary Side Pressure	1000 psi
Tubesheet Thermal Expansion	500°F
Shell Thermal Expansion	500°F
Channel Head Thermal Expansion	500°F

The three temperature loadings consist of applying a uniform thermal expansion to each of the three component members, one at a time, while the other two remain at ambient conditions. The boundary conditions imposed for all five cases are: $UX = 0$ at all nodes on the centerline, and $UY = 0$ at one node on the lower surface of the tubesheet support ring. In addition, an end cap load was applied to the top of the secondary side shell for the secondary side pressure unit load equal to:

$$P_{endcap} = -\frac{R_i^2}{R_o^2 - R_i^2} P$$

where, R_i = Inside radius of secondary shell in finite element model = 64.69 in.
 R_o = Outside radius of secondary shell in finite element model = 68.0 in.
 P = Secondary pressure unit load = 1000 psi.

This procedure yielded displacements throughout the tubesheet for the unit loads.

7.1.3 Tubesheet Rotation Effects

Loads are imposed on the tube OD as a result of tubesheet rotations under pressure and temperature conditions. Previous calculations performed [

]^{a,c,e}.

The radial deflection, UR, at any point within the tubesheet is found by scaling and combining the unit load radial deflections at that location according to:

$$\left[\begin{array}{c} \text{**} \\ \dots \\ \dots \\ \dots \end{array} \right]^{a,c,e}$$

This expression is used to determine the radial deflections along a line of nodes at a constant axial elevation (e.g., top of the tubesheet) within the perforated area of the tubesheet. The expansion of a hole of diameter D in the tubesheet at a radius R is given by:

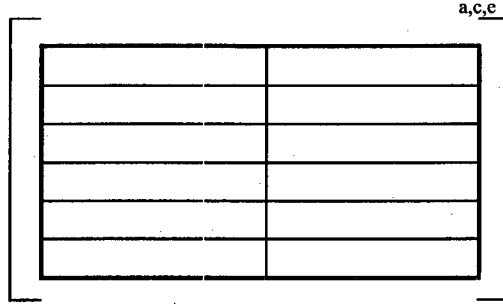
$$\left[\dots \right]^{a,c,e}$$

UR is available directly from the finite element results. dUR/dR may be obtained by numerical differentiation.

The maximum expansion of a hole in the tubesheet is in either the radial or circumferential direction. [

]^{a,c,e}

Where SF is a scale factor between zero and one. For the eccentricities typically encountered during tubesheet rotations, [^{a,c,e}]. These values are listed in the following table:



The data were fit to the following polynomial equation:

$$\left[\dots \right]^{a,c,c}$$

The hole expansion calculation as determined from the finite element results includes the effects of tubesheet rotations and deformations caused by the system pressures and temperatures. It does not include the local effects produced by the interactions between the tube and tubesheet hole. Standard thick shell equations, including accountability for the end cap axial loads in the tube (Reference 34), in combination with the hole expansions from above are used to calculate the contact pressures between the tube and the tubesheet.

The unrestrained radial expansion of the tube OD due to thermal expansion is calculated as:

$$\Delta R_t^{th} = c \alpha_t (T_t - 70)$$

and from pressure acting on the inside and outside of the tube as,

$$\Delta R_{to}^{pr} = \frac{P_i c}{E_t} \left[\frac{(2-\nu)b^2}{c^2-b^2} \right] - \frac{P_o c}{E_t} \left[\frac{(1-2\nu)c^2+(1+\nu)b^2}{c^2-b^2} \right],$$

- where:
- P_i = Internal primary side pressure, P_{pri} psi
 - P_o = External secondary side pressure, P_{sec} psi
 - b = Inside radius of tube = 0.33943 in.
 - c = Outside radius of tube = 0.382 in.
 - α_t = Coefficient of thermal expansion of tube, in/in/°F
 - E_t = Modulus of Elasticity of tube, psi
 - T_t = Temperature of tube, °F, and,
 - ν = Poisson's Ratio of the material.

The thermal expansion of the hole ID is included in the finite element results and does not have to be expressly considered in the algebra; however, the expansion of the hole ID produced by

pressure is given by:

$$\Delta R_{TS}^{pr} = \frac{P_1 c}{E_{TS}} \left[\frac{d^2 + c^2}{d^2 - c^2} + \nu \right],$$

where: E_{TS} = Modulus of Elasticity of tubesheet, psi
 d = Outside radius of cylinder which provides the same radial stiffness as the tubesheet, that is, []^{a,c,e}.

If the unrestrained expansion of the tube OD is greater than the expansion of the tubesheet hole, then the tube and the tubesheet are in contact. The inward radial displacement of the outside surface of the tube produced by the contact pressure is given by: (Note: The use of the term δ in this section is unrelated its potential use elsewhere in this report.)

$$\delta_t = \frac{P_2 c}{E_t} \left[\frac{c^2 + b^2}{c^2 - b^2} - \nu \right]$$

The radial displacement of the inside surface of the tubesheet hole produced by the contact pressure between the tube and hole is given by:

$$\delta_{TS} = \frac{P_2 c}{E_{TS}} \left[\frac{d^2 + c^2}{d^2 - c^2} + \nu \right]$$

The equation for the contact pressure P_2 is obtained from:

$$\delta_{to} + \delta_{TS} = \Delta R_{to} - \Delta R_{TS} - \Delta R_{ROT}$$

where ΔR_{ROT} is the hole expansion produced by tubesheet rotations obtained from finite element results. The ΔR 's are:

$$\Delta R_{to} = c\alpha_1(T_t - 70) + \frac{P_{pri} c}{E_t} \left[\frac{(2 - \nu)b^2}{c^2 - b^2} \right] - \frac{P_{sec} c}{E_t} \left[\frac{(1 - 2\nu)c^2 + (1 + \nu)b^2}{c^2 - b^2} \right]$$

$$\Delta R_{TS} = \frac{P_{sec} c}{E_{TS}} \left[\frac{d^2 + c^2}{d^2 - c^2} + \nu \right]$$

The resulting equation is:

$$\left[\text{Equation} \right]^{a,c,e}$$

For a given set of primary and secondary side pressures and temperatures, the above equation is solved for selected elevations in the tubesheet to obtain the contact pressures between the tube and tubesheet as a function of radius. The elevations selected ranged from the top to the bottom of the tubesheet. Negative “contact pressure” indicates a gap condition.

The OD of the tubesheet cylinder is equal to that of the cylindrical (simulate) collars (1.632 inches) designed to provide the same radial stiffness as the tubesheet, which was determined from a finite element analysis of a section of the tubesheet (References 35 and 36).

The tube inside and outside radii within the tubesheet are obtained by assuming a nominal diameter for the hole in the tubesheet (0.703 inch) and wall thinning in the tube equal to the average of that measured during hydraulic expansion tests. That thickness is 0.0396 inch for the tube. The following table lists the values used in the equations above, with the material properties evaluated at 600°F. (Note that the properties in the following sections are evaluated at the primary fluid temperature).

Thick Cylinder Equations Parameter	Value
b, inside tube radius, in.	0.3119
c, outside tube radius, in.	0.3515
d, outside radius of cylinder w/ same radial stiffness as TS, in.	[] ^{a,c,e}
α_t , coefficient of thermal expansion of tube, in/in °F	$7.83 \cdot 10^{-6}$
E_t , modulus of elasticity of tube, psi	$28.7 \cdot 10^6$
α_{TS} , coefficient of thermal expansion of tubesheet, in/in °F	$7.42 \cdot 10^{-6}$
E_{TS} , modulus of elasticity of tubesheet, psi	$26.4 \cdot 10^6$

7.1.4 Wolf Creek Contact Pressures

7.1.4.1 Normal Operating Conditions

The loadings considered in the analysis are based on an umbrella set of conditions as defined in References 31, 32 and 37. The current operating parameters from Reference 28 are used. The temperatures and pressures for normal operating conditions at Wolf Creek are bracketed by the following two cases:

Loading	Case 1 ⁽¹⁾	Case 2 ⁽²⁾
Primary Pressure	2235 psig	2235 psig
Secondary Pressure	792 psig	935 psig
Primary Fluid Temperature (T _{hot})	603.2°F	620.0°F
Secondary Fluid Temperature	519.3°F	538.4°F
⁽¹⁾ T _{hot} reduced.		
⁽²⁾ T _{max} maintained at 620°F.		

The primary pressure [

] ^{a,c,e}.

7.1.4.2 Faulted Conditions

Of the faulted conditions, Feedline Break (FLB) and Steamline Break (SLB) are the most limiting. FLB has a higher ΔP across the tubesheet, while the lower temperature of SLB results in less thermal tightening. Both cases are considered in this section.

Previous analyses have shown that FLB and SLB are the limiting faulted conditions, with tube lengths required to resist push out during a postulated loss of coolant accident (LOCA) typically less than one-fourth of the tube lengths required to resist pull out during FLB and SLB (References 34, 35 and 38). Therefore LOCA was not considered in this analysis.

7.1.4.3 Feedline Break

The temperatures and pressures for the FLB event at Wolf Creek are bracketed by the following two cases:

Loading	Case 1 ⁽¹⁾	Case 2 ⁽²⁾
Primary Pressure	2650 psig	2650 psig
Secondary Pressure	0 psig	0 psig
Primary Fluid Temperature (T _{hot})	579.2°F	596.0°F
Secondary Fluid Temperature	519.3°F	538.4°F
⁽¹⁾ T _{hot} reduced.		
⁽²⁾ T _{hot} maintained at a maximum value of 620°F.		

The FLB condition [

] ^{a,c,c}.

[

] ^{a,c,e}.

7.1.4.4 Steam Line Break

As a result of SLB, the faulted SG will rapidly blow down to atmospheric pressure, resulting in a large ΔP across the tubes and tubesheet. The entire flow capacity of the auxiliary feedwater system would be delivered to the dry, hot shell side of the faulted SG. The primary side re-pressurizes to the pressurizer safety valve set pressure. The pertinent parameters are listed below. The combination of parameters yielding the most limiting results is used.

Primary Pressure	=	2560 psig
Secondary Pressure	=	0 psig
Primary Fluid Temperature (T_{hot})	=	420°F
Secondary Fluid Temperature	=	260°F

For this set of primary and secondary side pressures and temperatures, the equations derived in Section 7.2 below are solved for the selected elevations in the tubesheet to obtain the contact pressures between the tube and tubesheet as a function of tubesheet radius for the hot leg.

7.1.4.5 Summary of FEA Results for Tube-to-Tubesheet Contact Pressures

For Wolf Creek, the contact pressures between the tube and tubesheet for various plant conditions are listed in Table 7-5 and plotted versus radius on Figure 7-3 through Figure 7-7. The application of these values to the determination of the required engagement length is discussed in Section 7.2.

7.2 Determination of Required Engagement Length of the Tube in the Tubesheet

The elimination of a portion of the tube within the tubesheet from the in-service inspection (ISI) requirement constitutes a change in the location of the pressure boundary. The technical justification of the omission of the lower portion of the tube from examination relies on knowledge of the tube-to-tubesheet interference fit contact pressure at all elevations in the tube joint. In order to maintain consistency with other reports on this subject, the required length of engagement of the tube in the tubesheet to resist tube end-cap loads associated with the structural performance criteria is designated as H^* . This length is based on structural requirements only and does not include any consideration of the potential leak rate, except perhaps in a supporting role with regard to the leak rate expectations relative to normal operating conditions. The contact pressure is used to calculate the magnitude of the force resisting pullout of the tube from the tubesheet over the H^* length. It is

also used in estimating the impact of changes in the contact pressure on potential primary-to-secondary leak rate during postulated accident conditions.

The end cap loads to be resisted during NOp and faulted conditions are:

$$\begin{aligned}\text{Normal (maximum): } & \pi \cdot (2235-792) \cdot (0.703)^2 / 4 = 560.10 \text{ lbs.} \\ \text{Faulted (FLB): } & \pi \cdot 2650 \cdot (0.703)^2 / 4 = 1028.60 \text{ lbs.} \\ \text{Faulted (SLB): } & \pi \cdot 2560 \cdot (0.703)^2 / 4 = 993.67 \text{ lbs.}\end{aligned}$$

Seismic loads have also been considered, but they are not significant in the tube joint region of the tubes. The normal operation load is multiplied by a factor of 3 and the faulted condition loads by a factor of 1.4 to obtain the associated structural performance criteria.

The tube-to-tubesheet contact pressure consists of the residual from the installation of the tube in the tubesheet plus the added effects discussed in Section 9.0 with regard to internal pressure in the tube, the differences in thermal expansion and tubesheet rotation effects. The residual contact pressure from the tube installation was evaluated semi-empirically. It was determined by test for the as-fabricated condition and then analytically projected to the pertinent plant conditions. The tests involved pullout testing of tube-in-tubesheet specimens using thick collars to simulate the tubesheet as described in Section 6.1.

The initial element in estimating the strength of the tube-to-tubesheet joint during normal operation or postulated accident conditions is the residual strength of the joint stemming from the expansion preload due to the manufacturing process, i.e., hydraulic expansion. During operation the preload increases because the thermal expansion of the tube is greater than that of the tubesheet and because a portion of the internal pressure in the tube is transmitted to the interface between the tube and the tubesheet. However, the tubesheet bows upward leading to a dilation of the tubesheet holes at the top of the tubesheet and a contraction at the bottom of the tubesheet when the primary-to-secondary pressure difference is positive. The dilation of the holes acts to reduce the contact pressure between the tubes and the tubesheet. The H^* lengths are based on the pullout resistance associated with the net contact pressure during normal or accident conditions. The calculation of the residual strength involves a conservative approximation that the strength is uniformly distributed along the entire length of the tube. This leads to a lower bound estimate of the strength for the determination of H^* .

For the partial-length RPC evaluation, tube-to-tubesheet contact pressure was calculated [

] ^{a,c,e}

The force resisting pullout acting on a length of a tube between elevations h_1 and h_2 is given by:

$$F_i = (h_2 - h_1)F_{HE} + \mu \pi d \int_{h_1}^{h_2} P dh$$

where: F_{HE} = Resistance per length to pull out due to the installation hydraulic expansion,
 P = Contact pressure acting over the incremental length segment dh , and,
 μ = Coefficient of friction between the tube and tubesheet, conservatively assumed to be 0.2 for the pullout analysis to determine H^* .

The contact pressure is assumed to vary linearly between adjacent elevations in the top part of Table 7-6 through Table 7-10, so that between elevations L_1 and L_2 ,

$$P = P_1 + \frac{(P_2 - P_1)}{(L_2 - L_1)}(h - L_1)$$

or,

$$\left[\begin{array}{c} \text{a,c,e} \\ \\ \\ \\ \end{array} \right]$$

so that,

$$\left[\begin{array}{c} \\ \\ \\ \\ \end{array} \right] \text{a,c,e}$$

The latter equation was used to accumulate the force resisting pullout from the top of the tubesheet to each of the elevations listed in the lower parts of Table 7-6 through Table 7-10. The above equation is also used to find the minimum contact lengths needed to meet the pullout force requirements; a summary for the various zones is provided in Table 7-11.

The top part of Table 7-8 lists the contact pressures through the thickness at each of the radial sections for the SLB faulted condition. The last parameter row, " $h(0)$," of the central portion of the table lists the maximum tubesheet elevation at which the contact pressure is greater than or equal to zero. The above equation is used to accumulate the force resisting pull out from the top of the tubesheet to each of the elevations listed in the lower part of Table 7-8. In Zone C for example, this length is 6.23 inches for the $1.4 \cdot \Delta P_{SLB}$ performance criterion which corresponds to a pullout force of 1391 lbs in the hot leg. The minimum contact length needed to meet the pullout force requirement of 1440 lbs for the Faulted (FLB) condition is less as is shown in Table 7-9 and Table 7-10. The H^* calculations for each loading condition at each of the radii considered are summarized in Table 7-11. The H^* results for each zone are summarized in Table 7-12. Therefore, the bounding condition for the determination of the H^* length is the SLB performance criterion.

In Zone D, The SLB performance criterion is controlling and the minimum contact length is 6.32 and 6.64 inches during a postulated SLB event for the hot and cold legs respectively. A summary for each of the zones is provided in Table 7-12. The smallest value occurs in Zone A where the tubesheet holes experience minimum dilation from the primary-to-secondary pressure difference.

Table 7-1. Summary of Material Properties Alloy 600 Tube Material							
Property	Temperature (°F)						
	70	200	300	400	500	600	700
Young's Modulus (psi·10 ⁶)	31.00	30.20	29.90	29.50	29.00	28.70	28.20
Thermal Expansion (in/in/°F·10 ⁻⁶)	6.90	7.20	7.40	7.57	7.70	7.82	7.94
Density (lb-sec ² /in ⁴ ·10 ⁻⁴)	7.94	7.92	7.90	7.89	7.87	7.85	7.83
Thermal Conductivity (Btu/sec-in-°F·10 ⁻⁴)	2.01	2.11	2.22	2.34	2.45	2.57	2.68
Specific Heat (Btu-in/lb-sec ² -°F)	41.2	42.6	43.9	44.9	45.6	47.0	47.9

Table 7-2. Summary of Material Properties for SA-508 Class 2a Tubesheet Material							
Property	Temperature (°F)						
	70	200	300	400	500	600	700
Young's Modulus (psi·10 ⁶)	29.20	28.50	28.00	27.40	27.00	26.40	25.30
Thermal Expansion (in/in/°F·10 ⁻⁶)	6.50	6.67	6.87	7.07	7.25	7.42	7.59
Density (lb-sec ² /in ⁴ ·10 ⁻⁴)	7.32	7.30	7.29	7.27	7.26	7.24	7.22
Thermal Conductivity (Btu/sec-in-°F·10 ⁻⁴)	5.49	5.56	5.53	5.46	5.35	5.19	5.02
Specific Heat (Btu-in/lb-sec ² -°F)	41.9	44.5	46.8	48.8	50.8	52.8	55.1

Table 7-3. Summary of Material Properties SA-533 Grade A Class 2 Shell Material							
Property	Temperature (°F)						
	70	200	300	400	500	600	700
Young's Modulus (psi·10 ⁶)	29.20	28.50	28.00	27.40	27.00	26.40	25.30
Thermal Expansion (in/in/°F·10 ⁻⁶)	7.06	7.25	7.43	7.58	7.70	7.83	7.94
Density (lb-sec ² /in ⁴ ·10 ⁻⁴)	7.32	7.30	7.283	7.265	7.248	7.23	7.211

Table 7-4. Summary of Material Properties SA-216 Grade WCC Channelhead Material							
Property	Temperature (°F)						
	70	200	300	400	500	600	700
Young's Modulus (psi·10 ⁶)	29.50	28.80	28.30	27.70	27.30	26.70	25.50
Thermal Expansion (in/in/°F·10 ⁻⁶)	5.53	5.89	6.26	6.61	6.91	7.17	7.41
Density (lb-sec ² /in ⁴ ·10 ⁻⁴)	7.32	7.30	7.29	7.27	7.26	7.24	7.22

Table 7-10. Cumulative Forces Resisting Pull Out from the TTS Wolf Creek
 FLB Conditions, $T_{hot} = 620^{\circ}\text{F}$

a,c,e

**Table 7-12. H* Summary Table
Structural Criteria Required Engagement**

Zone	Limiting Loading Condition	Engagement from TTS (inches)	
		Hot Leg	Cold Leg
A	$3 \cdot \Delta P_{\text{NOP}}^{(1,2)}$	2.16 ⁽³⁾	2.29 ^(3,4)
B	$1.4 \cdot \Delta P_{\text{SLB}}^{(1,2)}$	4.26 ⁽³⁾	4.54 ⁽³⁾
C	$1.4 \cdot \Delta P_{\text{SLB}}^{(1,2)}$	6.53 ⁽³⁾	6.83 ⁽³⁾
D	$1.4 \cdot \Delta P_{\text{SLB}}^{(1,2)}$	6.62 ⁽³⁾	6.94 ⁽³⁾

Notes:

1. Seismic loads have been considered and are not significant in the tube joint region (Reference 12).
2. The scenario of tubes locked at support plates is not considered to be a credible event in Model F SGs as they are manufactured with stainless steel support plates. However, conservatively assuming that the tubes become locked at 100% power conditions, the maximum force induced in an active tube as the SG cools to room temperature is [

$$]^{a,c,e}$$
3. 0.3 inches was added to the H* values to account for the BET location relative to the TTS.
4. $1.4 \cdot \Delta P_{\text{FLB}}$ conditions.
5. B* requirements for leak rate are provided in Table 9-2.



Figure 7-1. Definition of H* Zones.
(Zone D is the most inboard and Zone A the most outboard.)

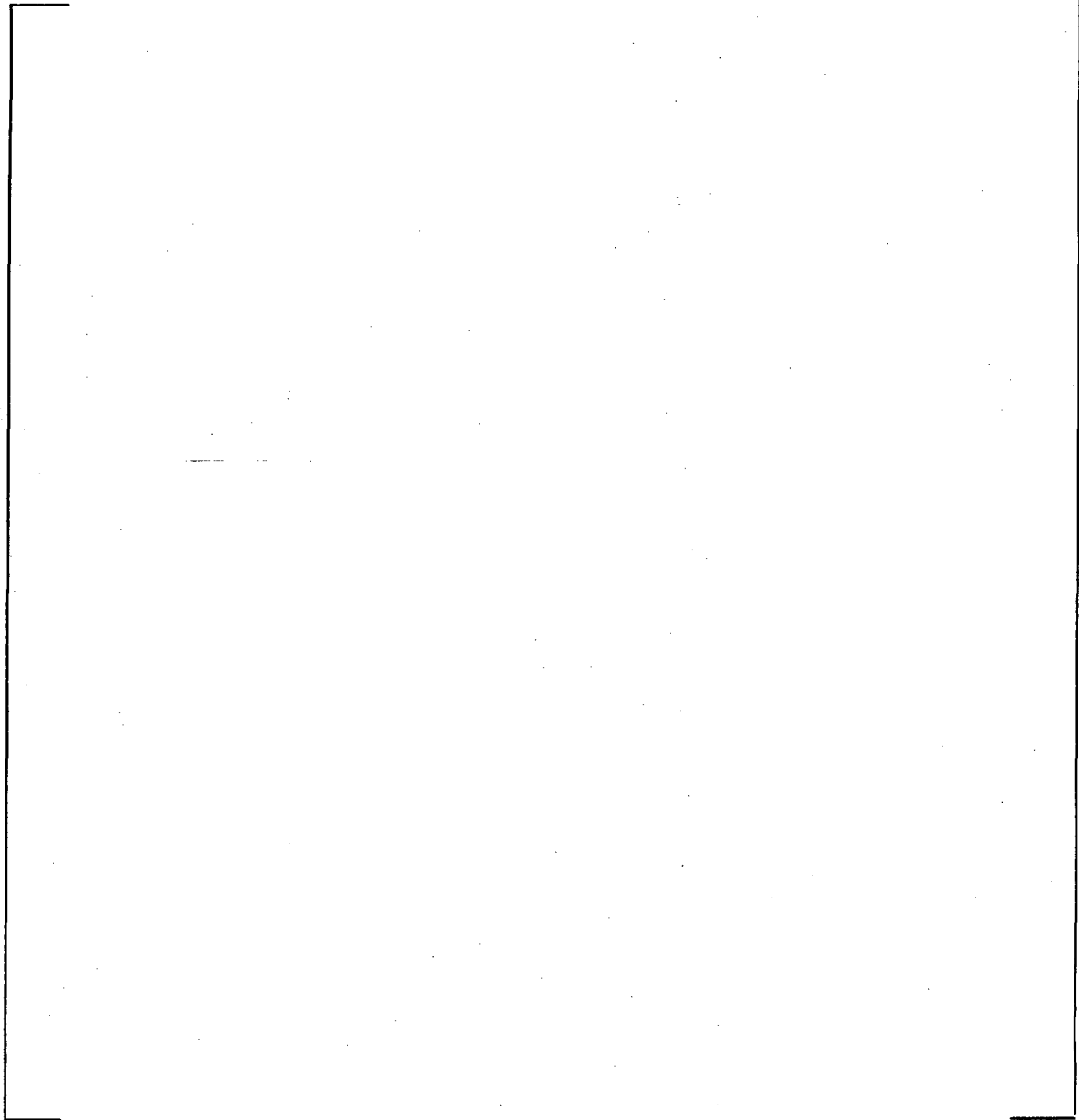


Figure 7-2. Finite Element Model of Model F Tubesheet Region

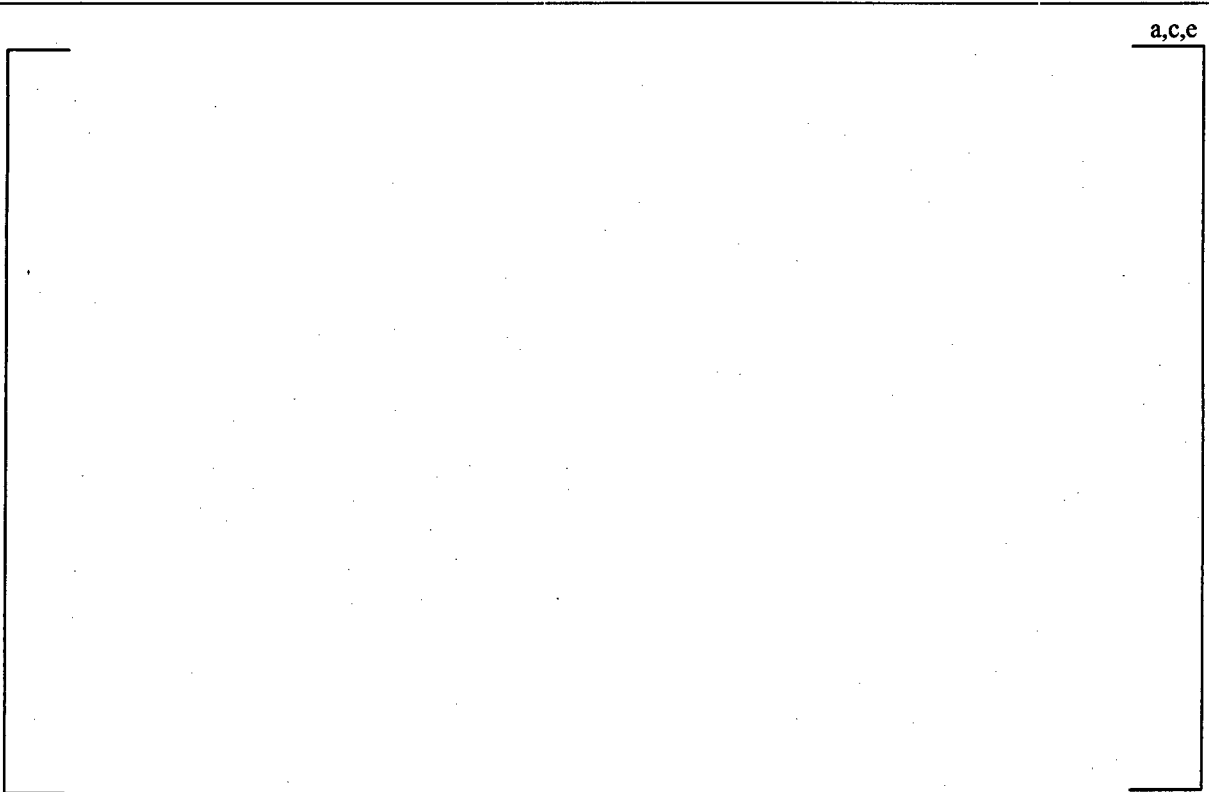


Figure 7-3. Contact Pressures for NOp at Wolf Creek, Reduced T_{hot} , $P_{sec} = 792$ psig



Figure 7-4. Contact Pressures for NOp at Wolf Creek, $T_{hot} = 620^{\circ}\text{F}$, $P_{sec} = 935$ psig



Figure 7-5. Contact Pressures for SLB Faulted Condition at Wolf Creek



Figure 7-6. Contact Pressures for FLB Condition at Wolf Creek, Reduced T_{hot}



Figure 7-7. Contact Pressures for FLB Condition at Wolf Creek, $T_{hot} = 620^{\circ}\text{F}$

This page intentionally blank.

8.0 Leak Rate Analysis of Cracked Tube-to-Tubesheet Joints

This section of the report presents a discussion of the leak rate expectations from axial and circumferential cracking confined to the tube-to-tubesheet joint region, including the tack expansion region, the tube-to-tubesheet welds and areas where degradation could potentially occur, due to bulges and overexpansions for example, within the tube at a distance at or below say 10 inches from the top of the tubesheet. Although the welds are not part of the tube per the technical specifications, consideration is given in deference to the discussions of the NRC staff in Information Notice 2005-09 and Generic Letter 2004-01, and References 2 and 13 respectively. It is noted that the methods discussed below support a permanent change to the Wolf Creek Technical Specification. With regard to the inherent conservatism embodied in the application of any predictive methods it is noted that the presence of cracking was not confirmed because removal of a tube section was not performed at Catawba 2 or Vogtle 1. This discussion was previously documented in Reference 5 in order to support a one-cycle omission of inspecting the lower 4 inches of the tube within the tubesheet.

8.1 The Bellwether Principle for Normal Operation to Steam Line Break Leak Rates

From an engineering expectation standpoint, if there is no meaningful primary-to-secondary leakage during normal operation, there should likewise be no meaningful leakage during postulated accident conditions from indications located approximately below the mid-plane of the tubesheet. The rationale for this is based on consideration of the deflection of the tubesheet with attendant dilation and diminution (expansion and contraction) of the tubesheet holes. In effect, the leakage flow area depends on the contact pressure between the tube and tubesheet and would be expected to decrease during postulated accident conditions below some distance from the top of the tubesheet. The primary-to-secondary pressure difference during normal operation is on the order of 1200 to 1400 psi, while that during a postulated accident, e.g., steam line and feed line break, is on the order of 2560 to 2650 psi.⁷ Above the neutral plane of the tubesheet the tube holes tend to experience a dilation due to pressure induced bow of the tubesheet. This means that the contact pressure between the tubes and the tubesheet would diminish above the neutral plane in the central region of the tubesheet at the same time as the driving potential would increase. Therefore, if there was leakage through the tube-to-tubesheet crevice during normal operation from a through-wall tube indication, that leak rate could be expected to increase during postulated accident conditions. Based on early NRC staff queries regarding the leak rate modeling code associated with calculating the expected leak rate, see Reference 5 for example, it was expected that efforts to license criteria based on estimating the actual leak rate as a function of the contact pressure during faulted conditions on a generic basis would be problematic.

As noted, the tube holes diminish in size below the neutral plane of the tubesheet because of the upward bending and the contact pressure between the tube and the tubesheet increases. When the differential pressure increases during a postulated faulted event the increased bow of the tubesheet

⁷ The differential pressure could be on the order of 2405 psi if it is demonstrated that the power operated relief valves will be functional.

leads to an increase in the tube-to-tubesheet contact pressure, increasing the resistance to flow. Thus, while the dilation of the tube holes above the neutral plane of the tubesheet presents additional analytic problems in estimating the leak rate for indications above the neutral plane, the diminution of the holes below the neutral plane presents definitive statements to be made with regard to the trend of the leak rate, hence, the bellwether principle. Independent consideration of the effect of the tube-to-tubesheet contact pressure leads to similar conclusions with regard to the opening area of the cracks in the tubes, thus further restricting the leak rate beyond that through the interface between the tube and the tubesheet.

In order to accept the concept of normal operation being a bellwether for the postulated accident leak rate for indications above the neutral plane of the tubesheet, the change in leak rate had to be quantified using a somewhat complex, physically sound model of the thermal-hydraulics of the leak rate phenomenon. This is not necessarily the case for cracks considered to be present below the neutral plane of the tubesheet. This is because a diminution of the holes takes place during postulated accident conditions below the neutral plane relative to normal operation. For example, at a radius of a little more than 30 inches from the center of the SG and 10.5 inches from the TTS, the contact pressure during normal operation is calculated to be about 1072 to 1157 psi⁸, see the third contact pressure column in Table 7-7 and Table 7-6 respectively, while the contact pressure during a postulated SLB would be on the order of 1670 psi, Table 7-8, and during a postulated FLB would be on the order of 2029 to 2075 psi at the bottom of the tubesheet, Table 7-9 and Table 7-10 respectively.

Note: The radii specified in the heading of the tables are the maximum values for the respective zones analyzed, hence the contact pressures in the center column correspond to the radius specified for the left column, etc. The leftmost column lists the contact pressure values for a radius of 4.02 inches, but is used to a radius of 12 inches, etc. Also, the values tabulated do not include the calculated residual preload from the tube installation, which is not necessary for this comparison.

The analytical model for the flow through the crevice, the Darcy equation for flow through porous media, indicates that flow would be expected to be proportional to the differential pressure. Thus, a doubling of the leak rate could be predicted if the change in contact pressure between the tube and the tubesheet were ignored. Examination of the correlation on Figure 6-6 indicates that the crevice resistance to flow per unit length (the loss coefficient) would increase during a postulated SLB event.

The leak rate from a crack located within the tubesheet is governed by the crack opening area, the resistance to flow through the crack, and the resistance to flow provided by the tube-to-tubesheet joint. The path through the tube-to-tubesheet joint is also frequently referred to as a crevice, but is not to be confused with the crevice left at the top of the tubesheet from the expansion process. The presence of the joint makes the flow from cracks within the tubesheet much different from the flow to be expected from cracks outside of the tubesheet. The tubesheet prevents outward

deflection of the flanks of cracks, a more significant effect for axial than for circumferential cracks, which is a significant contributor to the opening area presented to the flow. In addition, the restriction provided by the tubesheet greatly restrains crack opening in the direction perpendicular to the flanks regardless of the orientation of the cracks. The net effect is a large, almost complete restriction of the leak rate when the tube cracks are within the tubesheet.

The leak path through the crack and the crevice is very tortuous. The flow must go through many turns within the crack in order to pass through the tube wall, even though the tube wall thickness is relatively small. The flow within the crevice must constantly change direction in order to follow a path that is formed between the points of hard contact between the tube and the tubesheet as a result of the differential thermal expansion and the internal pressure in the tube. It is likely that there is both mechanical dispersion and molecular diffusion taking place. The net result is that the flow is best described as primary-to-secondary weepage. At its base, the expression used to predict the leak rate from tube cracks through the tube-to-tubesheet crevice is the Darcy expression for flow rate, Q , through porous media, i.e.,

$$Q = \frac{1}{K\mu} \frac{dP}{dz} \quad (8-1)$$

where μ is the viscosity of the fluid, P is the driving pressure, z is the physical dimension in the direction of the flow, and K is the "loss coefficient" which can also be termed the flow resistance if the other terms are taken together as the driving potential. The loss coefficient is found from a series of experimental tests involving the geometry of the particular tube-to-tubesheet crevice being analyzed, including factors such as surface finish, and then applied to the cracked tube situation.

If the leak rate during normal operation was 0.05 gpm (about 75 gpd), the postulated accident condition leak rate would be on the order of 0.1 gpm if only the change in differential pressure were considered; however, the estimate would be reduced if the increase in contact pressure between the tube and the tubesheet were to be included during a postulated steam line break event. An examination of the contact pressures as a function of depth in the tubesheet from the finite element analyses of the tubesheet as reported in Table 7-6 through Table 7-10 shows that the bellwether principle applies to a significant extent to all indications below the neutral plane of the tubesheet, and may apply to somewhat higher elevations. At the central plane of the tubesheet, the increase in contact pressure shown on Figure 8-4 is more on the order of 500 to 600 psi relative to that during NOP for all tubes regardless of radius. Still, the fact that the contact pressure increases means that the SLB leak rate would be expected to be bounded by no more than a factor of two relative to normal operation. The flow resistance would be expected to increase at a rate greater than that of the contact pressure and the increase in driving pressure would be mostly offset by the increase in the resistance of the joint.

⁸ The column headed 48.61 inches includes the range of $30 < R \leq 48.61$ inches.

The numerical results from the finite element analyses are presented on Figure 8-1 at the bottom of the tubesheet. A comparison of the contact pressure during postulated SLB conditions relative to that during NOP is also provided for depths of 16.9, 12.6, 10.5, 8.25, and 6.0 inches below the top of the tubesheet. The observations are discussed in what follows:

- At the bottom of the tubesheet, Figure 8-1, the contact pressure increases by 1679 psi near the center of the tubesheet, exhibits no change at a radius of about 55 inches, and diminishes by 424 psi at the extreme periphery, a little less than 61 inches from the center.
- At 16.9 inches below the top of the tubesheet (about 4.13 inches from the bottom of the tubesheet) the contact pressure increases by about 1249 psi at the center to a minimum of about 332 psi at a radius of 56 inches, Figure 8-2. The contact pressure during a SLB is everywhere greater than that during NOP. The influence of the channelhead and shell at the periphery causes the deformation to become non-uniform near the periphery.
- At a depth of 12.6 inches, Figure 8-3, the contact pressure increase ranges from a maximum of 753 psi near the center of the tubesheet to 543 psi at a radius of about 51 inches as shown on Figure 8-3.
- At roughly the neutral surface, about 10.5 inches, Figure 8-4, the contact pressure during SLB is uniformly greater than that during normal operation by about 533 psi (ranging from 513 to 619 psi traversing outward).
- At a depth of 8.25 inches from the TTS, Figure 8-5, the contact pressure increases by about 266 psi near the center of the TS to a maximum increase of 623 psi near the periphery.
- At a depth of about 6 inches from the TTS, Figure 8-6, the contact pressure increases by about 9 psi at the center of the TS, i.e., is invariant, and increases by 610 psi near the periphery.
- Although not depicted, the contact pressure at a depth of 4 inches decreases by 232 psi at 6 inches from the center of the tubesheet, exhibits no change at a radius of 29 inches, and increases by about 600 psi at a radius of 58 inches.

The absolute value of the contact pressure is not as important as the change in contact pressure because the parameter of interest in applying the B* criteria is the relative leak rate between NOP and SLB conditions. The analysis results indicate that there is an axial location within the tubesheet as a function of radius from the center where the contact pressure is invariant between NOP and SLB. The analysis results discussed in the next section include a plot of the invariant elevation for the Wolf Creek SGs (Figure 9-11). The distribution of the contact pressure would decrease near the TTS in the central region. Thus, it would not be sufficient to simply use an arbitrary depth value and suppose that the leak rate would be relatively unchanged even if the pressure potential difference were the same without further analysis. However, the fact that the

contact pressure generally increases below that elevation indicates that the leak rate would be relatively unaffected for indications a little deeper into the tubesheet.

The leak rate from any indication is determined by the total resistance of the crevice from the elevation of the indication to the top of the tubesheet in series with the resistance of the crack itself, which is also expected to increase with contact pressure (The effect of hoop compression on axial cracks would overwhelm the effect of the fluid pressure on the flanks.). A comparison of the curves on Figure 8-6 relative to those on Figure 8-4 indicates that the contact pressure generally increases for a length of at least 4 inches upward from the mid-plane for all tubes.

The trend is consistent, at radii where the contact pressure decreases or the increase is not as great near the bottom of the tubesheet, the increase at higher elevations would be expected to compensate. For example, the contact pressures on Figure 8-1 at the bottom of the tubesheet show a decrease beyond a radius of 55 inches; however, the increase at 8.4 inches above the bottom, Figure 8-2 is significant. For the outboard tubes the increase in contact pressure extends all the way to the top of the tubesheet.

A comparison of the curves at the various elevations leads to the conclusion that for a length of 11 inches upward from an elevation of about 4.1 inches from the bottom of the tubesheet, there is always an increase in the contact pressure in going from normal operation conditions to postulated SLB conditions. At a depth 6.0 inches, the information on Figure 8-6 indicates the contact pressure is the same at the worst location, while Figure 8-2 illustrates that the SLB contact pressure is everywhere greater at a depth of 16.9 inches. Hence, it is reasonable by inspection to expect that omission of the examination of bulges or other artifacts below a depth of a somewhat more than 6 inches from the top of the tubesheet would lead to a high level of confidence that the potential leak rate from indications below the lower bound inspection elevation during a postulated SLB event will be bounded by twice the normal operation primary-to-secondary leak rate. The reason that 6 inches cannot be used is that although the contact pressure is no less than the same at that depth, the integrated contact pressure must be used to obtain the total resistance and the contact pressure above 6 inches depth decreases during the SLB event. A detailed derivation of the actual required depth is provided in Section 9.0.

Noting that the density of the number of tubes populating the tubesheet increases with the square of the radius, the number of tubes for which the contact pressure is greater during a SLB than during NOp at the H^* depth from the TTS is far greater than the number for which the contact pressure decreases, i.e., 96% of the tubes are at a radius greater than 12 inches from the center of the tubesheet.

8.2 Ligament Tearing Discussion

One of the concerns that must be addressed in dealing with cracks in SG tubes is the potential for ligament tearing to occur during a postulated accident when the differential pressure is significantly greater than during normal operation. While this is accounted for in the strength evaluations that demonstrate a resistance to pullout in excess of $3 \cdot \Delta P$ for normal operation and

1.4· ΔP for postulated accident conditions, the potential for ligament tearing to significantly affect the leak rate predictions needs to be accounted for.

Ligament tearing considerations for circumferential tube cracks that are located below the H^* depths within the tubesheet are significantly different from those for potential cracks at other locations. The reason for this is that H^* has been determined using a factor of safety of three relative to the normal operating pressure differential and 1.4 relative to the most severe accident condition pressure differential. Therefore, the internal pressure end cap loads which normally lead to an axial stress in the tube are not transmitted below about 1/3 of the H^* depth. This means that the only source of stress acting to extend the crack is the primary pressure acting on the flanks of the crack. Since the tube is captured within the tubesheet, there are additional forces acting to resist opening of the crack. The contact pressure between the tube and tubesheet results in a friction induced shear stress acting opposite to the direction of crack opening. Moreover, the pressure on the flanks is compressive on the tube material adjacent to the plane of the crack, hence a Poisson's ratio radial expansion of the tube wall in the immediate vicinity of the crack plane is induced, increasing the contact pressure and also acting to restrain the opening of the crack. In addition, the differential thermal expansion of the tube is greater than that of the carbon steel tubesheet, thereby inducing a compressive stress in the tube below the H^* length.

A scoping evaluation of the [

] ^{a,c,e}.

In summary, considering the worst-case scenario, the likelihood of ligament tearing from radial circumferential cracks resulting from an accident pressure increase is small since at most, only 9% of the cross-sectional area is needed to maintain tube integrity. Also, since the crack face area will

be less than the total cross-sectional area used above, the difference in the force applied as a result of normal operating and accident condition pressures will be less than the 35 lbs associated with the above numbers. Therefore, the potential for ligament tearing is considered to be a secondary effect of essentially negligible probability and should not affect the results and conclusions reported for the H* evaluation. The leak rate model does not include provisions for predicting ligament tearing and subsequent leakage, and increasing the complexity of the model to attempt to account for ligament tearing has been demonstrated to be not necessary (Reference 41).



Figure 8-1. Change in contact pressure at 20.0 inches below the TTS



Figure 8-2. Change in contact pressure at 16.9 inches below the TTS



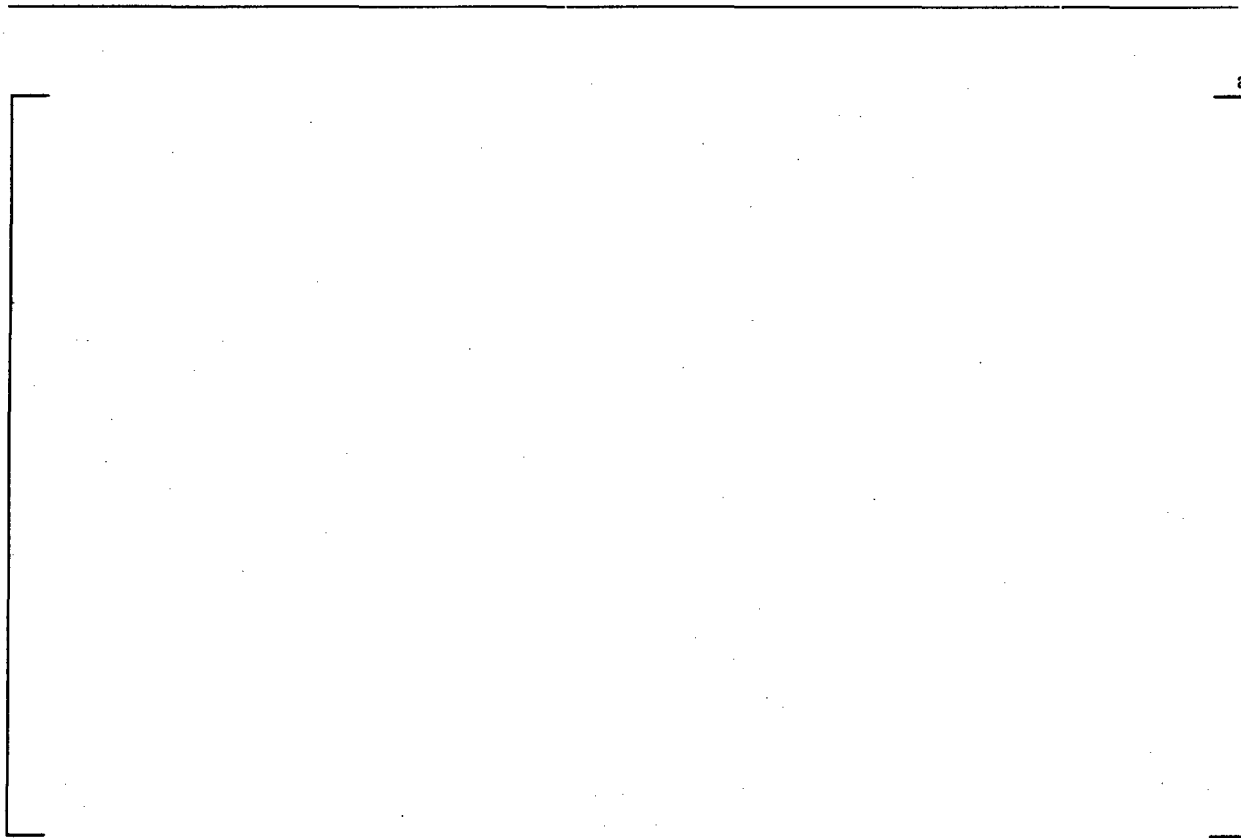
a,c,e

Figure 8-3. Change in contact pressure at 12.6 inches below the TTS



a,c,e

Figure 8-4. Change in contact pressure at 10.5 inches below the TTS



a,c,e

Figure 8-5. Change in contact pressure at 8.25 inches below the TTS



a,c,e

Figure 8-6. Change in contact pressure at 6.0 inches below the TTS

9.0 Determination of the B* Distance

B* is the length of engagement in the tubesheet needed for the leak rate during a postulated steam line break (SLB) event to be bounded by a specified multiple of the leak rate during normal operation (NOp). The rationale for the determination of B* is that there are changes during a SLB relative to NOp that lead to the expectation of an increase in the leak rate and other changes that lead to the expectation of a higher resistance to leakage. The determination of B* is based on analyzing the contributing factors and making an estimate of the change in leak rate that would be expected. The factors that lead to an expectation of an increase in the leak rate are as follows:

1. An increase in the primary-to-secondary differential pressure induced force on the water inside a postulated tube crack and the tube-to-tubesheet interface. For Wolf Creek this is a factor of about 1.79 to 1.99.
2. A decrease in the tube-to-tubesheet contact pressure above the neutral plane of the tubesheet resulting from dilation of the tubesheet holes in response to an increase in the bending deformation from the primary-to-secondary pressure difference increase. This does not apply to the periphery of the tubesheet where the opposite effect occurs.
3. A decrease in the tube-to-tubesheet contact pressure associated with the higher coefficient of thermal expansion of the tube material relative to that of the tubesheet if the temperature of the tubesheet decreases.

The factors that lead to an expectation of a decrease in the leak rate are:

1. The increase in primary pressure within the tube expands the tube into tighter contact with the tubesheet, resulting in an increase of the resistance of the material interface to flow between the tube and the tubesheet.
2. An increase in the tube-to-tubesheet contact pressure below the neutral plane of the tubesheet resulting from diminution of the tubesheet holes in response to the increase in the bending deformation from the primary-to-secondary pressure difference increase. Again, the effect is opposite for most tubes on the periphery of the tubesheet.
3. An increase in the resistance to flow associated with an increase in the viscosity of the water in the crevice if the temperature of the tubesheet decreases.

The basis for the determination of B* is the consideration of each of the above effects using results from finite element analyses of the tubesheet and results from leak rate testing of the tube-to-tubesheet interface. The analyses and testing are described Section 6.0 of this report. In summary, the leak rate is characterized by the Darcy equation for flow through a porous medium, an equation of the same form as the Hagen-Poiseuille equation for fully developed flow. The resistance to flow was developed from test data as a function of the contact pressure between the tube and the tubesheet in accord with expectations. The finite element analysis results provide calculated results

for the contact pressure as a function of tube location and depth into the tubesheet based on the NOp and postulated SLB pressure and temperature conditions of the plant.

The following are discussed: background information giving a qualitative overview supporting the development of B^* , flow through a crevice formulation, tube-to-tubesheet contact pressure variation, the determination of the B^* distance, and conclusions regarding the B^* values.

9.1 Background Information

A natural question regarding the development and application of the B^* criterion is whether or not numerical studies were performed to verify that the reduction in leak rate resistance above the neutral surface of the tubesheet associated with tubesheet bowing was adequately bounded by the increase in resistance below the neutral surface. The following discussion is intended to provide technical insight into the behavior of the leak rate from throughwall tube indications within the tubesheet by presenting:

- 1) the theoretical detail that is the basis for the observations from the test data and extrapolation of the test data for leak rate as function of joint length as expressed as the flow loss coefficient, and,
- 2) the explanation as to why the leak rate at normal operating conditions provides a bellwether for and can be used to establish a bounding value for the leak rate during steam line break conditions.

For most of the tube locations in the tubesheet the bow is convex upwards, like a dome. The tube-to-tubesheet contact pressure is an increasing linear function of the depth from the top of the tubesheet, thus, for any specified location within the tubesheet the contact pressure increases below and decreases above that location. The resistance to leakage through the tube-to-tubesheet interface is an increasing function of the contact pressure between the tube and the tubesheet. The bellwether principle is based on considering the leak rate during a postulated steam line break (SLB) event relative to that during normal operating conditions (NOp). The primary-to-secondary differential pressure during a SLB event is greater than that during NOp so that bowing of the tubesheet increases with an associated change in the slope of the contact pressure versus depth relation as a function of tube location. For all tubes, except for the small percentage of tubes that are located on the periphery, the slope increases. For tubes on the periphery the slope increases in an absolute sense since there is an inflection point near the periphery. Regardless, the evaluation applies because increasing the contact pressure has a greater influence on the leak rate than decreasing the contact pressure.

Numerical studies were not initially performed because the subject was considered to be adequately addressed based on a qualitative evaluation using first principles considerations as follows:

- 1) In the limiting case of no dependence of the leak rate loss coefficient, i.e., the resistance per unit length, on the contact pressure, the leak rate during NOp and postulated SLB would be

a function of the length of the crevice and pressure difference only. Using the Darcy equation, the leak rate is a direct function of the differential pressure and the inverse of the crevice length. Since the length remains the same and the driving pressure increases by a factor of about 2, almost 1300 psi to 2560 psi, the leak rate change is bounded by a similar factor. Any other theoretical dependence of leak rate on pressure difference, e.g., the square root of the pressure difference à la the Bernoulli equation, results in a reduction of the bounding factor relative to the result obtained using the Darcy equation.

- 2) The test data have demonstrated that the resistance per unit length is a monotonically increasing, non-linear function of the contact pressure with a positive second derivative. The deflection of the TS in combination with the increase in internal pressure results in the change in the contact pressure being zero between NOp and SLB at some depth below the TTS that is above the neutral surface of the tubesheet. The net contact pressure decreases above and increases below that depth, which is a function of location within the tube bundle. Using this elevation as a reference, the increase in resistance per unit length below the zero-change location must always be more than the absolute value of the decrease in resistance per unit length above the zero-change elevation. Thus, the average resistance in going from NOp to SLB must increase and the average leak rate must decrease. This is independent of the individual leak rates involved and only depends on the trend. The latter observation is apparent by inspection of the figure relating loss coefficient to contact pressure in all submittals on the subject of leak rate through tube-to-tubesheet crevices, see Figure 6-6 in this report for example.

There are alternate approaches to proving the above statements from the observations regarding the leak rate from test specimens.

9.2 Flow Through a Crevice (Darcy's Equation)

The equation that is solved for flow through a crevice is Darcy's model for flow through a porous media, that is, the volumetric flow, Q , is a function of the differential driving pressure, ΔP , and the respective inverse values of the viscosity, μ , the loss coefficient, K , and the length of the path, L , as,

$$Q = \frac{1}{\mu K} \frac{\Delta P}{L} \quad (9-1)$$

The driving pressure is based on the upstream minus the downstream values, else a negative sign would be needed in front of the equation. The viscosity is a function of the temperature and pressure of the fluid. The Darcy equation is also of the same form as the Hagen-Poiseuille flow equation for fully developed, laminar, axial flow in an annular gap, i.e.,

$$Q = \frac{1}{\mu} \frac{6}{\pi R a^3} \frac{\Delta P}{L} \quad (9-2)$$

Here, R is the average radius of the gap and a is a characteristic or effective gap dimension for the rough tube-to-tubesheet interface, expected to be very small, on the order of $4 \cdot 10^{-5}$ inch. Thus, the loss coefficient would be expected to be proportional to the inverse of the cube of the effective gap. The Hagen-Poiseuille form of the leak rate equation gives insight into the relationship between the average resistance, characterized by the loss coefficient, K , and the contact pressure, i.e.,

$$K = \frac{6}{\pi R a^3} \quad (9-3)$$

If the characteristic gap were proportional to the contact pressure between the tube and the tubesheet, doubling the pressure would increase the leak resistance by a factor of 8, although this is not necessarily expected to be the case because of the complex nature of the interface. In addition, it would not be unexpected that a plot of the $\ln(K)$ versus the contact pressure would approximate a straight line. For the rough tube-to-tubesheet interface, the length of the tortuous path can also be considered to be characterized as being effective because the flow does not necessarily have a straight path to follow to the TTS (top of the tubesheet). Approximation of the path as the legs of an equilateral triangle would essentially double the distance traveled from the throughwall location to the TTS. Hence, the use of the loss coefficient integrates the accounting of the effective gap and effective length.

The electrical analogy for the flow considers Q as the current flow and ΔP as the potential, hence the quantity $\mu K L$ is the resistance to flow, R . Since K is a function of the contact pressure, P_c , the resistance is a function of the location within the tubesheet. The total resistance can be found as the average value of the quantity μK , the resistance per unit length, multiplied by L , or by integrating the incremental resistance, $dR = \mu K dL$ over the length L , i.e.,

$$R = \mu \bar{K} (L_2 - L_1) = \int_{L_1}^{L_2} \mu K dL, \quad (9-4)$$

where both μ and K could be functions of location L . The viscosity is a very weak function of the pressure of the water in the crevice and can be considered to be constant for a given plant condition with negligible error, Figure 9-13, Reference 42 and 43. However, the viscosity is a strong function of the temperature of the water in the crevice, Figure 9-14, and the tubesheet temperature for the condition being analyzed must be considered. A decrease in the temperature can lead to a significant increase in flow resistance.

9.3 Tube-to-Tubesheet Contact Pressure Variation

Six tubesheet radial locations for which the contact pressure as a function of depth was determined were used in calculating the length of sound tubing below the TTS required to resist the NOP and SLB axial loads, i.e., the H^* depth. The intercept, b_0 , and slope, b_1 , parameters for the calculation of the contact pressure as a function of length, L , into the tubesheet for the six radial locations are listed in Table 9-1. The relationships are always in linear first order form,

$$P_c = b_0 + b_1 L \quad (9-5)$$

where the coefficients b_0 and b_1 vary as a function of the radial location of the tube in the tubesheet. This is simply a consequence of the fact that in the linear elastic stress analysis, no yielding occurs. A comparison of the FEA results with first order, linear representations is provided on Figure 9-5 for NOp and SLB conditions at a radius of 34 inches from the center of the tubesheet.

Further calculations examined the relationship between the intercept and slope of the prediction equations as a function of tube location radius. It was found that second order polynomial expressions can be used to describe the parameters almost exactly, i.e., with negligible error. A plot of the operating contact pressures, which do not include the residual contact pressure from the hydraulic expansion process, is provided on Figure 9-6 for each location during NOp and Figure 9-7 provides similar information during the postulated SLB event. The polynomial coefficients that were used to determine the values of the intercept and slope, i.e., b_0 and b_1 , for any given radius, R , from the center of the tubesheet for NOp conditions are illustrated on Figure 9-8. Here, the following relationships are depicted where the g and h values were determined from the regression analyses (recall that R in the following two equations represents radius),

$$\begin{aligned} \text{Normal Operation} \quad b_0 &= g_0 + g_1 R + g_2 R^2 && \text{(Intercept)} \\ b_1 &= h_0 + h_1 R + h_2 R^2 && \text{(Slope)} \end{aligned} \quad (9-6)$$

The coefficients, u and v , of a similar set of expressions were calculated for determining the contact pressure at all locations within the tubesheet during a SLB event, i.e.,

$$\begin{aligned} \text{SLB Conditions} \quad b_0 &= u_0 + u_1 R + u_2 R^2 && \text{(Intercept)} \\ b_1 &= v_0 + v_1 R + v_2 R^2 && \text{(Slope)} \end{aligned} \quad (9-7)$$

The polynomial coefficients that were used to determine the values of the intercept and slope for use in calculating the contact pressure during a SLB are illustrated on Figure 9-9. A comparison of the coefficients for the two conditions is provided on Figure 9-10.

9.4 Determination of the B* Distance

The results from multiple leak rate testing programs indicate that the logarithm of the loss coefficient is a linear function of the contact pressure, i.e.,

$$\ln K = a_0 + a_1 P_c, \quad (9-8)$$

where the coefficients, a_0 and a_1 of the linear relation are found from a regression analysis of the test data; both coefficients are greater than zero. Simply put, the loss coefficient is greater than zero at the point where the contact pressure is zero and the loss coefficient increases with

increasing contact pressure. Thus,

$$K = e^{a_0 + a_1 P_c}, \quad (9-9)$$

and the loss coefficient is an exponential function of the contact pressure. Combining Equation 9-9 for the loss coefficient as a function of the contact pressure with Equation 9-5 for the contact pressure as a function of length yields,

$$K = e^{a_0 + a_1 (b_0 + b_1 L)} = e^{c_0 + c_1 L} \quad (9-10)$$

where L is reckoned downward from the lower of the top of the tubesheet or the bottom of the expansion transition and the joined coefficients are given by $c_0 = a_0 + a_1 b_0$ and $c_1 = a_1 b_1$. Away from the periphery of the tubesheet, b_1 is greater than zero, hence c_1 is also greater than zero and the loss coefficient increases with depth into the tubesheet. Alternatively, the relation also means that near the periphery of the tubesheet the resistance to flow increases above any depth when the tubesheet bows upward. Since the B^* distance into the tubesheet is based on finding the depth for which the resistance to leak during SLB is the same as that during NOp, the meaningful radial region of the tubesheet is away from the periphery, that is, where the resistance to leakage decreases near the top of the tubesheet. Another point to note from the above expression is that in the region of interest the second derivative of the loss coefficient with respect to depth is positive. This means that the resistance per unit length is always increasing with depth into the tubesheet. One consequence of the relation is that the decrease in resistance for a specified distance above any reference point is balanced by the increase in resistance over a shorter distance below that reference point. The coefficients for the contact pressure as a function of location are given by Equations 9-6 and 9-7 for NOp and SLB respectively.

The B^* distance is designated by L_B in the following equations and is the depth at which the resistance to leak during SLB is the same as that during NOp. Note that the product of the viscosity and the loss coefficient is the resistance per unit length for any location in the tubesheet. The resistance to leak, R , as a function of the viscosity, μ , average loss coefficient, \bar{K} , and length of the leak path from some uppermost location, L_0 , to L_B for any condition is given by,

$$R = \mu \bar{K} (L_B - L_0) = \int_{L_0}^{L_B} e^{c_0 + c_1 L} dL. \quad (9-11)$$

The limits of the integration define the range over which there is a contact pressure between the tube and the tubesheet that is greater than zero, i.e., ignoring any resistance to flow above that elevation. The lower limit is the lower of the TTS, the BET (bottom of the expansion transition), or the point where the contact pressure is zero. Carrying out the integration,

$$R = \mu \frac{e^{c_0}}{c_1} [e^{c_1 L_B} - e^{c_1 L_0}]. \quad (9-12)$$

The equation can be used directly when the point of zero contact pressure between the tube and the tubesheet is at or below the TTS or BET, whichever is lower.

In order to account for the condition wherein L_0 is < 0 , i.e., at or above the TTS or BET, whichever is lower, the equation is written as,

$$R = \mu \frac{e^{c_1}}{c_1} \left[e^{c_1 L_B} - \text{if}(L_0 > 0, e^{c_1 L_0}, 1) \right]. \quad (9-13)$$

Here, the first argument of the “if” statement is the condition to be tested, the second argument is the value used if the condition is true, and the third argument is used if the condition is false, that is, when zero contact pressure is predicted above the TTS or BET. For normal operation the resistance to leakage is given by,

$$R_N = \mu_N \frac{e^{c_{1N}}}{c_{1N}} \left[e^{c_{1N} L_B} - \text{if}(L_{0N} > 0, e^{c_{1N} L_{0N}}, 1) \right], \quad (9-14)$$

and for SLB by,

$$R_S = \mu_S \frac{e^{c_{1S}}}{c_{1S}} \left[e^{c_{1S} L_B} - \text{if}(L_{0S} > 0, e^{c_{1S} L_{0S}}, 1) \right]. \quad (9-15)$$

The B^* distance is such that the resistance during SLB is the same as that during NOp, limiting the leak rate to be no more than a factor of two times that during normal operation, thus the solution is obtained for the value of L_B that makes $R_S = R_N$.

For the Wolf Creek SGs the value of B^* varies from a maximum of 7 inches at a radius of 2 inches, about row 1 at the center of the bundle, to 5 inches at a radius of 20 inches, about row 29 between columns 57 and 58, and 3 inches at a radius of 26 inches. Thereafter, the integrated leak resistance is always greater during a SLB event than during NOp. A plot of the calculated B^* values is provided on Figure 9-15. Here, any values less than 1 inch were truncated to 1 inch. For example, the top of the tubes at the extreme periphery of the tubesheet are in compression during NOp because of contraction of the tube holes due to convex downward bending. The level of compression increases during a SLB event because the magnitude of the convex bending increases. Thus, any leak rate during NOp would bound the leak rate during SLB. While the driving pressure would increase by a factor of up to 2, the contact pressure between the tube and the tubesheet would increase toward the top of the tubesheet.

9.5 Sensitivity of the B^* Calculation

Two approaches were taken to examine the sensitivity of the determination of the B^* distance to the parameters of the analysis. The first was to vary the loss coefficient versus contact pressure parameters based on the confidence values from the regression calculations. The value of the largest B^* depth changed by about 0.25, 0.12, and 0.04 inch in going from an upper to a lower 95% confidence bound on the slope at radii of 2, 12, and 32 inches respectively. Changes in the intercept coefficient did not have any meaningful effect. Regardless, the most conservative values were used for the reported analysis results.

As an alternative approach, the depths for which the integration of the product of the viscosity with the contact pressure remained constant were also calculated. Compared to the previous section this is simply a pseudo-resistance, R_p , that is found as,

$$R_p = \int_{L_0}^{L_B} \mu P_c dL = \int_{L_0}^{L_B} \mu (b_0 + b_1 L) dL \quad (9-16)$$

so,

$$R_p = \mu \left[b_0 (L_B - L_0) + \frac{1}{2} b_1 (L_B^2 - L_0^2) \right] \quad (9-17)$$

Setting $R_{PN} = R_{PS}$ at a radius of 2 inches leads to a value of L_B of 6.3 inches. A value of 8 inches results from the same calculation at a radius of 5.4 inches. At radii of 15 and 20 inches the depths for equal values of R_p during NOp and SLB conditions were found to be 4.0 and 2.6 inches respectively. The result for a radius of 8 inches is illustrated on Figure 9-18 to be a depth of 5.4 inches. The results are comparable to those of the previous section and diminish more rapidly with radius than the approach that accounts for the loss coefficient from the testing program. For radii greater than about 50 inches the value of R_p is always greater during NOp than during SLB regardless of the depth into the tubesheet. The inherent assumption here is that the resistance is proportional to the contact pressure. This is not an unreasonable assumption in light of the dependence on the inverse third power of the effective gap thickness as implied by the Hagen-Poiseuille equation. Therefore, the results from the B^* analysis based on the consideration of the slope of the loss coefficient are considered to be effectively confirmed, i.e., validated.

Finally, additional insight into the effect of cold leg indications on the relative leak rate is illustrated by examining the plots of depth for zero contact pressure on Figure 9-19 for the hot leg and Figure 9-20 for the cold leg. The change in differential pressure and the change in temperature result in the depth for zero contact pressure during NOp increasing on the cold leg, i.e., depth from the TTS, relative to the hot leg. This means that leakage during normal operation will be closer to that during a postulated SLB event and the relative increase smaller. Depending on the relative change in differential pressure and temperature, the leak rate during a postulated SLB event could decrease for locations outboard of a radius of about 17 to 20 inches. The conclusion regarding the cold leg indications is that the application of a hot leg derived B^* is conservative.

9.6 Conclusions Relative to B^*

The resistance equations above can be used to show that the resistance is always bounded by the region through the thickness of the tubesheet where the contact pressure increases relative to the region where the contact pressure decreases. This simply means that the leak rate resistance increases during a SLB event relative to that during normal operation for similar lengths about a reference depth from the TTS, for example, B^* . The resistance equations were used to calculate B^* as the distance from the TTS for which the resistance during a postulated SLB event is the same as that during NOp. This means that the leak rate during SLB from any and all indications below B^* will be bounded by a multiple of the leak rate during NOp based on the relative driving

pressure for the two conditions. The differential pressure during a SLB at Wolf Creek is 1.79 to 2 for the cases described in Section 7.1.4.1, times that during NOP depending on the operating conditions considered, e.g., differences in plugging level. Hence, the leak rate during a postulated SLB event would be expected to be no more than 2 times the leak rate being experienced during normal operation. Moreover, the B* analysis did not take into consideration the effect of the increase in the contact pressure below the B* elevation on the leak rate through postulated tube cracks within the tubesheet. For axial cracks the flanks would be compressed and the leak rate through the cracks themselves would be expected to decrease. For circumferential cracks the resistance to flank displacement in the axial direction would be expected to negate the effect of the slight increase in pressure on the crack flanks. In conclusion, the use of a factor of 2 would usually be expected to be conservative.

Table 9-1. First Order Equation Coefficients for the Variation of Contact Pressures Through Tubesheet

a,c,e

Table 9-2. B* Summary Table Leak Rate Required Engagement Lengths

Zone	Leak Resistance Ratio $R_{SLB} / R_{NOp}^{(1,2)}$	Engagement from TTS (inches)	
		Hot Leg	Cold Leg
A	1.0	< 1.0	< 1.0
B	1.0	< 1.0	< 1.0
C	1.0	4.6	3.4
D	1.0	6.8	5.4

Notes:

1. Conditions for the analyses are specified in Sections 7.1.4.1 for NOp, 7.1.4.3 for FLB, and 7.1.4.4 for SLB.
2. Equal resistance assures leak rate during accident conditions is not more than twice that during normal operation.
3. H* structural summary is provided in Table 7-12.

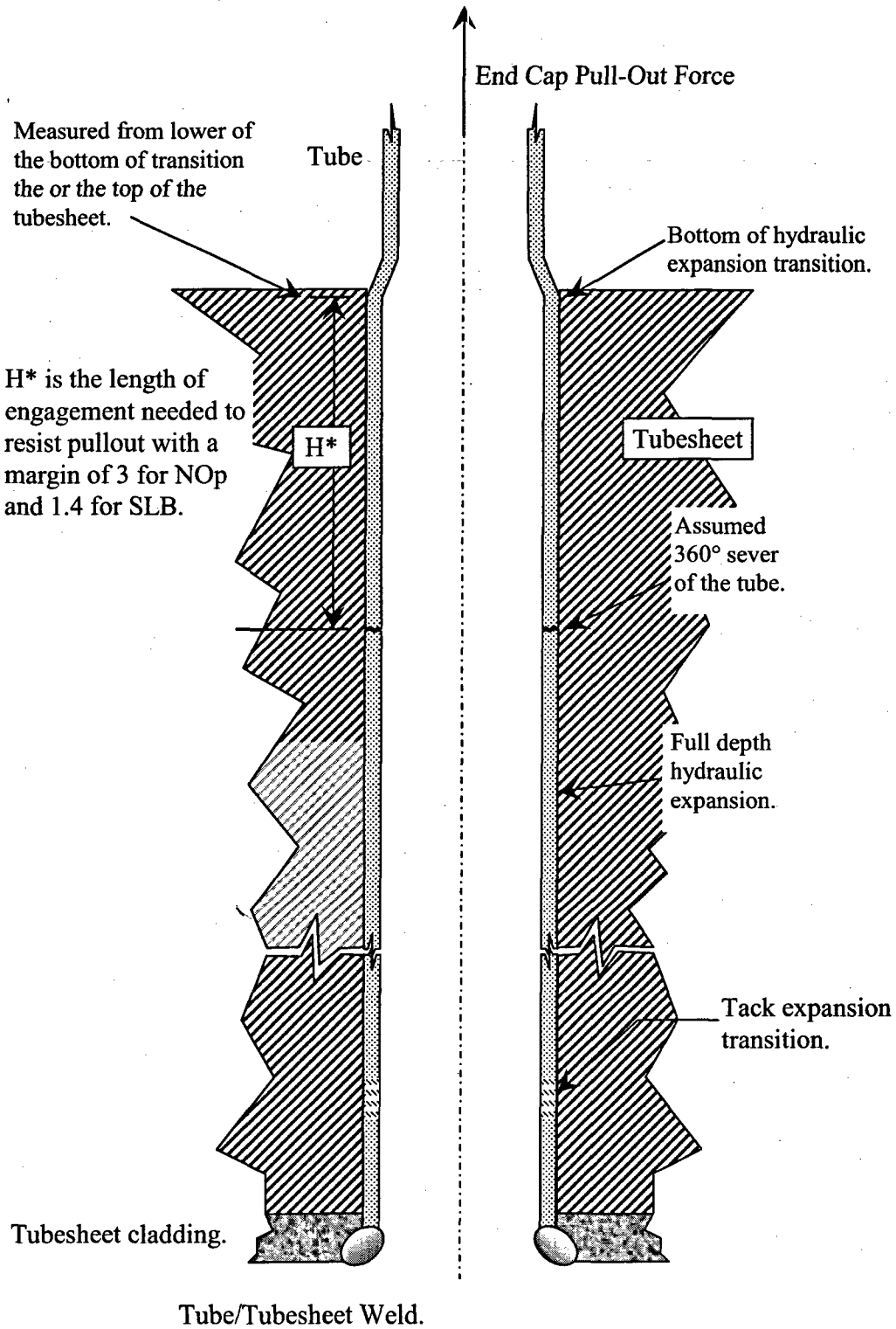


Figure 9-1. Determination of H^*

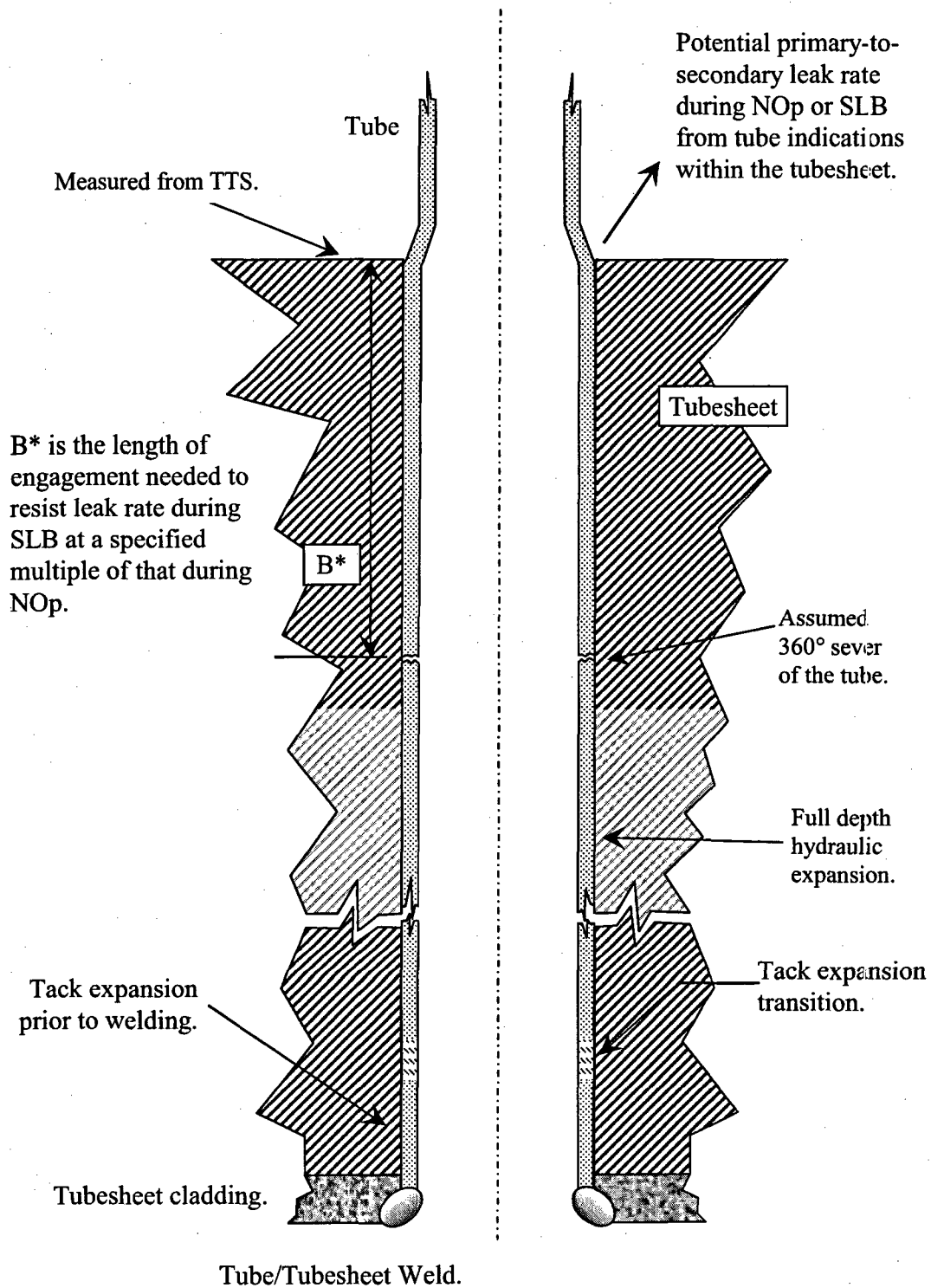


Figure 9-2. Determination of B^*

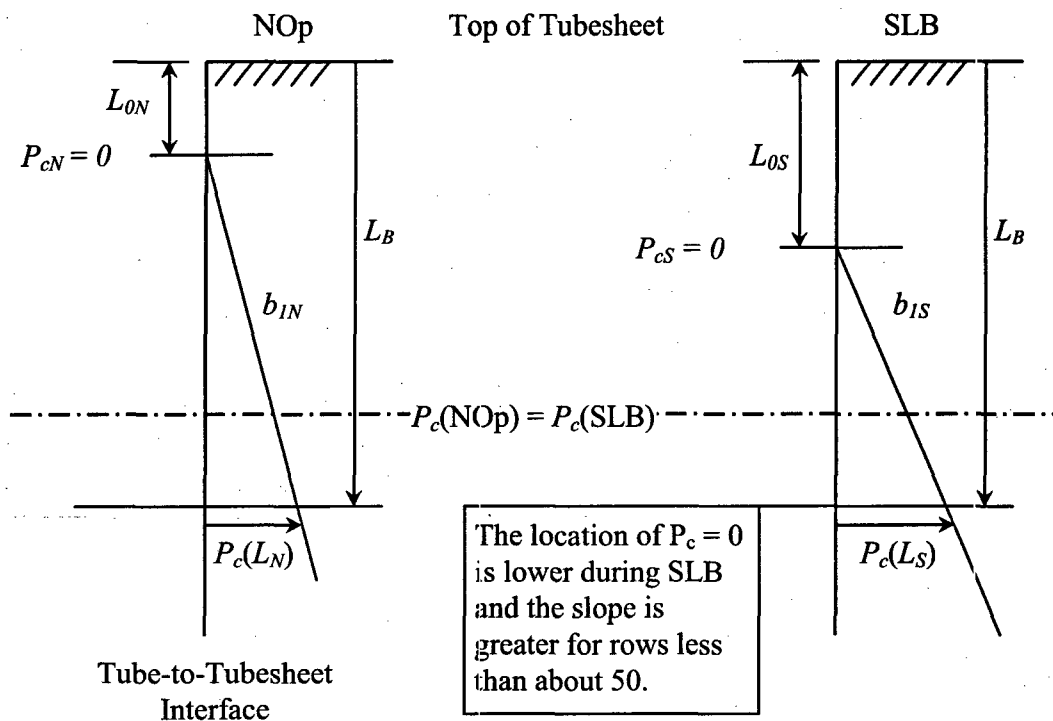


Figure 9-3. Concepts for the Determination of B*

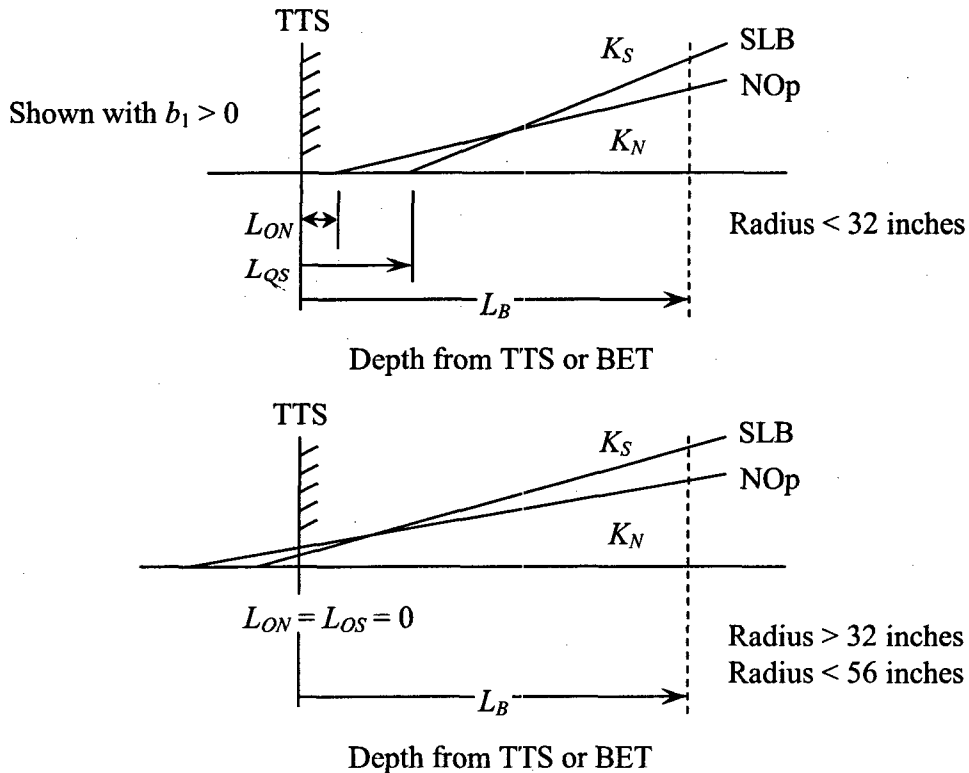


Figure 9-4. Schematic for the Determination of B* Parameters

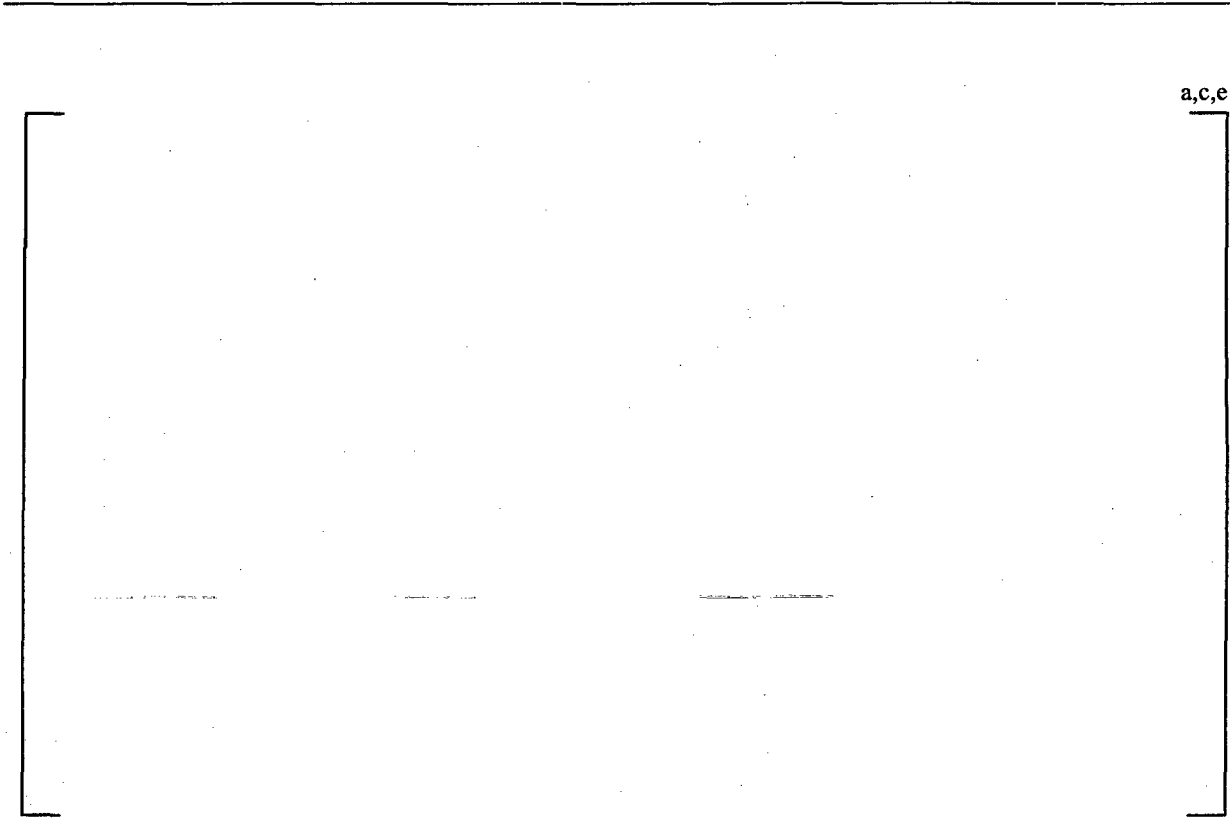


Figure 9-5. First Order Linear Representation of Contact Pressure



Figure 9-6. Contact Pressure During Normal Operation (Model F)



a,c,e

Figure 9-7. Contact Pressure During SLB (2560 psi at 297°F)



a,c,e

Figure 9-8. NOp Contact Pressure vs. Depth Coefficients by Radius



Figure 9-9. SLB Contact Pressure vs. Depth Coefficients by Radius



Figure 9-10. Comparison of Contact Pressure Coefficients for NOP & SLB Conditions



Figure 9-11. Elevation Below the TTS for Invariant Contact Pressure

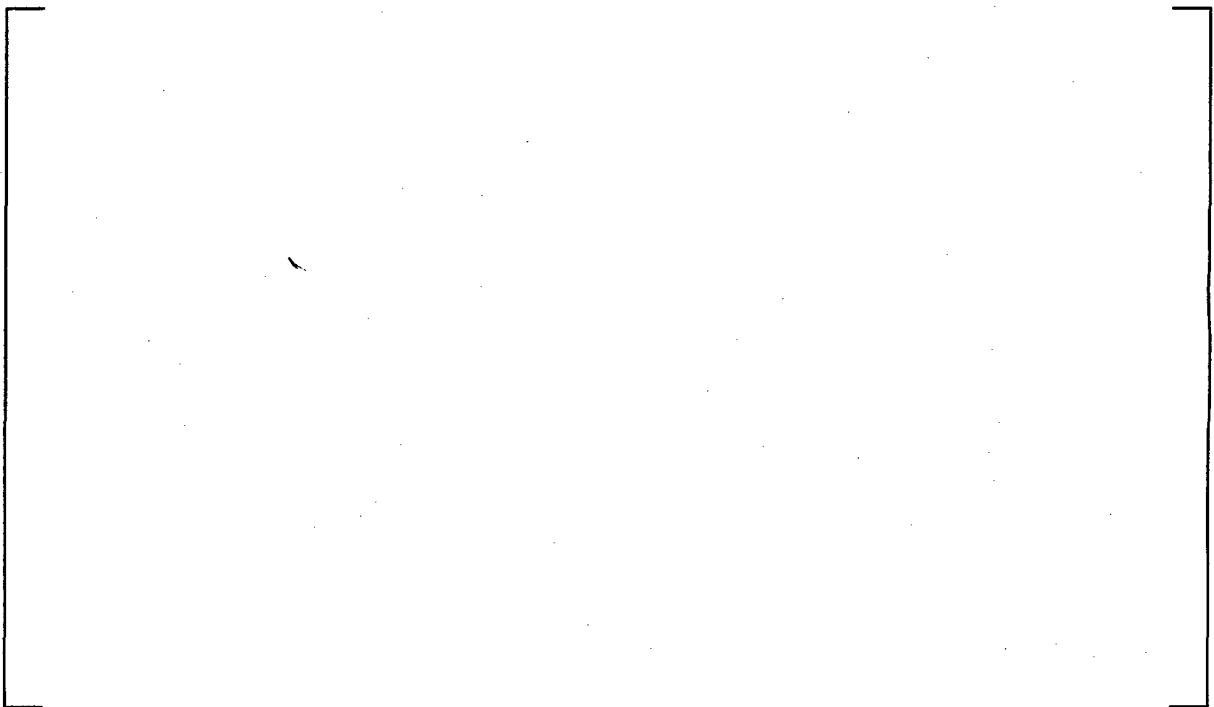


Figure 9-12. TTS Contact Pressure for NOP & SLB Conditions



Figure 9-13. Viscosity of Water as a Function of Pressure



Figure 9-14. Viscosity of Water at 2560 psi as a Function of Temperature



Figure 9-15. Upper Bound B^* for Wolf Creek SGs for No Change in Resistance



Figure 9-16. Nominal B^* for Wolf Creek SGs for No Change in Leak Rate



Figure 9-17. Graphical Determination of B* Depth from Flow Resistance



Figure 9-18. Approximate Determination of B* Depth from Contact Pressure



Figure 9-19. Elevation of Zero Contact Pressure for the Hot Leg



Figure 9-20. Elevation of Zero Contact Pressure for the Cold Leg

10.0 NRC Staff Discussion for One-Cycle B* Approval for Braidwood 2 & Wolf Creek

10.1 Joint Structural Integrity Discussion

In Section 5.1, "Joint Structural Integrity," of Reference 7 the NRC staff stated that the analyses that were performed by Westinghouse that led to the determination of the required engagement distances were not reviewed in detail and more qualitative arguments were used by the NRC staff for one time approval of the applicable 17 inch tube joint length. The qualitative arguments are stated below.

- The NRC staff estimates based on the Westinghouse pullout tests that the radial contact pressure produced by the hydraulic expansion and differential radial thermal expansion is such to require an engagement distance of 8.6 inches to ensure the appropriate safety margins against pullout based on no-slip. This estimate is a mean minus one standard deviation estimate based on 6 pull out tests. This estimate ignores the effect on needed engagement distance from internal primary pressure in the tube and tubesheet bore dilations associated with the tubesheet bow. The NRC staff notes from a tube pullout standpoint, the use of a 0.25 inch displacement criterion is conservative. Allowing slippage of about 0.2 to 0.3 inches decreases the necessary engagement distance to 5.1 inches, again ignoring the effect on needed engagement distance from internal primary pressure in the tube and tubesheet bore dilations associated with tubesheet bow.
- The internal primary pressure inside the tube under normal operating and accident conditions also acts to tighten the joint relative to unpressurized conditions, thus reducing the necessary engagement distance.
- Tubesheet bore dilations caused by the tubesheet bow under primary to secondary pressure can increase or decrease contact pressure depending on tube location within the bundle and the location along the length of the tube in the tubesheet region. Basically, the tubesheet acts as a flat, circular plate under an upward-acting net pressure load. The tubesheet is supported axially around its periphery with a partial restraint against tubesheet rotation provided by the steam generator shell and the channel head. The SG divider plate provides a spring support against upward displacement along a diametral mid-line. Over most of the tubesheet away from the periphery, the bending moment resulting from the applied primary to secondary pressure load can be expected to put the tubesheet in tension at the top and compression at the bottom. Thus, the resulting distortion of the tubesheet bore (tubesheet bore dilation) tends to be such as to loosen the tube to tubesheet joint at the top of the tubesheet and to tighten the joint at the bottom of the tubesheet. The amount of dilation and resulting change in joint contact pressure would be expected to vary in a linear fashion from the top to the bottom of a tubesheet. Given the neutral axial to be at approximately the mid-point of the tubesheet thickness (i.e., 10.5 inches below the TTS to 17 inches below the TTS), tubesheet bore dilation effects would be expected to further tighten the joint from 10 inches below the TTS to 17 inches below the TTS which would be the lower limit of the proposed tubesheet region inspection

zone. Combined with the effects of the tube joint tightening associated with the radial differential thermal expansion and primary pressure inside the tube, contact pressure over at least a 6.5 inch distance should be considerably higher than the contact pressure simulated in the above mentioned pullout tests. A similar logic applied to the periphery of the tubesheet leads the staff to conclude that at the top 10.5 inches of the tubesheet region, contact pressure over at least a 6.5 inch distance should be considerably higher than the contact pressure simulated in the above mentioned pull out tests. Thus, the staff concludes that the proposed 17-inch engagement distance (or inspection zone) is acceptable to ensure the structural integrity of the tubesheet joint.

The NRC qualitative arguments are further supported on a more quantitative basis based on a study completed for the Model F steam generators for another plant. Moreover, similar statements were made in Reference 8 in approving a similar amendment for a plant with Model D5 SGs.

10.1.1 Discussion of Interference Loads

There are four source terms that must be considered relative to the determination of the interface pressure between the tube and the tubesheet. These are,

1. the initial preload from the installation of the tube,
2. internal pressure in the tube that is transmitted from the ID to the OD,
3. thermal expansion of the tube relative to the tubesheet, and
4. bowing of the tubesheet that results in dilation of the tubesheet holes.

The initial preload results from the plastic deformation of the tube material relative to that of the tubesheet. The material on the inside diameter experiences more plastic deformation than the material on the outside and thus has a deformed diameter which is incrementally greater. Equilibrium of the hoop forces and moments in the tube means that the OD is maintained in a state of hoop tension at a diameter greater than a stress free state. The model for the determination of the initial contact pressure between the tube and the tubesheet, P_c , is illustrated on Figure 10-1 for the elements of the unit cell and on Figure 10-2 for the analysis schematic. Both the tube and the tubesheet behave as elastic springs after the expansion process is applied. The normal stress on the tube must be equal in magnitude to the normal stress on the tubesheet and the sum of the elastic springback values experienced by each must sum to the total interference.

As long as the tube and the tubesheet remain in contact the radial normal stresses must be in equilibrium. Thus, the problem of solving for the location of the interface and the contact pressure is determinate. The elements considered in the analysis are illustrated on Figure 10-3 for all operating and postulated accident conditions; the centerline of the tube and tubesheet hole are to the left in the figure. Each source of deformation of the tube outside surface starting from the installed equilibrium condition can be visualized starting from the top left side of the figure. The sources of deformation of the tubesheet inside surface can be visualized starting from the lower left side of the figure. As illustrated, although not to scale, the tube material has a coefficient of

thermal expansion that is greater than that of the tubesheet. The radial flexibility⁹, f , of the tube relative to that of the tubesheet determines how much of the pressure is actually transmitted to the interface between the tube and the tubesheet. Positive radial deformation of the tube in response to an internal pressure is found as the product of the pressure, P_p , and the tube flexibility associated with an internal pressure, discussed in the next section. Thus, the tube gets tighter in the tubesheet hole as the temperature of the tube and tubesheet increase. The deformation of the tube in response to an external or secondary pressure, P_s , is the product of the pressure times the flexibility associated with an external pressure. The normal operation contact pressure, P_N , is found from compatibility and equilibrium considerations. The deformation of the tubesheet hole in response to an internal pressure, P_s , is found as the product of the pressure and the flexibility of the tubesheet associated with an internal pressure. The opening or closing of the tubesheet hole, δr_i , resulting from bow induced by the primary-to-secondary pressure difference is in addition to the deformations associated with temperature and internal pressure. Once the tube has been installed, the deformations of the tube and tubesheet associated thermal expansion, internal pressure, and tubesheet bow remain linearly elastic.

Because of the potential for a crack to be present and the potential for the joint to be leaking, the pressure in the crevice is assumed to vary linearly from the primary pressure at the crack elevation to the secondary pressure at the top of the tubesheet. If the joint is not leaking, it would be expected that there was no significant fluid pressure in the crevice. The pressure assumption is considered to be conservative because it ignores the pressure drop through the crack, and the leak path is through the crevice will not normally be around the entire circumference of the tube. In addition, the leak path is believed to be between contacting microscopic asperities between the tube and the tubesheet, thus the pressure in the crevice would not be acting over the entire surface area of the tube and tubesheet. In any event, pressure in the crevice is always assumed to be present for the analysis.

There is no bow induced increase in the diameter of the holes during normal operation or postulated accident conditions below the mid span elevation within the tubesheet, hence most analyses concentrate on locations near the top of the tubesheet. The tubesheet bow deformation under postulated accident conditions will increase because of the larger pressure difference between the bottom and top of the tubesheet. The components remain elastic and the compatibility and equilibrium equations from the theory of elasticity remain applicable. Below the mid span elevation within the tubesheet the tubesheet holes will contract. The edges of the tubesheet are not totally free to rotate and there is some suppression of the contraction near the outside radius. This also means that the dilation at the top of the tubesheet is also suppressed near the outside radius of the tubesheet. The maximum hole dilations occur near the center of the tubesheet.

The application of the theory of elasticity means that the individual elements of the analysis can be treated as interchangeable if appropriate considerations are made. The thermal expansion of the tube can be thought of as the result of some equivalent internal pressure by ignoring Poisson

⁹ Flexibility is the ratio of deformation to load and is the inverse of the stiffness.

effects, or that tubesheet bow could be analytically treated as an increase in temperature of the tubesheet while ignoring associated changes in material properties.

10.1.2 Flexibility Discussion

Recall that the flexibility, f , is defined as the ratio of deflection relative to applied force; it is the inverse of stiffness which commonly used to relate force to deformation. There are four flexibility terms associated with the radial deformation of a cylindrical member depending on the surface to which the loading is applied and the surface for which the deformation is being calculated, e.g., for transmitted internal pressure one is interested in the radial deformation of the OD of the tube and the ID of the tubesheet. The deformation of the OD of the tube in response to external pressure is also of interest. The geometry of the tube-to-tubesheet interface is illustrated on Figure 10-3. The flexibility of the tubesheet, designated herein by the subscript c , in response to an internal pressure, P_{ci} , is found as,

$$\left[\frac{r_{ci}}{r_{co}} \right]^{a,c,c} \quad \text{Tubesheet (10-1)}$$

where, r_{ci} = inside radius of the tubesheet and outside radius of the tube,
 r_{co} = outside radius of the tubesheet hole unit cell,
 E_c = the elastic modulus of the carbon steel tubesheet material, and
 ν = Poisson's ratio for the tubesheet material.

Here, the subscripts on the flexibility stand for the component, c for tubesheet (and later t of tube), the surface being considered, i for inside or o for outside, and the surface being loaded, again, i for inside and o for outside. The superscript designates whether the cylinder is open, o , or closed, c , of interest in dealing with the end cap load from pressure in the tube. The former case is a state of plane stress and the latter is not since a closed cylinder has an end cap load. The flexibility of the tube in response to the application of an external pressure, P_{ro} , e.g., the contact pressure within the tubesheet, is,

$$\left[\frac{r_{ci}}{r_{co}} \right]^{a,c,o} \quad \text{Open Tube (10-2)}$$

Poisson's ratio is the same for the tube and the tubesheet. When the external pressure can act on the end of the tube,

$$\left[\frac{r_{ci}}{r_{co}} \right]^{a,c,c} \quad \text{Closed Tube (10-3)}$$

where E_t is the elastic modulus of the tube material. The flexibility of the tube in response to an external pressure is different when the secondary side pressure is present because that pressure also acts to compress the tube in the axial direction giving rise to a Poisson expansion effect, resisting the radial compression due to the pressure.

Finally, the flexibility of the outside radius of the tube in response to an internal pressure, P_{ti} , is,

$$\left[\frac{r_{ti}^3}{E_t} \left(\frac{1}{r_{ti}^3} + \frac{1}{r_{to}^3} \right) \right]^{a,c,e} \quad \text{Closed Tube (10-4)}$$

where r_{ti} is the internal radius of the tube and the tube is assumed to be closed. For an open tube the term in parentheses in the numerator is simply 2. A closed tube expands less due to Poisson contraction associated with the end cap load from the internal pressure. A summary of the applicable flexibilities is provided in Table 10-1. Note that during normal operation there is an end cap load on the tube from the secondary pressure but not from that associated with the fluid in the crevice if the joint is leaking. Both flexibilities would then be involved in calculating the radial deformation of the outside of the tube. Only the open tube flexibility is used with the pressure in the crevice for postulated accident conditions.

When the inside of the tube is pressurized, P_{ti} , some of the pressure is absorbed by the deformation of the tube within the tubesheet and some of the pressure is transmitted to the OD of the tube, P_{to} , as a contact pressure with the ID of the tubesheet. The magnitude of the transmitted pressure is found by considering the relative flexibilities of the tube and the tubesheet as,

$$\left[\frac{r_{ti}^3}{E_t} \left(\frac{1}{r_{ti}^3} + \frac{1}{r_{to}^3} \right) \right]^{a,c,e} \quad (10-5)$$

Note that the tube flexibility in response to the contact pressure is for an open tube because there is no end cap load associated with the contact pressure. The denominator of the fraction is also referred to as the interaction coefficient between the tube and the tubesheet. About 85 to 90% of the pressure internal to the tube is transmitted through the tube in Westinghouse designed SGs. However, the contact pressure is not increased by that amount because the TS acts as a spring and the interface moves radially outward in response to the increase in pressure. The net increase in contact pressure is on the order of 67 to 74% of the increase in the internal pressure, depending on the constraint conditions. For example, the contact pressure between the tube and the tubesheet is increased by about 1970 psi during normal operation relative to ambient conditions. Likewise, the increase in contact pressure associated with SLB conditions is about 2250 psi relative to ambient conditions.

When the temperature increases from ambient conditions to operating conditions the differential thermal expansion of the tube relative to the tubesheet increases the contact pressure between the tube and the tubesheet. The mismatch in expansion between the tube and the tubesheet, δ , is given

by,

$$\delta = (\alpha_t \Delta T_t - \alpha_c \Delta T_c) r_{to} \quad \text{Thermal Mismatch} \quad (10-6)$$

where: α_t, α_c = thermal expansion coefficient for the tube and tubesheet respectively,
 $\Delta T_t, \Delta T_c$ = the change in temperature from ambient conditions for the tube and tubesheet respectively.

During normal operation the temperature of the tube and tubesheet are effectively identical to within a very short distance from the top of the tubesheet and the individual changes in temperature can usually be replaced by ΔT_t , thus,

$$\delta = (\alpha_t - \alpha_c) \Delta T_t r_{to}. \quad (10-7)$$

The change in contact pressure due to the increase in temperature relative to ambient conditions, P_T , is given by,

$$\left[\begin{array}{c} \text{a,c,e} \\ \square \end{array} \right] \quad (10-8)$$

Likewise, the same equation can be used to calculate the reduction in contact pressure resulting from a postulated reduction the temperature of the tube during a postulated SLB event.

The net contact pressure, P_C , between the tube and the tubesheet during operation or accident conditions is given by,

$$\text{Net Contact Pressure} \quad P_C = P_0 + P_p + P_T - P_B \quad (10-9)$$

where P_B is the loss of contact pressure due to dilation of the tubesheet holes, P_0 is the installation preload, P_p is the pressure induced load, and P_T is the thermal induced contact load. There is one additional term that could be considered as increasing the contact pressure. When the temperature increases the tube expands more in the axial direction than the tubesheet. This is resisted by the frictional interface between the tube and the tubesheet and a compressive stress is induced in the tube. This in turn results in a Poisson expansion of the tube radius, increasing the interface pressure. The effect is not considered to be significant and is essentially ignored by the analysis.

10.1.3 Analysis

From the preceding discussions it is apparent that the contact pressure during normal operation can be found by equating the total deformation of the outside radius of the tube, r_{to} , to the total deformation of the inside radius of the tubesheet hole, r_{ci} , where the net deformation of the outside of the tube, δ_{to} , is given by,

$$\text{Tube Deformation} \quad \delta_{to} = \alpha_t \Delta T_t r_{to} + P_p f_{toi}^c + P_s f_{100}^c + P_N f_{100}^o \quad (10-10)$$

and the net deformation of the tubesheet hole, δ_{ci} , is given by,

$$\text{TS Deformation} \quad \delta_{ci} = \alpha_c \Delta T_c r_{ci} + P_s f_{cii}^o + \delta r_i + P_N f_{cii}^o \quad (10-11)$$

The inclusion of the P_N terms assures compatibility and the two net deformations must be equal. It can usually be assumed that the secondary fluid pressure does not penetrate the tubesheet hole and the terms involving P_s may be ignored. All of the terms except for the final contact pressure, P_N , are known and the tubesheet bow term, δr_i , is found from the finite element model analysis of the tubesheet. The total contact pressure during operation is then found as P_N plus P_c , the installation contact pressure. For postulated SLB conditions the solution is obtained from,

$$\alpha_t \Delta T_t r_{to} + P_p f_{toi}^c + P_N f_{too}^o = \alpha_c \Delta T_c r_{ci} + \delta r_i + P_N f_{cii}^o, \quad (10-12)$$

or, the total contact pressure during a postulated SLB event is given by,

$$\text{SLB Contact Pressure} \quad P_T = P_c + \frac{\alpha_t \Delta T_t r_{to} - \alpha_c \Delta T_c r_{ci} + P_p f_{toi}^c - \delta r_i}{f_{cii}^o - f_{too}^o}, \quad (10-13)$$

where $r_{to} = r_{ci}$. A similar expression with more terms is used to obtain the contact pressure during normal operation. The denominator of the above equation is referred to as the tube-to-tubesheet influence coefficient because it related deformations associated with the interfacing components to the interface pressure. The influence coefficient for Westinghouse Model F SG tubes is calculated using the information tabulated in Table 10-1 as $3.33 \cdot 10^{-6}$ psi/inch.

By taking partial derivatives with respect to the various terms on the right the rate of change of the contact pressure as a function of changes in those parameters can be easily calculated. For example, the rate of change of the contact pressure with the internal pressure in the tube is simply,

$$\frac{\Delta P_N}{\Delta P_p} = \frac{f_{toi}^c}{f_{cii}^o - f_{too}^o}. \quad (10-14)$$

Thus, the rate of change of contact pressure with internal pressure in the tube is 0.564 psi/psi. Likewise, the rate of change of the contact pressure with change in the tube temperature or tubesheet temperature is given by,

$$\frac{\Delta P_N}{\Delta T_t} = \frac{\alpha_t r_{to}}{f_{cii}^o - f_{too}^o} \quad \text{and} \quad \frac{\Delta P_N}{\Delta T_c} = - \frac{\alpha_c r_{ci}}{f_{cii}^o - f_{too}^o}, \quad (10-15)$$

respectively. Again using the values in Table 10-1, the rate of change of contact pressure with tube temperature is 18.3 psi/°F if there is no increase in tubesheet temperature. The corresponding change with an increase in tubesheet temperature without an increase in tube temperature is -17.36 psi/°F leave a net increase in contact pressure of 0.94 psi/°F with a uniform increase in temperature of the tube and the tubesheet.

Finally, the rate of change of contact pressure with tubesheet bow is calculated as,

$$\frac{\Delta P_N}{\Delta \delta r_{ci}} = \frac{1}{f_{cii}^o - f_{100}^o} \quad (10-16)$$

The effect of the dilation associated with the tubesheet bow can be calculated using the information tabulated in Table 10-1. For each 0.1 mil of diameter dilation the interface pressure is reduced on the order of 380 psi. A summary of all of the contact pressure influence factors is provided in Table 10-1. A summary of tubesheet bow induced hole dilation values is provided in Table 10-2.

10.1.4 Conclusions

Although the study was completed for another Model F SG, the results listed in Table 10-2 indicate that the effect of tubesheet bow can result in a significant average decrease in the contact pressure during postulated accident conditions above the neutral plane. However, for the most severe case in one plant, in tube R18C77, the diametral change at the worst case location is less than 0.2 mils at the H* depth during postulated accident conditions. This same type of result would be expected to be the case for the Model F SGs at the Wolf Creek Generating Station. Below the neutral plane, tubesheet bow is shown not to result in any tube dilation thus supporting the NRC staff conclusion that:

“Given the neutral axis to be at approximately the mid-point of the tubesheet thickness (i.e., 10.5 inches below the TTS to 17 inches below the TTS), tubesheet bore dilation effects would be expected to further tighten the joint from 10 inches below the TTS to 17 inches below the TTS which would be the lower limit of the proposed tubesheet region inspection zone. Combined with the effects of the tube joint tightening associated with the radial differential thermal expansion and primary pressure inside the tube, contact pressure over at least a 6.5 inch distance should be considerably higher than the contact pressure simulated in the above mentioned pullout tests.”

10.2 Joint Leakage Integrity Discussion

As noted in Sections 5.2 and 4.2, “Joint Leakage Integrity,” respectively of References 7 and 8, the NRC staff reviewed the qualitative arguments developed by Westinghouse regarding the conservatism of the conclusion that a minimum 17 inch engagement length ensures that leakage during a main steam line break (MSLB) will not exceed two times the observed leakage during normal operation. The NRC staff reviewed the qualitative arguments developed by Westinghouse regarding the conservatism of the “bellwether approach,” but the NRC staff’s depth of review did not permit it to credit Westinghouse’s insights from leak test data that leak flow resistance is more sensitive to changes in joint contact pressure as contact pressure increases due to the log normal nature of the relationship. The staff was still able to conclude that there should be no significant reduction in leakage resistance when going from normal operating to accident conditions.

The basis for the Westinghouse conclusion that flow resistance varies as a lognormal linear function of joint contact pressure is provided in detail below. The data from the worst case tube in a comparative study analytically supports the determination that there is at least an eight inch zone in the upper 17 inches of the tubesheet where there is an increase in joint contact pressure due to a higher primary pressure inside the tube and changes in tubesheet bore dilation along the length of the tubes. The NRC concurred (Reference 24) that the factor of 2 increase in leak rate as an upper bound by Westinghouse is reasonable given the stated premise that the flow resistance between the tube and the tubesheet remains unchanged between normal operating and accident pressure differential. The NRC staff noted in Reference 8 that the assumed linear relationship between leak rate and differential pressure is conservative relative to alternative models such as the Bernoulli or orifice models, which assume the leak rate to be proportional to the square root of the differential pressure.

The comparative study supported the NRC staff conclusion that “considering the higher pressure loading when going from normal operating to accident conditions, Westinghouse estimates that contact pressures, and, thus, leak flow resistance, always increases over at least an 8 inch distance above 17 inches below the top of the tubesheet appears reasonable to the NRC Staff.”

a,c,e

a,c,e

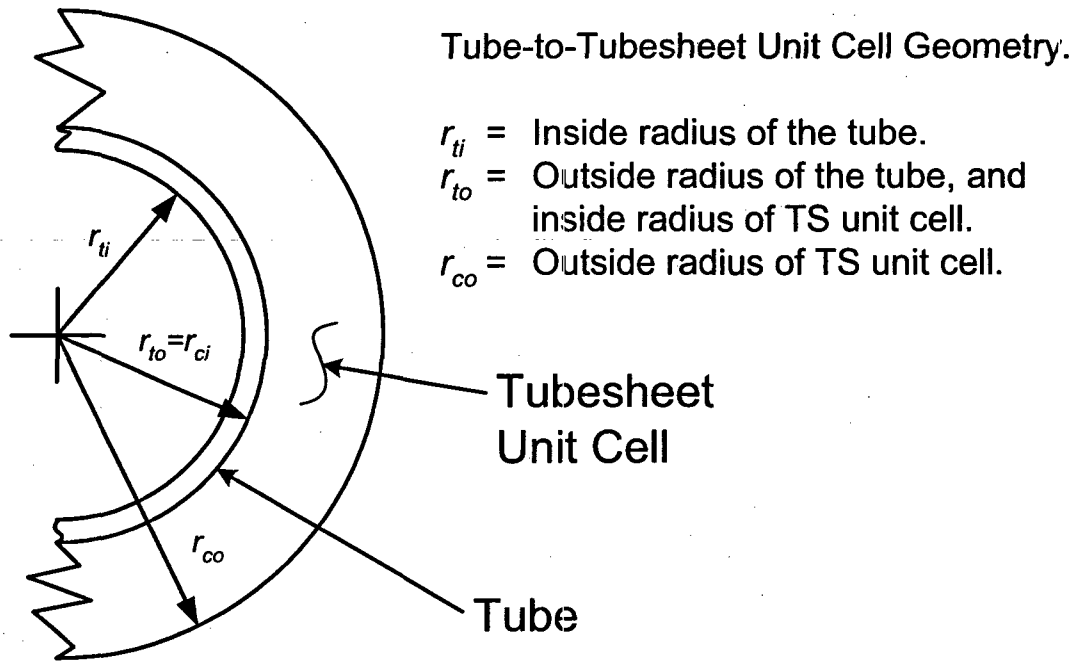


Figure 10-1. Geometry of the Tube-to-Tubesheet Interface



Figure 10-2. Model for Initial Contact Pressure



Figure 10-3. Determination of Contact Pressure, Normal or Accident Operation
(As illustrated, the bow does not result in a loss of contact; however, there are situations where the bow is sufficient to result in a loss of contact between the tube and the tubesheet at the top of the tubesheet.)

11.0 Conclusions

11.1 Analysis

The evaluation of Section 7.0 of this report provides a technical basis for assuring that the structural performance criteria of NEI 97-06 are inherently met for degradation of any extent below the H^* depth identified in Table 7-12, i.e., depths ranging from 2.2 to 6.9 inches below the TTS (including allowance of 0.3 inches to account for the hydraulic expansion transition) selected to be bounding for all tubes in all zones. The corresponding evaluation presented in Section 9.0 provides a technical basis for bounding the potential leak rate from non-detected indications in the tube region below about 6.8 inches from the top of the tubesheet as no more than twice the leak rate during normal operation, see Figure 9-15. A similar analysis obtained a depth of about 9.8 inches based on restricting the expected leak rate to being the same as that during normal operation, Figure 9-16. The evaluation is independent of the magnitude of any degradation that might occur because it is based solely on the resistance of the interface between the tube and the tubesheet. In other words, the tube may be nonexistent below the B^* depth. The conclusion is general in that the depths determined are for the most severely affected region of the tubesheet, the central region. The conclusions also apply to any postulated indications in the tack expansion region and in the tube-to-tubesheet welds, although the level of conservatism would be significantly more. As noted in the introduction to this report, the reporting of crack-like indications in the tube-to-tubesheet welds would be expected to occur inadvertently since no structural or leak rate technical reason exists for a specific examination to take place.

A graphical summary of the findings are presented on Figure 11-1. The depths associated with H^* ¹⁰ and B^* are presented relative to the left ordinate while the leak rates are presented relative to the right ordinate as a function of radial location from the center of the tubesheet.

- The H^* depths are bounding relative to a B^* for equal leak rate resistance during NOP and SLB for radii ≥ 4 inches. The B^* depths are bounding by about 0.3 inch maximum at a radius of 2 inches. This means that if the structural limits, H^* , are satisfied, the leakage limit, B^* , will also be satisfied, except in the area inside of a tubesheet radius of 4 inches.
- Using the H^* values of Table 7-12 results in leak rate per tube increasing on average by a factor of 2 in Zone D, 1.3 in Zone C, 0.95 in Zone B, and 0.43 in Zone A. (Conservatively based on a uniform density of tubes.)
- The SLB leak resistance is greater than that at NOP outside a radius of 4 inches, thus for a differential pressure during SLB of 2.0 times that during NOP the leak rates would be expected to be less than twice that at NOP. Beyond 4 inches the resistance to leak during SLB increases relative to that for NOP and the leak rate would be expected to decrease, becoming about a factor of 2.5 less at 45 inches and 4.6 less at the periphery.

¹⁰ The presented H^* depths are depicted for individual radii from the center of the tubesheet rather than by zone for comparative purposes.

The conclusions to be drawn from the performed analyses are that:

- 1) There is no structural integrity concern associated with tube or tube weld cracking of any extent provided it occurs below the H^* distance as reported in Section 7.0 of this report. The pullout resistance of the tubes has been demonstrated for axial forces associated with 3 times the normal operating differential pressure and 1.4 times differential pressure associated with the most severe postulated accident.
- 2) Contact forces during postulated LOCA events are sufficient to resist axial motion of the tube. Also, if the tube end welds are not circumferentially cracked, the resistance of the tube-to-tubesheet hydraulic joint is not necessary to resist push-out. Moreover, the geometry of any postulated circumferential cracking of the weld would result in a configuration that would resist pushout in the event of a loss of coolant accident. In other words, the crack flanks would not form the cylindrical surface necessary such that there would be no resistance to expulsion of the tube in the downward direction.
- 3) The leak rate for indications below a B^* depth of about 6.8 inches from the top of the tubesheet would be bounded by twice the leak rate that is present during normal operation of the plant regardless of tube location in the bundle. This is initially apparent from comparison of the contact pressures from the finite element analyses over the full range of radii from the center of the tubesheet, and ignores any increase in the leak rate resistance due to the contact pressure changes and associated tightening of the crack flanks. The expectation that this would be the case was confirmed by the detailed analysis of the relative leak rates of Section 9.0.
- 4) The H^* depth bounds the relocation of the pressure boundary for radii greater than about 4 inches. The B^* depth slightly exceeds the H^* depth inside a radius of about 4 inches. The B^* evaluations were performed utilizing the same operating parameters that were used for the determination of the depths required to meet the structural performance criteria, that is, conservative values for the operating temperature.

In conclusion, a relocation of the pressure boundary to the deeper of the H^* or B^* values is acceptable from both a structural and leak rate considerations depending to the relative allowable leak rate during accident conditions. The prior conclusions rely on the inherent strength and leak rate resistance of the hydraulically expanded tube-to-tubesheet joint, a feature which was not considered or permitted to be considered for the original design of the SG. Thus, omission of the inspection of the weld constitutes a reassignment of the pressure boundary to the tube-to-tubesheet interface. Similar considerations for tube indications require NRC staff approval of a license amendment. Consideration of the allowable leak rate during accident conditions may necessitate locating the reassigned pressure boundary to a depth greater than that required for structural integrity, i.e., H^* .

The analyses demonstrate that the evaluation of the conditions on the hot leg bound those for the cold leg with regard to leak rate performance. However, as previously noted, the structural results

for the cold leg are bounding relative to the hot leg. The difference is approximately 0.3 inch. A summary is provided in Table 7-12.

It is important to note that all of the evaluations performed considered the tube to be severed at the reassigned pressure boundary location with no resistance to flow from the leak path within the tube itself, i.e., cracks. At the specified depths the crack flanks would be restricted from opening or parting, and may be held tighter, thus reducing the accident condition leak to below that anticipated herein.

With regards to the preparation of a significant hazards determination, the results of the testing and analyses demonstrate that the relocation of the pressure boundary to a depth based on the more conservative of either H^* or B^* does not lead to an increase in the probability or consequences of the postulated limiting accident conditions because the margins inherent in the original design basis are maintained and the expected leak rate during the postulated accident is not expected to increase beyond the plant specific limit. In addition, the relocation of the pressure boundary does not create the potential for a new or departure from the previously evaluated accident events. Finally, since the margins inherent in the original design bases are maintained, no significant reduction in the margin of safety would be expected.

11.2 Application for Wolf Creek

This document provides a technical justification for limiting the RPC inspection in the tubesheet expansion region to less than the full depth of the tubesheet (21.1 in.).

The justification includes two necessary parts to satisfy both the structural requirements and the leakage requirements under normal operating conditions and under limiting accident conditions:

H^* addresses the structural requirements. H^* defines the minimum length of engagement required for hydraulically expanded tubes to prevent tube pullout from the tubesheet under limiting accident conditions. The principal loads acting to pull a tube from the tubesheet are end-cap loads resulting from the primary to secondary pressure differentials. H^* varies with radial position from the tubesheet centerline due to tubesheet bow resulting from the primary-to-secondary pressure differential. The bow increases during accident conditions due to a greater pressure differential across the tubesheet. Increased tubesheet bow causes tube-hole bore dilation above the neutral axis resulting in reduced interface loads between the tube and the tubesheet. Tubesheet bending varies with the radial distance from the centerline of the tubesheet as dictated by the structural constraints of the tubesheet, e.g., shell and support ring on the OD and divider plate at the centerline.

B^* addresses leakage requirements. As defined in this document, B^* is the distance from the top of the tubesheet where the leakage flow resistance at SLB conditions equals the leakage flow resistance at the H^* distance under normal operating conditions. This definition of B^* is useful in that the accident leakage will be equal to the ratio of the accident pressure differential to the normal operating pressure differential times the normal operating leakage. If effect, the normal operating leakage becomes a "bellwether" for the accident leakage; therefore, if normal operating leakage is within acceptable limits, accident induced leakage will also be within acceptable limits.

The Technical Specification allowable normal operating leak rate for Wolf Creek will be 150 gpd (0.1 gpm) with the approval of the changes submitted to the NRC by WCNOG letter dated November 3, 2005. The allowable accident induced leak rate is 1 gpm total in the affected SG per USAR Table 15.1-3, "Parameters Used in Evaluating the Radiological Consequences of a Main Steam Line Break."

For Wolf Creek, the SLB pressure differential is a factor of 2, or less, greater than the normal operating pressure differential depending on the plugging status of the steam generators. The accident induced primary to secondary pressure differential is never more than a factor of 2 greater than the normal primary to secondary operating pressure differential. Therefore, if the current normal operating leakage is at its limiting value, 0.1 gpm, the accident induced leakage will not exceed 0.2 gpm, a factor of 5, or greater, less than its allowable value if the bounding values of H^* and B^* are applied.

With the exception of the area between approximately 2 inch radius to 4 inch radius on the Hot Leg of the tubesheet, H^* is limiting at Wolf Creek. That is, a greater distance is required to prevent tube pullout than that required to achieve equal NOP and SLB flow resistances except inside a tubesheet radius of about 4 inches. Near the TS centerline (radius of approximately 2 in.), the B^* distance is 6.8 in. and the H^* distance is 6.5 inches. Both B^* and H^* decrease to a point of equality at about 4 in. radius where their distance is 6.6 in. At a TS radius greater than 4 in., the structural requirement, H^* , is limiting. The H^* distance decreases from 6.6 in. depth at 4 inch radius to 1.7 in. depth at a radius of 59 in.

For the Cold Leg, the H^* distance is limiting at all points radially across the tubesheet. The H^* distance is 6.8 in. depth at 2 in. radius, increases to 6.9 in. depth at 8 in. radius, then decreases to 1.7 in. depth at 59 in. radius. Since the B^* distance is smaller at all points, it can be inferred that, at the H^* distance, the SLB flow resistance is greater than the NOP flow resistance, and the factor of safety to the limiting SLB leakage is much greater than 5 if only the cold leg is considered.

Table 11.1 summarizes the pertinent H^* and B^* distances based on Figures 11-1 and 11-2 and their underlying calculations (Note that 1 inch is used as a lower bound): The H^* distances include 0.3 inch conservatively added to the calculated numbers to account for the potential variation of the position of the bottom of the expansion transition relative to the top of the tubesheet.

Since the required inspection depths for the hot leg differ from those of the cold leg as indicated in the prior table, separate inspection plans are recommended for the hot leg and the cold leg to achieve a conservative and efficient inspection. Both the HL and CL inspection schemes assure that the structural criteria against tube pullout are satisfied, and that the SLB leakage at all locations will be a factor of less than 2 times the NOP leak rate. Therefore, if the NOP leakage is at its limit of 0.1 gpm, the integral SLB leakage will be less than 0.2 gpm compared to its limit of 1.0 gpm.

Figure 11-3 shows the bounding inspection requirement for the Hot Leg of the tubesheet and the recommended inspection depths. The bounding requirement is taken from Figure 11-1 and the

Table 11.1 where the H* depth governs for essentially the entire tubesheet. A stepwise representation that bounds the depth requirement at all points is recommended to provide conservative inspection coverage of the tubesheet while maintaining data management requirements at a reasonable level.

Similarly, Figure 11-4 shows the bounding inspection requirement for the Cold Leg of the tubesheet and the recommended inspection depths. The bounding requirement for the Cold Leg is taken from Figure 11-2 and the Table 11.1.

Table 11.2 lists the recommended inspection depths for the HL and the CL of the tubesheet vs. the radial location on the tubesheet. Figure 11-5 and Figure 11-6 illustrate the resulting rows and columns that would be inspected. These are called out as zones, i.e., H1, H2..., C1, C2.... These zones are also identified in Table 11.2.

Table 11-2. Inspection Program for H*/B*

TS Radius (in.)		Hot Leg		Cold Leg	
From	To	Zone	Depth (in.)	Zone	Depth (in.)

a.c.e



Figure 11-1. Comparison of H* and B* Hot Leg Results



Figure 11-2. Comparison of H* and B* Cold Leg Results

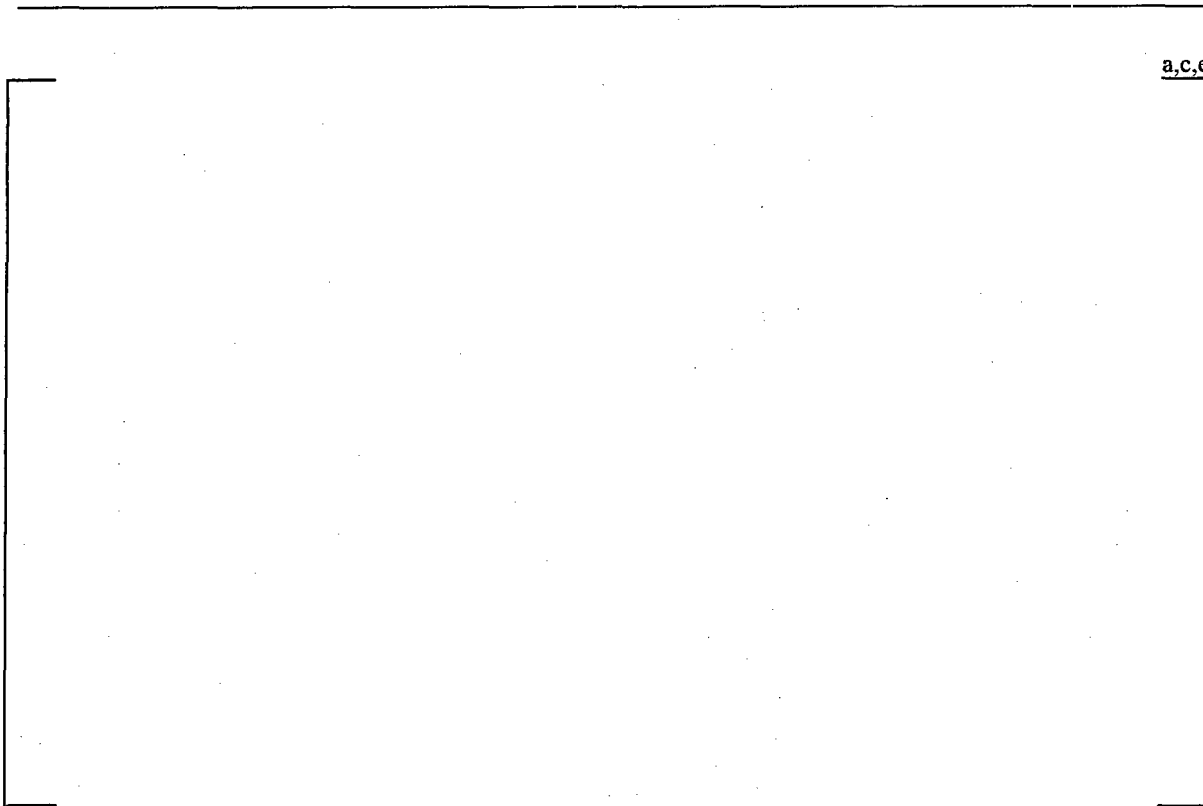


Figure 11-3. Wolf Creek Hot Leg Inspection Depth Profile



Figure 11-4. Wolf Creek Cold Leg Inspection Depth Profile

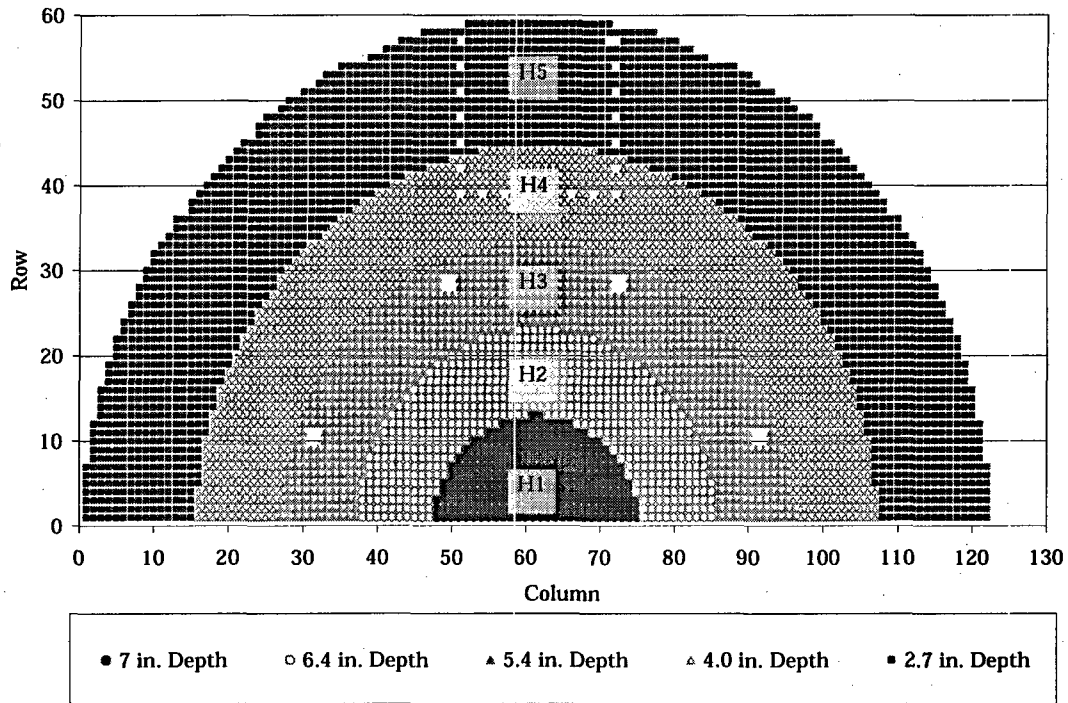


Figure 11-5. Wolf Creek Hot Leg Inspection Depth Zones

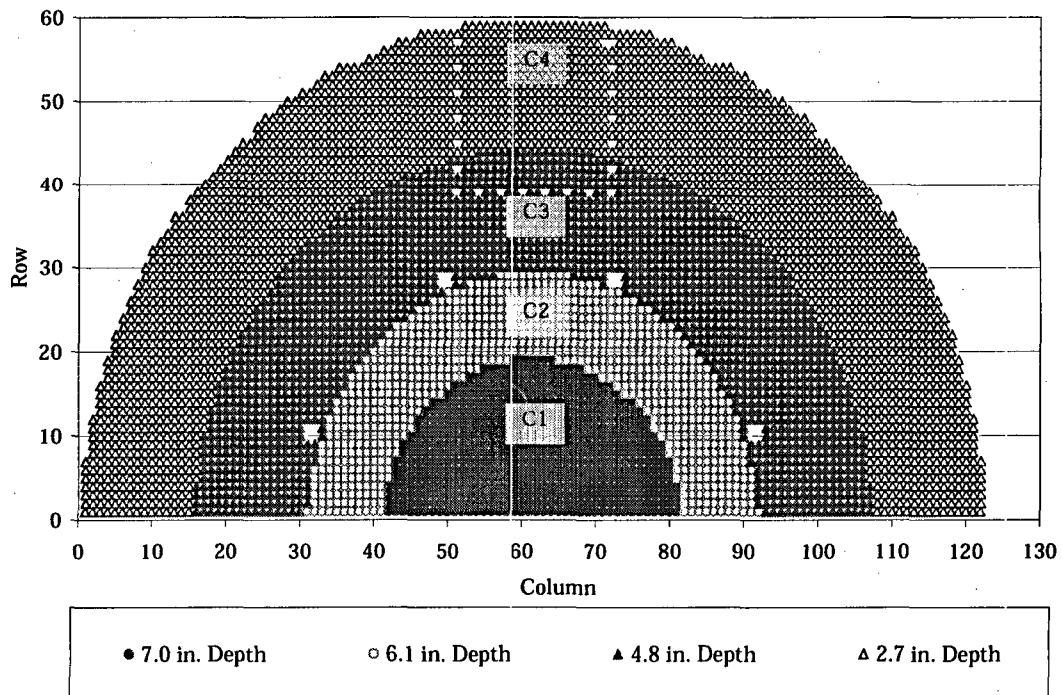


Figure 11-6. Wolf Creek Cold Leg Inspection Depth Zones

12.0 References

1. OE19662 (Restricted & Confidential), "Steam Generators (Catawba Nuclear Power Station)," Institute of Nuclear Power Operations (INPO), Atlanta, GA, USA, December 13, 2004.
2. IN 2005-09, "Indications in Thermally Treated Alloy 600 Steam Generator Tubes and Tube-to-Tubesheet Welds," United States Nuclear Regulatory Commission, Washington, DC, April 7, 2005.
3. SGMP-IL-05-01, "Catawba Unit 2 Tubesheet Degradation Issues," EPRI, Palo Alto, CA, March 4, 2005.
4. OE20339, "Vogtle Unit 1 Steam Generator Tube Crack Indications," Institute of Nuclear Power Operations (INPO), Atlanta, GA, USA, April 4, 2005.
5. LTR-CDME-05-82, "Limited Inspection of the Steam Generator Tube Portion Within the Tubesheet as Wolf Creek Generation Station," Westinghouse Electric Company LLC, Pittsburgh, PA, April 2005.
6. "Docket NO. 50-482: Exigent Request for Revision to Technical Specification (TS) 5.5.9, 'Steam Generator (SG) Tube Surveillance Program'," Wolf Creek Nuclear Operating Corporation, Burlington, KS, April 19, 2005.
7. NRC Letter, "Wolf Creek Generating Station – Issuance of Exigent Amendment Re: Steam Generator (SG) Tube Surveillance Program (TAC No. MC6757)," United States Nuclear Regulatory Commission, Washington, DC, April 28, 2005.
8. NRC Letter, "Braidwood Station, Units 1 and 2 – Issuance of Exigent Amendments Re: Revision of Scope of Steam Generator Inspections for Unit 2 Refueling Outage 11 – (TAC Nos. MC6686 and MC6687)," United States Nuclear Regulatory Commission, Washington, DC, April 25, 2005.
9. NRC Letter, "Vogtle Electric Generating Plant, Units 1 and 2 RE: Issuance of Amendments Regarding the Steam Generator Tube Surveillance Program (TAC Nos. MC8078 and MC8079)," United States Nuclear Regulatory Commission, Washington, DC, September 21, 2005.
10. WCAP-16124, "Justification of the Partial-Length Rotating Pancake Coil (RPC) Inspection of the Tube Joints of the Wolf Creek Model F Steam Generators," Westinghouse Electric Company LLC, Pittsburgh, PA, December 2003.
11. ASME Boiler and Pressure Vessel Code, Section III, "Nuclear Power Plant Components," American Society of Mechanical Engineers, New York, New York, 1971, Summer 1973 Addenda.
12. WNET-180 (Proprietary), Volume 11, "Model F Steam Generator Stress Report," Westinghouse Electric Company LLC, Pittsburgh, PA, September 1980.
13. GL 2004-01, "Requirements for Steam Generator Tube Inspections," United States Nuclear Regulatory Commission, Washington, DC, August 30, 2004.

-
14. NEI 97-06, Rev. 2, "Steam Generator Program Guidelines," Nuclear Energy Institute, Washington, DC, October 2005.
 15. RG 1.121 (Draft), "Bases for Plugging Degraded PWR Steam Generator Tubes," United States Nuclear Regulatory Commission, Washington, DC, August 1976.
 16. Federal Register, Part III, Nuclear Regulatory Commission, National Archives and Records Administration, Washington, DC, pp. 10298 to 10312, March 2, 2005.
 17. NPD/E/PEN-99-255, "Applicable ASME Codes for the Original and Replacement Steam Generators," Westinghouse Electric Company LLC, Pittsburgh, PA, June 29, 1999.
 18. ASME Boiler and Pressure Vessel Code, Section XI, "Rules for Inservice Inspection of Nuclear Power Plant Components," American Society of Mechanical Engineers, New York, New York, 1971.
 19. ASME Boiler and Pressure Vessel Code, Section XI, "Rules for Inservice Inspection of Nuclear Power Plant Components," American Society of Mechanical Engineers, New York, New York, 2004.
 20. WCAP-11224, Rev. 1, "Tubesheet Region Plugging Criterion for the Duke Power Company McGuire Nuclear Station Units 1 and 2 Steam Generators," Westinghouse Electric Company LLC, Pittsburgh, PA, October 1986.
 21. Drawing 1104J40 (Proprietary), Rev. 4, "Steam Generator Model 'F' Tube Bundle Assembly," Westinghouse Electric Company LLC, Pittsburgh, PA, December 1978.
 22. WCAP-13532, Rev. 1, "Sequoyah Units 1 and 2 W* Tube Plugging Criteria for SG Tubesheet Region of WEXTEx Expansions," Westinghouse Electric Company LLC, Pittsburgh, PA, 1992.
 23. WCAP-14797, "Generic W* Tube Plugging Criteria for 51 Series Steam Generator Tubesheet Region WEXTEx Expansions," Westinghouse Electric Company LLC, Pittsburgh, PA, 1997.
 24. "Safety Evaluation by the Office of Nuclear Reactor Regulation Related to Amendment No. 129 to Facility Operating License No. DPR-80 and Amendment No. 127 to Facility Operating License No. DPR-82 Pacific Gas and Electric Company Diablo Canyon Nuclear Power Plant, Units 1 and 2 Docket Nos. 50-275 and 50-323," United States Nuclear Regulatory Commission, Washington, DC, 1999.
 25. NSD-RFK-96-015, "Vogtle 1 Tube Integrity Evaluation, Loose Part Affected SG," Westinghouse Electric Company LLC, Pittsburgh, PA, June 9, 1996.
 26. WCAP-14871 (Proprietary), "Vogtle Electric Generating Plant (VEGP) Steam Generator Tube-to-Tubesheet Joint Evaluation," Westinghouse Electric Company LLC, Pittsburgh, PA, May 1997.
 27. LTR-SGDA-02-162 (Proprietary), Revision 1, "Bounding Evaluation for Operation of Wolf Creek Nuclear Operating Corporation Steam Generator D with Impacted Channelhead Components," Westinghouse Electric Company LLC, Pittsburgh, PA, November 2003.

-
28. CN-SGDA-03-85 (Proprietary), Rev. 1, "H*/P* Input for Model D5 and Model F Steam Generators," September 2003.
 29. CN-SGDA-03-87 (Proprietary), "Evaluation of Tube/Tubesheet Contact Pressures and H* for Model D5 Steam Generators at Byron, Braidwood, Catawba, and Comanche Peak," Westinghouse Electric Company LLC, Pittsburgh, PA, October 2003 (Proprietary Report.)
 30. WCAP-16932-P (Proprietary), Rev. 1, Improved Justification of Partial-Length RPC Inspection of the Tube Joints of Model F Steam Generators of Ameren-UR Callaway Plant," Westinghouse Electric Company LLC, Pittsburgh, PA, May 2003.
 31. Porowski, J.S. and O'Donnell, W.J., "Elastic Design Methods for Perforated Plates," Transactions of the ASME Journal of Engineering for Power, Vol. 100, p. 356, 1978.
 32. Slot, T., "Stress Analysis of Thick Perforated Plates," PhD Thesis, Technomic Publishing Co., Westport, CN 1972.
 33. Computer Program WECAN/Plus, "User's Manual," 2nd Edition, Revision D, Westinghouse Government Services LLC, Cheswick, PA, May 1, 2000.
 34. SM-98-102 (Proprietary), Rev. 2, "Tube/Tubesheet Contact Pressures for Yonggwang 2," Westinghouse Electric Company LLC, Pittsburgh, PA, November 1998.
 35. Nelson, L.A., "Reference for Model D Tubesheet Simulate [sic] of 1.800 Inch Diameter," electronic mail, Westinghouse Electric Company LLC, Pittsburgh, PA, August 6, 2003.
 36. CN-SGDA-03-87 (Proprietary), "Evaluation of the Tube/Tubesheet Contact Pressures and H* for Model D5 Steam Generators at Byron, Braidwood, Catawba and Comanche Peak," Westinghouse Electric Company LLC, Pittsburgh, PA, October 2003.
 37. ASME Boiler and Pressure Vessel Code Section III, "Rules for Construction of Nuclear Power Plant Components," 1989 Edition, The American Society of Mechanical Engineers, New York, NY.
 38. CN-SGDA-02-152 (Proprietary), Rev. 1, "Evaluation of the Tube-to-Tubesheet Contact Pressures for Callaway Model F Steam Generators," Westinghouse Electric Company LLC, Pittsburgh, PA, March 2003.
 39. CN-SGDA-03-123 (Proprietary), "Leakage Calculations to Support H* Criterion for Model D5 Steam Generators," Westinghouse Electric Company LLC, Pittsburgh, PA, October 2003.
 40. CN-SGDA-03-133 (Proprietary), Rev. 0, "Evaluation of the H* Zone Boundaries for Specific Model D-5 and Model F Steam Generators," Westinghouse Electric Company LLC, Pittsburgh, PA, October 2003.
 41. CN-SGDA-03-121 (Proprietary), "H* Ligament Tearing for Models F and D5 Steam Generators," 10/03.
 42. VBA/Excel compatible version of the steam67.dll (dynamic link library) from Winsim.com, Internet available

-
43. ChemicalLogic SteamTab Companion, "Thermodynamic and Transport Properties of Steam, Version 2.0, Based on the IAPWS-95 Formulation," ChemicalLogic Corporation, Burlington, MA, 2003.
 44. NCE-88-271 (Proprietary), "Assessment of Tube-to-Tubesheet Joint Manufacturing Processes for Sizewell B Steam Generators Using Alloy 690 Tubing," Westinghouse Electric Company LLC, Pittsburgh, PA, November 1988.
 45. WCAP 15932-P, Revision 1 (Proprietary), "Improved Justification of Partial-Length RPC Inspection of Tube Joints of Model F Steam Generators of Ameren-UE Callaway Plant," Westinghouse Electric Company LLC, Pittsburgh, PA May 2003.
 46. NEI Letter, "Federal Register Notice of Availability for Generic Steam Generator Program Technical Specifications", September 2,2005.

Enclosure III to ET 06-0004

**Westinghouse Electric Company LLC LTR CAW-05-2084, "Application for Withholding
Proprietary Information from Public Disclosure."**



Westinghouse Electric Company
Nuclear Services
P.O. Box 355
Pittsburgh, Pennsylvania 15230-0355
USA

U.S. Nuclear Regulatory Commission
Document Control Desk
Washington, DC 20555-0001

Direct tel: (412) 374-4419
Direct fax: (412) 374-4011
e-mail: maurerbf@westinghouse.com

Our ref: CAW-05-2084

February 16, 2006

**APPLICATION FOR WITHHOLDING PROPRIETARY
INFORMATION FROM PUBLIC DISCLOSURE**

Subject: LTR-CDME-05-209-P, "Steam Generator Tube Alternate Repair Criteria for the Portion of the Tube Within the Tubesheet at the Wolf Creek Power Station," dated January 2006 (Proprietary)

The proprietary information for which withholding is being requested in the above-referenced report is further identified in Affidavit CAW-05-2084 signed by the owner of the proprietary information, Westinghouse Electric Company LLC. The affidavit, which accompanies this letter, sets forth the basis on which the information may be withheld from public disclosure by the Commission and addresses with specificity the considerations listed in paragraph (b)(4) of 10 CFR Section 2.390 of the Commission's regulations.

Accordingly, this letter authorizes the utilization of the accompanying affidavit by the Wolf Creek Nuclear Operating Corporation

Correspondence with respect to the proprietary aspects of the application for withholding or the Westinghouse affidavit should reference this letter, CAW-05-2084, and should be addressed to B. F. Maurer, Acting Manager, Regulatory Compliance and Plant Licensing, Westinghouse Electric Company LLC, P.O. Box 355, Pittsburgh, Pennsylvania 15230-0355.

Very truly yours,

A handwritten signature in black ink, appearing to read "B. F. Maurer", with a horizontal line extending to the right.

B. F. Maurer, Acting Manager
Regulatory Compliance and Plant Licensing

Enclosures

cc: B. Benney, NRC
L. Feizollahi, NRC

bcc: B. F. Maurer (ECE 4-7) 1L
R. Bastien, 1L (Nivelles, Belgium)
C. Brinkman, 1L (Westinghouse Electric Co., 12300 Twinbrook Parkway, Suite 330, Rockville, MD 20852)
RCPL Administrative Aide (ECE 4-7A) 1L, 1A (letter and affidavit only)
G. W. Whiteman, Waltz Mill
R. F. Keating, Waltz Mill
H. O. Lagally Waltz Mill
D. E. Peck, ECE 5-10
P. J. McDonough, ECE 5-10

AFFIDAVIT

COMMONWEALTH OF PENNSYLVANIA:

SS

COUNTY OF ALLEGHENY:

Before me, the undersigned authority, personally appeared B. F. Maurer, who, being by me duly sworn according to law, deposes and says that he is authorized to execute this Affidavit on behalf of Westinghouse Electric Company LLC (Westinghouse), and that the averments of fact set forth in this Affidavit are true and correct to the best of his knowledge, information, and belief:

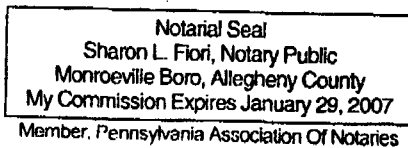


B. F. Maurer, Acting Manager
Regulatory Compliance and Plant Licensing

Sworn to and subscribed
before me this 16th day
of February, 2006



Notary Public



- (1) I am Acting Manager, Regulatory Compliance and Plant Licensing, Nuclear Services, Westinghouse Electric Company LLC (Westinghouse), and as such, I have been specifically delegated the function of reviewing the proprietary information sought to be withheld from public disclosure in connection with nuclear power plant licensing and rule making proceedings, and am authorized to apply for its withholding on behalf of Westinghouse.
- (2) I am making this Affidavit in conformance with the provisions of 10 CFR Section 2.390 of the Commission's regulations and in conjunction with the Westinghouse "Application for Withholding" accompanying this Affidavit.
- (3) I have personal knowledge of the criteria and procedures utilized by Westinghouse in designating information as a trade secret, privileged or as confidential commercial or financial information.
- (4) Pursuant to the provisions of paragraph (b)(4) of Section 2.390 of the Commission's regulations, the following is furnished for consideration by the Commission in determining whether the information sought to be withheld from public disclosure should be withheld.
 - (i) The information sought to be withheld from public disclosure is owned and has been held in confidence by Westinghouse.
 - (ii) The information is of a type customarily held in confidence by Westinghouse and not customarily disclosed to the public. Westinghouse has a rational basis for determining the types of information customarily held in confidence by it and, in that connection, utilizes a system to determine when and whether to hold certain types of information in confidence. The application of that system and the substance of that system constitutes Westinghouse policy and provides the rational basis required.

Under that system, information is held in confidence if it falls in one or more of several types, the release of which might result in the loss of an existing or potential competitive advantage, as follows:

- (a) The information reveals the distinguishing aspects of a process (or component, structure, tool, method, etc.) where prevention of its use by any of Westinghouse's competitors without license from Westinghouse constitutes a competitive economic advantage over other companies.

- (b) It consists of supporting data, including test data, relative to a process (or component, structure, tool, method, etc.), the application of which data secures a competitive economic advantage, e.g., by optimization or improved marketability.
- (c) Its use by a competitor would reduce his expenditure of resources or improve his competitive position in the design, manufacture, shipment, installation, assurance of quality, or licensing a similar product.
- (d) It reveals cost or price information, production capacities, budget levels, or commercial strategies of Westinghouse, its customers or suppliers.
- (e) It reveals aspects of past, present, or future Westinghouse or customer funded development plans and programs of potential commercial value to Westinghouse.
- (f) It contains patentable ideas, for which patent protection may be desirable.

There are sound policy reasons behind the Westinghouse system which include the following:

- (a) The use of such information by Westinghouse gives Westinghouse a competitive advantage over its competitors. It is, therefore, withheld from disclosure to protect the Westinghouse competitive position.
- (b) It is information that is marketable in many ways. The extent to which such information is available to competitors diminishes the Westinghouse ability to sell products and services involving the use of the information.
- (c) Use by our competitor would put Westinghouse at a competitive disadvantage by reducing his expenditure of resources at our expense.
- (d) Each component of proprietary information pertinent to a particular competitive advantage is potentially as valuable as the total competitive advantage. If competitors acquire components of proprietary information, any one component may be the key to the entire puzzle, thereby depriving Westinghouse of a competitive advantage.

- (e) Unrestricted disclosure would jeopardize the position of prominence of Westinghouse in the world market, and thereby give a market advantage to the competition of those countries.
 - (f) The Westinghouse capacity to invest corporate assets in research and development depends upon the success in obtaining and maintaining a competitive advantage.
-
- (iii) The information is being transmitted to the Commission in confidence and, under the provisions of 10 CFR Section 2.390, it is to be received in confidence by the Commission.
 - (iv) The information sought to be protected is not available in public sources or available information has not been previously employed in the same original manner or method to the best of our knowledge and belief.
 - (v) The proprietary information sought to be withheld in this submittal is that which is appropriately marked in LTR-CDME-05-209-P, "Steam Generator Tube Alternate Repair Criteria for the Portion of the Tube Within the Tubesheet at the Wolf Creek Power Station," dated January 2006 (Proprietary). The information is provided in support of a submittal to the Commission, being transmitted by the Wolf Creek Nuclear Operating Corporation and Application for Withholding Proprietary Information from Public Disclosure, to the Document Control Desk. The proprietary information as submitted for use by Westinghouse for the Wolf Creek Power Station is expected to be applicable to other licensee submittals in support of implementing a limited inspection of the tube joint with a rotating probe within the tubesheet region of the steam generators.

This information is part of that which will enable Westinghouse to:

- (a) Provide documentation of the analyses, methods, and testing for the implementation of an alternate repair criteria for the portion of the tubes within the tubesheet of the Wolf Creek Power Station steam generators.
- (b) Provide a primary-to-secondary side leakage evaluation for the Wolf Creek Power Station during all plant conditions.

- (c) Assist the customer to respond to NRC requests for information.

Further this information has substantial commercial value as follows:

- (a) Westinghouse plans to sell the use of similar information to its customers for purposes of meeting NRC requirements for licensing documentation.
- (b) Westinghouse can sell support and defense of this information to its customers in the licensing process.
- (c) The information requested to be withheld reveals the distinguishing aspects of a methodology which was developed by Westinghouse.

Public disclosure of this proprietary information is likely to cause substantial harm to the competitive position of Westinghouse because it would enhance the ability of competitors to provide similar licensing support documentation and licensing defense services for commercial power reactors without commensurate expenses. Also, public disclosure of the information would enable others to use the information to meet NRC requirements for licensing documentation without purchasing the right to use the information.

The development of the technology described in part by the information is the result of applying the results of many years of experience in an intensive Westinghouse effort and the expenditure of a considerable sum of money.

In order for competitors of Westinghouse to duplicate this information, similar technical programs would have to be performed and a significant manpower effort, having the requisite talent and experience, would have to be expended.

Further the deponent sayeth not.

PROPRIETARY INFORMATION NOTICE

Transmitted herewith are proprietary and/or non-proprietary versions of documents furnished to the NRC in connection with requests for generic and/or plant-specific review and approval.

In order to conform to the requirements of 10 CFR 2.390 of the Commission's regulations concerning the protection of proprietary information so submitted to the NRC, the information which is proprietary in the proprietary versions is contained within brackets, and where the proprietary information has been deleted in the non-proprietary versions, only the brackets remain (the information that was contained within the brackets in the proprietary versions having been deleted). The justification for claiming the information so designated as proprietary is indicated in both versions by means of lower case letters (a) through (f) located as a superscript immediately following the brackets enclosing each item of information being identified as proprietary or in the margin opposite such information. These lower case letters refer to the types of information Westinghouse customarily holds in confidence identified in Sections (4)(ii)(a) through (4)(ii)(f) of the affidavit accompanying this transmittal pursuant to 10 CFR 2.390(b)(1).

COPYRIGHT NOTICE

The reports transmitted herewith each bear a Westinghouse copyright notice. The NRC is permitted to make the number of copies of the information contained in these reports which are necessary for its internal use in connection with generic and plant-specific reviews and approvals as well as the issuance, denial, amendment, transfer, renewal, modification, suspension, revocation, or violation of a license, permit, order, or regulation subject to the requirements of 10 CFR 2.390 regarding restrictions on public disclosure to the extent such information has been identified as proprietary by Westinghouse, copyright protection notwithstanding. With respect to the non-proprietary versions of these reports, the NRC is permitted to make the number of copies beyond those necessary for its internal use which are necessary in order to have one copy available for public viewing in the appropriate docket files in the public document room in Washington, DC and in local public document rooms as may be required by NRC regulations if the number of copies submitted is insufficient for this purpose. Copies made by the NRC must include the copyright notice in all instances and the proprietary notice if the original was identified as proprietary.

Wolf Creek Nuclear Operating Corporation

Letter for Transmittal to the NRC

The following paragraphs should be included in your letter to the NRC:

Enclosed is:

1. 1 copy of LTR-CDME-05-209-P, "Steam Generator Tube Alternate Repair Criteria for the Portion of the Tube Within the Tubesheet at the Wolf Creek Power Station," dated January 2006 (Proprietary).
2. 1 copy of LTR-CDME-05-209-NP, "Steam Generator Tube Alternate Repair Criteria for the Portion of the Tube Within the Tubesheet at the Wolf Creek Power Station," dated January 2006 (Non-proprietary).

Also enclosed is Westinghouse authorization letter CAW-05-2084 with accompanying affidavit, Proprietary Information Notice, and Copyright Notice.

As Item 1 contains information proprietary to Westinghouse Electric Company LLC, it is supported by an affidavit signed by Westinghouse, the owner of the information. The affidavit sets forth the basis on which the information may be withheld from public disclosure by the Commission and addresses with specificity the considerations listed in paragraph (b) (4) of Section 2.390 of the Commission's regulations.

Accordingly, it is respectfully requested that the information which is proprietary to Westinghouse be withheld from public disclosure in accordance with 10 CFR Section 2.390 of the Commission's regulations.

Correspondence with respect to the copyright or proprietary aspects of the items listed above or the supporting Westinghouse affidavit should reference CAW-05-2084 and should be addressed to B. F. Maurer, Acting Manager, Regulatory Compliance and Plant Licensing, Westinghouse Electric Company LLC, P.O. Box 355, Pittsburgh, Pennsylvania 15230-0355.